Ingenieurfakultät Bau Geo Umwelt
Technische Universität München

Agent-based Modelling and Simulation of Urban Air Mobility Operation

An Evaluation of Travel Times and Transport Performance

Raoul Leander Rothfeld

Vollständiger Abdruck der von der Ingenieurfakultät Bau Geo Umwelt der Technischen Universität München zur Erlangung des akademischen Grades eines

Doktor-Ingenieurs (Dr.-Ing.)

genehmigten Dissertation.

Vorsitzender:
Prof. Dr.-Ing. Rolf Moeckel

Prüfende der Dissertation:
1. Prof. Dr. Constantinos Antoniou
2. Prof. Dr.-Ing. Kay Axhausen,
   Eidgenössische Technische Hochschule Zürich / Schweiz

Die Dissertation wurde am 17.02.2021 bei der Technischen Universität München eingereicht und durch die Ingenieurfakultät Bau Geo Umwelt am 02.06.2021 angenommen.

In memory of Ursula and Bernhard Rothfeld.

Abstract

Improving aerial mobility of citizens in Europe is a political objective of the European Commission. Three preceding studies that approached access to and by aerial mobility are consolidated within this dissertation and supplemented by accompanying analyses. An initial European airport access and egress time analysis shows substantial differences in airports' car and Public Transport (PT) average access/egress speeds and concludes that—in line with the European Commission's goals—aerial mobility needs to become more accessible for intra-European travel times to decrease.

With novel, electrified Vertical Take-off and Landing (VTOL) vehicles, an initial inner-city airport concept can be advanced into the idea of widespread introduction of commercial, on-demand, inter- and intra-urban aerial passenger transport, i.e. Urban Air Mobility (UAM). UAM has elevated hopes of utilizing airspace capacity to reduce ground-based traffic volumes—especially for congested urban areas. An overview of contemporary UAM literature in topics such as passenger adoption, modelling and simulation, and welfare effects provides the basis for a following study that explicitly analyses UAM's potential travel time savings. The study's outcome indicates that UAM is not expected to provide significant travel time savings for a vast majority of motorized trips. By reviewing the results of multiple analyses, the conclusion is drawn that UAM will not provide mass transportation, nor be able to alleviate traffic congestion.

To facilitate UAM transport modelling, a UAM-extension has been developed for the Multi-agent Transport Simulation (MATSim) and has since been published as an open-source project for public use. This dissertation provides technical documentation, usage instructions, and pointers for further development, besides adding to the above-mentioned analyses and the general discussion on UAM-related literature. With that, modelling and simulation capabilities for intermodal, intra-urban, station-based, on-demand aerial passenger transport have been established that facilitate further research into the potential benefits of UAM.

Zusammenfassung

Die Verbesserung der Luftverkehrsmobilität und deren Erreichbarkeit für europäische Bürger ist ein politisches Ziel der Europäischen Kommission. Drei vorangegangene Studien, die sich mit der Zugänglichkeit zu und der Mobilität durch Lufttransport befassten, werden in dieser Dissertation konsolidiert und durch begleitende Analysen ergänzt. Eine erste Analyse von An- und Abreisedauern zu und von europäischen Flughäfen zeigt erhebliche Unterschiede in den durchschnittlichen An- und Abreisegeschwindigkeiten von Autos und öffentlichen Verkehrsmitteln und schlussfolgert, dass Luftmobilität—in Übereinstimmung mit den Zielen der Europäischen Kommission—zugänglicher werden muss, um innereuropäische Reisezeiten zu senken.

Mit neuartigen, elektrifizierten Vehikeln—welche vertikal starten und landen können (VTOL)—kann die anfängliche Idee eines innerstädtischen Flughafens zu einem flächendeckenden Konzept von kommerziellem, bedarfsgesteuertem, inter- und intraurbanem Personenluftverkehr—dem so-genannten Urban Air Mobility (UAM) Konzept—weiterentwickelt werden. Mit UAM verbindet man die Hoffnung, bisher ungenutzte Luftraumkapazitäten zu verwenden, um das bodengebundene Verkehrsaufkommen zu reduzieren—vor allem in staugeplagten Stadtgebieten. Ein Überblick über aktuelle UAM-Literatur zu Themen wie dessen Passagierakzeptanz, der Modellierung und Simulation von UAM, sowie dessen Wohlfahrtseffekte bildet die Grundlage für eine Folgestudie, die explizit die potenziellen Reisezeiteinsparungen durch UAM analysiert. Das Ergebnis dieser Reisezeitstudie zeigt, dass UAM für die überwiegende Mehrheit von motorisierten Fahrten keine signifikanten Zeiteinsparungen erwarten lässt. Durch das Zusammenführen von Ergebnissen mehrerer Analysen wird die Schlussfolgerung gezogen, dass UAM weder Massentransport bereitstellen kann, noch in der Lage sein wird, Bodenverkehrsaufkommen zu reduzieren.

Zur Verkehrsmodellierung und -simulation von UAM wurde eine entsprechende Erweiterung für die Multi-Agenten-Transport-Simulation (MATSim) entwickelt und inzwischen als Open-Source-Projekt zur allgemeinen Nutzung veröffentlicht. Diese Dissertation liefert neben den oben genannten Analysen und der allgemeinen Diskussion UAM-bezogener Literatur auch technische Dokumentation und Nutzungs- und Weiterentwicklungshinweise. Folglich wurden Modellierungs- und Simulationsmöglichkeiten für intermodalen, innerstädtischen, stationsbasierten und bedarfsgesteuerten Personenluftverkehr geschaffen, die zur weiteren Erforschung der potenziellen Vorteile von UAM befähigen.

Contents

List of Figures

List of Tables

1 Introduction

In an ever-more connected world with interwoven exchange of passengers, goods, and information, the speed of transportation has never before been more significant. Within their strategy paper, Flightpath 2050, the European Commission, set forth a challenging vision of ensuring that 90% of all intra-European travel can be done in less than four hours. Especially for longer-range trips, aerial mobility is seen as the main enabler of shortened travel times.

With the overdue push towards more sustainable mobility, electrification has made its way into mobility technology—as can be seen by the emergence of fully-electric cars, for example. Electrification, though, has also spurred the development of novel aircraft that make use of this progress with electrified distributed propulsion. Whereas conventional helicopters use single main rotors, that are usually driven by gas-powered turboshaft engines, these novel aircraft make use of electrical—instead of mechanical—energy transmission. This allows these vehicles to be equipped with multiple smaller rotors, rather than one large one, which promises a substantial reduction in cost and noise emission, while increasing safety. Numerous start-ups and established road and aviation Original Equipment Manufacturers (OEMs) are building prototypes of such aircraft. A main driver for these developments is the potential for using these vehicles for inter- and intra-urban, on-demand passenger transport missions, sometimes called air taxis. This dissertation compounds, summarizes, and documents the author's studies, [1]–[3] in particular, and developments towards understanding and modelling the accessibility and impact of this potentially-novel form of aerial mobility.

1.1 Emergence of Urban Air Mobility

Motivated by the previously-mentioned Flighpath 2050 goal of enabling below four-hour intra-European door-to-door travel times [4, p. 13], Rothfeld *et al.* [1] set out to analyse European airport access and egress times given that there is little room for aircraft flight speed improvements [1, p. 148]. By analysing the airport access and egress trip times gathered via Google Maps for 22 European airport for various distances and times of day, airport access/egress time estimations are presented for car and PT. They indicate, that out of the four-hour goal, "merely 50 min remain for airport access and egress" [1, p. 157], which itself has to be split near-equally between both access and egress trips. While PT access/egress time estimations are consistently larger than 25 minutes, car estimations are below 25 minutes for trips with Euclidean distances of less than 25 km.

Two-thirds of the European Union (EU) population live further than 25 km away from their nearest international airport, Rothfeld *et al.* [1, p. 157] state and conclude that "[r]educing European airport access and egress times is [..] an inevitable step in order to achieve the four hours door-to-door goal."

While airports' PT connections could see substantial improvements, those alone will not change the study's outcome that—for most people—international airports are out of reach in terms of being able to satisfy the four-hour time frame. Given that average driving and PT speeds are not expected to fundamentally change in the near future, one could turn to access and egress distances in hopes of reducing airport access/egress trip times. In this context, Urban *et al.* [5] proposed a "transport concept [that] consists of an inner-city airport combined with a short takeoff and landing (STOL) capable, short-range aircraft" [5, p. 1] in order to make aerial mobility more accessible. Their idea places multi-story, single-building airports, whose roof acts as a runway, within urban settings such as on top of main train stations. These inner-city airports, with a minimum length and width of 640 by 80 m, could substantially decrease access and egress trip lengths if placed centrally in or closely around cities. Granted, the accompanying STOL aircraft is shorter-range and lower-capacity [5, p. 6] than conventional airport-operated aircraft.

The before-noted emerging prevalence of electrified distributed propulsion for aerial vehicles "revitalize[d] the idea of using urban airspace for intracity passenger transport" [2, p. 267]. Initially, these novel aircraft were often called Personal Air Vehicle (PAV) (e.g. [6]–[10]). However, with the spread of the idea of operating such vehicles as so-called air or flying taxis (e.g. [11]–[13]), the reference to personal ownership in the term PAV could be questioned. Nonetheless, these Vertical Take-off and Landing (VTOL) vehicle promise to allow the inner-city airport concept to be advanced by potentially enabling on-demand, intra-city passenger transport operations from so-called sky- or vertiports (cf. [14]–[16])—the concept of Urban Air Mobility (UAM). Technically, UAM in itself can describe any aerial transportation within a—usually—densely-populated space and, with that, is very broad in its applicability. Interpretations can range from, for example, video or package-delivery drones to conventional helicopters—all of which do provide the ability to fly or be flown in urban settings. Recently, however, the term UAM has increasingly been used to specifically refer to on-demand, station-based, inter- and intra-urban aerial passenger transport using novel and electrified VTOL aircraft architectures.

Arellano [17] summarised the emerging UAM vision in stating that "[t]he concept is expected to provide speedier, time-reducing travel with vehicles envisioned to be cleaner, cheaper and more efficient than presently available short-distance crafts" [17, p. I]. Further, Lim and Hwang [10] state that UAM has the "potential means of providing the freedom of fast door-to-door mobility beyond what is widely available today via automobiles" and add that it "would alleviate the traffic issue" [10, p. 260] that cities face. Similarly, Rothfeld *et al.* [2] explain that "[b]y making use of aerial transport capacity, UAM is aimed at reducing problems facing the growing demand for mobility in an increasingly crowded environment, such as congestion, pollution, and scarcity of urban space" [2, p. 268].

Defining aspects of UAM vehicles are their ability to take off and land vertically and the general expectation that these vehicles will operate autonomously at some point in

the future. The requirement for VTOL capability is given by the nature of its urban area of operation, with little space for take-off and landing infrastructure. Even though some UAM prototypes exist that advertise no need for dedicated VTOL infrastructure (see, e.g., entries 11 and 32 in [6, Table 1]), it is—by now—consensus that urban passenger transport will require some form of UAM stations for take-off and landing (cf. [10], [14]–[17]). UAM vehicle's autonomous operation is desired in order to evade the weight, cost, and errors of human pilots. The potential cost saving through autonomous operation, reduced noise emission, and assumed ability to operate within densely-populated areas are the primary reasons for industry and research interest in UAM.

This promises-spurred interest is reflected in the wide range of topics that are currently being studied, such as vehicle design (e.g. [18]), station placement (e.g. [10], [14]–[17], [19]), environmental impact (e.g. [20], [21]), passenger adoption (e.g. [13], [22], [23]), cost structures (e.g. [24]), and potential demand (e.g. [3], [24]–[27]). Goyal [28] provides an extensive review of UAM's potential markets whereas Straubinger *et al.* [8] offer a comprehensive—yet, non-exclusive—overview of current research and developments regarding UAM. Besides technical prototyping, market demand analyses receive special attention in this early stage of potential UAM realisation.

1.2 UAM Demand & Supply

In 2019, Fu *et al.* [13] conducted a stated-preference survey to gain insights into potential user's choice behaviour regarding currently available urban transportation modes and autonomous transportation services. Based on survey data, collected in Munich, Germany, logistic mode choice models were developed considering four transportation alternatives: private car, Public Transport (PT), autonomous taxi, and autonomous flying taxi—with autonomous flying taxi being the representation of UAM within that study. It has been revealed that travel time, travel cost, and safety may be critical determinants with regard to the adoption of autonomous transportation modes. The results also indicate a high willingness to pay for using autonomous transportation modes—particularly for UAM. Meanwhile, among different market segments, younger individuals, as well as older individuals with relatively high household income, are more likely to adopt UAM, especially for performing non-commuting trips during a potential market entry stage. Further factors of UAM adoption in the Munich Metropolitan Region have been studied by Al Haddad *et al.* [22], who identified potential user's trust and perceived safety as key factors for UAM adoption. An additional factor, that might influence adoption, lies in its expected autonomy; in that passenger can use their travel time more productively instead of having to drive themselves, similar to time spent in PT as studied by Gripsrud and Hjorthol [29]. With that, Gripsrud and Hjorthol [29] even question the assumption that travel times need to be minimized, which contrasts the major expected benefit of UAM.

The results of Fu *et al.* [13] and Al Haddad *et al.* [22] have been used in further UAM analyses studying potential UAM implementations within the Munich Metropolitan Region. Using an incremental approach (see [30], [31]), a new—UAM-including—utility function was defined, where most of the coefficients were derived from a reference mode.

The mode train was chosen as reference mode, under the assumption of using UAM as a complement to public transport, and due to the equivalence of rail networks with the simulated UAM network (i.e. requirement for accessing stations combined with high travel speeds). With that, Pukhova *et al.* [27] estimated a potential UAM trip market share of up to 0.4%. Other studies identified potential modal shares of 0.5% [24] and 1.3% [32]. The results of studies of Zurich, Switzerland, by Balać *et al.* [9], [26] yielded comparable results with UAM trip shares of below 0.3%. A very early UAM study [7] on Sioux Falls, United States, found a potential UAM market share of 4% but—more importantly—outlined the substantial impact of process times on UAM travel times. Even the potential of inducing demand was found to be insignificant with regards to UAM market share by Pukhova *et al.* [27] and Moreno *et al.* [33].

These above-mentioned studies included UAM pricing in their market share calculations, often with various scenarios, even though UAM service pricing—unfortunately—very much remains speculation at this point, as discussed by Rothfeld *et al.* [3, p. 14]. While UBER estimates that long-term VTOL usage cost could be as low as that of a privately owned car [34, pp. 95], no indicative studies have proven that such low prices can be realized in an economically feasible manner. With that, UAM's potential for travel time savings over ground-based transportation remains the primary anticipated benefit of UAM introduction. Hence, a dedicated analysis of travel time savings through UAM was conducted by Rothfeld *et al.* [3], which analysed the study areas of Munich Metropolitan Area, Île-de-France, and San Francisco Bay Area. Through large-scale travel time calculations for car, PT, and various implementations of UAM, they found that in their base case scenario between 3% and 13% of motorized trips, i.e. 2–7% of all trips, would see their travel times reduced through the use of UAM—most of those trips originally being PT trips. Thus, calling the often proclaimed benefit of UAM, in that it provides substantial and widespread travel time savings, into question.

Additionally, the study [3] confirmed the importance of short process times and UAM station placement, while also discussing the impact of vehicle parameters such as cruise flight speed. Focusing on these novel VTOL aircraft, Baur *et al.* [35] illustrated various types of UAM vehicles and their potential use cases depending on cruising speeds and operation ranges. Shamiyeh *et al.* [18] and Liu *et al.* [36] provide an overview regarding characteristics and mission performance of different configurations of air vehicles, as well as technologies that enable these vehicle developments. Remaining challenges of air vehicle design, such as safety issues and helipad distribution, were also highlighted by Liu *et al.* [36]. Since UAM itself is an emerging transportation mode, with novel VTOL vehicles which have not seen widespread commercial use yet, the number and range of assumptions on a potential UAM implementations is quite large (see [6, Table 1]). UAM vehicle cruise speeds, for example, are advertised in a range of 70–630 km/h according to Shamiyeh *et al.* [6].

With higher speeds, however, comes increased energy usage. Thus, discussions surrounding the sustainability of UAM operations have rightfully emerged. As discussed in Rothfeld *et al.* [3], Pukhova [20] and Kasliwal *et al.* [37] offer slightly contradictory conclusions on the environmental friendliness of UAM services. While Pukhova [20] "found that UAM can only be of environmental benefit if the electricity used by eVTOL ve-

hicles originates from renewable sources" [3, p. 3], Kasliwal *et al.* [37] claim that UAM emits fewer greenhouse gas emissions per passenger-kilometre than conventional cars and even electric cars. Their core assumption lies in full utilisation of UAM passenger capacity while the ground-based counterparts are assumed to only be filled with an average occupancy of 1.5 passengers despite having ample spare capacity. The assumption that UAM flights will consistently operate with maximum occupancy, however, remains highly questionable. Noise emission is another aspect of sustainability and is often discussed as the primary factor hindering UAM's public acceptance (see [38]). Precise noise levels, that occur during UAM operation, have yet to be measured with full-scale and fully-loaded prototypes. Nevertheless, first studies emerge that model and analyse possible noise profiles of UAM of different sizes as done by Jia and Lee [39]. Fortunately, sustainability is gaining in importance in transportation, which is also reflected by the recent call for research proposals within the European Union's Horizon 2020 programme, titled "Towards sustainable urban air mobility", that focuses on UAM's "overall environmental footprint (e.g. energy demand; local emissions and global greenhouse gas emissions); and [...] noise and visual pollution, including those aspects dealing with perception, monitoring and mitigation in urban environments" [40]. As done by Jia and Lee [39], it is fundamental to develop and apply modelling techniques in order to gain insights into the impacts of potential UAM implementations before those might—either in the near or far future—be in operation.

1.3 Transport Modelling & Simulation

For transportation modelling, one can look back on more than 140 years of research with several important milestones. As outlined by Trattner [41], one of the early roots of transport modelling is the first isochronic map of travel times by Galton [42] in 1881 (see Figure 1.1). The following major advancements in transport modelling occurred in 1955 (cf. [43]) with the emergence of aggregate trip-based models, i.e. the so-called four-step model, which, according to Moeckel *et al.* [44], is "[b]y far, the most common approach for travel demand modeling." Though, Moeckel *et al.* [44] adds, "[t]he form of this model used nowadays is largely based on the framework proposed by Manheim [45]." The four-step model outlines the process of analysing mobility behaviour in subsequent—usually flow-based—steps: (1) trip generation, (2) trip distribution, (3) mode choice, and (4) traffic assignment. Building on the four-step model, the concept of activity-based modelling is introduced in 1983 by Jones [46] and sees continues development and usage to this day (see, e.g., [44], [47], [48]).

Shortly thereafter, in 1984, Hillier and Hanson [49] present the so-called space syntax which facilitated the representation of transport infrastructure as—what is now called—graphs with nodes and links, allowing for the analysis of spaces "as a system of syntactic relations" [49, pp. 93]. The following transport modelling milestone, agent-based transport modelling—enabled by the exponential growth in computational processing power (cf. Moore's law [50])—combines the methods of activity-based modelling and space syntax to simulate individuals entities such as vehicles and persons, so-called agents,

Figure 1.1: Isochronic map of travel times from London, United Kingdom, made 1881 by Galton [42] and is in the public domain.

on transport networks. Agent-based systems, Van Dyke Parunak *et al.* [51] specify, begin "with behaviors through which individuals interact with one another" where "[d]irect relationships among the [agents] are an output of the process, not its input." Such agent-based approaches have established themselves within transport modelling as Bazzan and Klügl [52] explain. Agent-based models are capable of integrating the various phases of the four-step method into one coherent system while "offer[ing] many advantages compared with conventional approaches in traffic simulation" [52, p. 4], such as facilitating modelling data and behaviour heterogeneity [52, pp. 4]. Transportation, in particular, is seen as a prominent field for the application of agent-based approaches (cf. [52], [53]).

The Multi-agent Transport Simulation (MATSim) [54] is a framework that facilitates such agent- and activity-based transportation simulations and has seen continuous refinement after its inception "[a]t the end of the 1990s" [55, p. 4]. Zwick *et al.* [56, p. 5] accurately and concisely summarised the functioning of MATSim in that it "utilizes an iterative, co-evolutionary learning approach in which each agent tries to [optimise] their daily plan of activities." While MATSim does provide microscopic modelling of traffic and agent behaviour [55, p. 3], it is fundamentally "designed for large-scale scenarios" [55, p. 4] and is, thus, often described as a mesoscopic transport simulation framework. With that, MATSim has established itself as a highly versatile, open-source, and modular simulation framework that is still being further developed and extended (see, e.g., [57], [58]). Particularly, MATSim is extensively used with regards to modelling emerging transport concepts, such as car-sharing (e.g. [59]–[61]), ride-hailing and -sharing (e.g. [62], [63]), or Shared Autonomous Vehicle (SAV) services (e.g. [64]–[67]).

Most of these studies, that simulate novel concepts of mobility, build upon the developments by Maciejewski [57] who introduced the ability of modelling dynamic vehicle routing with his Dynamic Vehicle Routing Problem (DVRP) extension for MATSim. As such, Maciejewski [57, p. 146] clarifies that "[his] contribution is designed to be highly general and customizable to model and simulate a wide range of dynamic vehicle rout-

ing and scheduling processes." This enabled DVRP's reuse in further extensions, such as Demand Responsive Transport (DRT) for shared-service ([68], [69]) or Autonomous Vehicle (AV) ([70]). Thus, the MATSim environment with its numerous extensions provides all required functionality to model most emerging modes of transportation such as AV/SAV operation, taxi and ride-hailing, or car- and ride-sharing. With the emergence of UAM, however, it became evident that additional developments are required to be able to properly include UAM operations within MATSim besides existing modes. While also being a shared, autonomous, on-demand service, UAM also requires its own dedicated transport infrastructure, process times, and—most importantly—fully intermodal access and egress to and from its dedicated VTOL stations by any ground-based transport mode. Even though Rieser [71] introduced intermodal station access with walking trips to PT stations, the unique combination of those numerous and versatile aspects of UAM operations was not yet implemented within MATSim.

1.4 Objectives & Contributions

In light of the discussed literature, this dissertation intends to address the current shortcoming in the ability to model and simulate intermodal travel itineraries which include on-demand aerial mobility. Thus, this doctoral research aims to:

- advance the understanding of aerial mobility in an urban context, its accessibility and ground-based traffic impact;
- provide modelling and simulation capabilities for intermodal, intra-urban, station-based, on-demand aerial passenger transport;
- evaluate potential travel time impacts of intra-urban aerial passenger transport systems.

With regards to the above-mentioned objectives, this dissertation comprises three peer-reviewed studies, that delve into travel time analyses covering various facets of aerial mobility:

- Rothfeld *et al.* [1] (see Appendix A) analyse access and egress times to and from selected European international airports using Google Maps data. The results, which include linear access/egress speed regression models, show great discrepancies in-between European airports, car and Public Transport (PT) travel times, and the need for a significant increase in accessibility to aerial mobility.
- Rothfeld *et al.* [2] (see Appendix B) provide an overview of current research and developments in the field of Urban Air Mobility (UAM). In particular, the study summarises literature surrounding UAM passenger adoption, provides an outlook on UAM modelling, offers an introduction into a self-developed simulation framework extension, and adds to the discussion of UAM's potential effects on societal welfare and land-use.

- Rothfeld *et al.* [3] (see Appendix C) present an extensive analysis of potential travel time savings and motorized trip shares of UAM for three study areas: Munich Metropolitan Region, Île-de-France, and San Francisco Bay Area. The study's conclusions state that UAM would provide travel time savings to a relatively small share of motorized trips and, on average, only beyond Euclidean trip distances of 50–55 km.

Together with further research that has been conducted with fellow colleagues from, for example, the Munich-based aviation think-tank Bauhaus Luftfahrt e.V. and the Eidgenössische Technische Hochschule Zürich, these studies and—hence—this dissertation facilitate the scientific discourse around aerial mobility and make the following contributions:

- a regression model for estimating access and egress travel speeds/times of car or PT usage to and from European airports;
- a comprehensive review and discussion of UAM-related literature, covering facets such as modelling and simulation, public acceptance, vehicle parameters, and sustainability of aerial mobility;
- providing agent-based, intermodal, station-based, on-demand aerial modelling and simulation capabilities in a systematic, extendable, and transparent way by developing, documenting, and publishing an adaptable open-source extension to MATSim;
- proposing replicable methods for semi-automated UAM station placement and non-Euclidean UAM flight path routing;
- providing a large-scale experimental exploration of various (potential) UAM implementations in three diverse metropolitan regions, which identifies maximum-attainable UAM trip shares, the impact of ground congestion on UAM travel times, and distances beyond which UAM-usage, on average, provides time savings when compared to conventional modes.

The following remainder of this thesis is structured as follows: Chapter 2 introduces the reader to the transport simulation framework MATSim, its extension for dynamic transport services and, finally, guides towards the development of UAM modelling capabilities within MATSim. Chapter 3 provides technical documentation and usage tutorials for the self-developed framework extension, MATSim-UAM [72], that allows for the modelling and simulation of UAM. Discussion of two alternative use cases, besides UAM, close Chapter 3. Thereupon, Chapter 4 continues and enhances the UAM travel time savings analyses of Rothfeld *et al.* [3], which makes heavy use of said MATSim-UAM [72]. Finally, a list of limitations and potential topics for further research and some summarizing remarks, in Chapters 5 and 6 respectively, conclude this dissertation.

2 The MATSim Framework

As previously discussed, MATSim is an open-source, research-driven, multi-agent transport simulation framework that evolved as a joint project between Eidgenössische Technische Hochschule Zürich and Technische Universität Berlin [54]. By now, MATSim is entirely written in the object-oriented Java programming language and provides the ability to perform mesoscopic transport simulations to the general public.

2.1 Core Concepts

In MATSim, an agent- and activity-based transportation framework, persons are represented as agents that—throughout a simulated day—perform a plan of daily activities. While MATSim is not limited to simulating a singular day, it is MATSim's default behaviour that is being used almost exclusively. By including many agents, each of which has their own plan and behaviour, that share common resources (e.g. road capacity), the multi-agent system is able to "describe macroscopic phenomena as a result of many microscopic (inter-)actions" [73, p. 16]. Each agent's plan describes a "chain of activities (e.g. home–work–shop–home), including their locations and end times", as Ziemke *et al.* [74] explain. Since, commonly, each activity is based at a different location than the previous one (e.g. home-work), the need arises for each agent to travel in-between the activities' locations—generating the to-be-simulated trips. Collectively, all agents' plans represent the input population, i.e. the initial demand, which constitutes the starting point of the so-called MATSim execution loop depicted in Figure 2.1.

Besides the initial demand, each MATSim scenario, i.e. a complete set of input files that allow the simulation of a specific study area, also requires a transport network. For MATSim, these networks typically represent road and rail infrastructure that provides the agents with the ability to traverse in-between activity locations. Rieser *et al.* [75] and Neumann and Zilske [76] outline different ways to create such input networks for

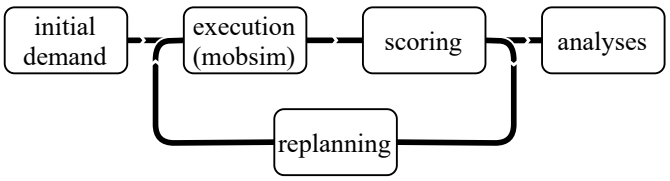

Figure 2.1: MATSim execution loop (based on [55, p. 4]).

Figure 2.2: Exemplary MATSim simulation of Munich with road and rail infrastructure and travelling agents (black triangles) visualised with Simunto Via.

MATSim, which—most commonly—are conversions of OpenStreetMap data. As Rieser *et al.* [77, pp. 14] describe, MATSim networks consist of nodes and links, each with their own set of variables. Nodes define specified locations by providing longitudes, latitudes, and—optionally—elevations of points within any given study area. Links are directed connections between two such nodes and provide traffic-related information such as the link's (hourly) vehicle capacity, the maximum (i.e. uncongested free-flow) vehicle speed, and a list of transport modes that are permitted to use that link. Using nodes and links together allows for the representation of sophisticated, multimodal transport networks, as illustrated in Figure 2.2, and conceptionally stems from the previously-discussed space syntax introduced by Hillier and Hanson [49].

The before-mentioned MATSim execution loop (see Figure 2.1) consists of three recurring steps that constitute MATSim's core functionality: (1) the mobility simulation (mobsim), (2) scoring, and (3) replanning. As described by Rothfeld *et al.* [78], "the mobility simulation executes each agent's plan using the provided transport network." The predominant way of controlling the order and amount of agents that can pass through links in MATSim is the so-called Queue-based Simulation (QSim). QSim uses queues, where the first agent to enter a link is also the first to exit (FIFO), to track and move agents throughout the network for every time step of the simulation. By default, MATSim does not include microscopic traffic behaviour such as, for example, overtaking. If the number of agents that traverse a particular link in a given time frame exceeds that link's capacities, then succeeding agents have to wait until spare capacity is—once more—available for that link. The potential wait of those succeeding agents increases their experienced travel times and, as such, embody emerging traffic congestion. During this mobility simulation, each event (e.g. an agent entering/leaving a link or starting/ending an activity) is being recorded and stored by MATSim, allowing for in-depth post-simulation analyses of each agent's itineraries. Rieser *et al.* [77], [79] provide further detail on MATSim's QSim and MATSim events.

After the mobility simulation, each agent's executed plan is given a utility score during the so-called scoring phase (cf. Figure 2.1). This artificial score rises or falls depending on

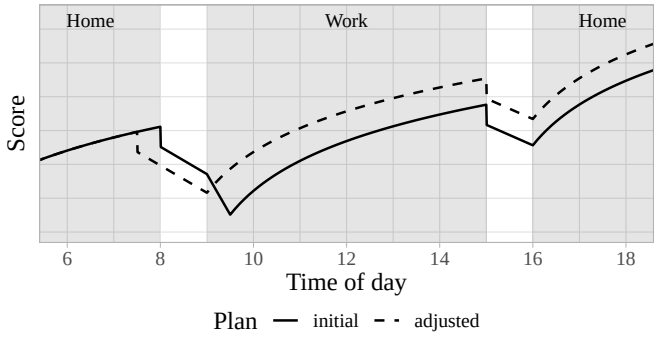

Figure 2.3: Exemplary MATSim score development of an agent's initial and adjusted plan throughout a simulated day, which includes planned home and work activities (based on [80]).

that plan's simulated performance, as explained in detail by Nagel *et al.* [80]. Commonly, time spent doing any activity increases a plan's score while travelling has a negative effect. Each mode and activity has their own set of scoring parameters, i.e. (dis-)utility values, within MATSim that specify how much, e.g., a minute of walking or driving influences a plan's overall score. It is important to note, however, that a plan's score by itself cannot be seen as a indicator for its performance, yet only becomes meaningful once it is compared to other plans' scores. Figure 2.3 illustrates the course of two exemplary home-work-home plans throughout a simulated day. At the start of the simulation the agent is at home (i.e. pursues the home activity). Consequently, due to the agent performing an activity, that plan's score rises—though, with diminishing marginal increases in utility. Once the agent ends their activity and commences their morning commute, the score decreases as travelling is commonly seen as a disutility. In the example of the initial plan in Figure 2.3, the agent expects a one-hour commute to work. Due to traffic congestion, which might occur during mobility simulation, the agent arrives at work 30 minutes too late—leading to a stark drop in the plan's score, before recovering during the following work activity. The score value at the end of the simulated day is stored as each plan's overall score.

Once the mobility simulation and scoring has been completed, agents are given the chance to adjust their plans during the so-called replanning phase (cf. Figure 2.1) as to increase their plans' scores. During this phase, agents' plans are altered via—so-called—innovative strategies which change details of one or more plan elements, such as changing the mode, departure time, or route of a trip within said plan (see [81]). In the following MATSim iteration, this altered plan is simulated and scored, in hopes of achieving a higher score than the initial plan. For each agent, a predefined number of plans can be stored that are generated, simulated, and scored during a MATSim run that, in itself, involves many such iterations. However, not all agents are set to adjust their plans for each iteration. Based on a predefined share, a random sample of agents is newly selected for each iteration that may alter their plans with said innovative strategies. The remaining majority of agents follows non-innovative strategies, which, e.g., instruct the

agent to select the best scoring plan (either directly or based on probabilities) out of the already-scored plans for that agent without modifying them. While this method, of allowing innovative strategies for a minority of agents, increases the number of required iterations, it prevents oscillation. The number of MATSim iterations is usually set by trial and error or through expert experience so that the systems nears "a Nash equilibrium-like state" [78], i.e. until the marginal increase in agents' scores has sufficiently diminished. Further, for the last iterations, all innovative strategies are shut-off to ensure score and plan convergence. In the above-illustrated example of Figure 2.3, an adjusted plan is shown with an earlier home departure so that the agent arrives at their work activity on time—thus, achieving a higher score at the end of the simulated day.

2.2 Dynamic Transport Services

By default, MATSim provides transport modes such as car, walking, cycling, and—after the inclusion into MATSim's core functionality—also PT. Dynamic, i.e. on-demand, services, however, require use of the DVRP extension by Maciejewski [57], which—among other things—is capable of "monitoring the simulation state (e.g., movement of vehicles)", "computing schedules for drivers/vehicles", and "coordinating interaction/cooperation between drivers, passengers and dispatchers" [57, p. 146]. With DVRP, vehicles with dedicated drivers can be defined that move within the MATSim simulation, based on a dynamically-adjusted schedule, and are able to pick-up and drop-off passengers. For said schedules, DVRP provides four states: (1) unplanned, where no (pick-up) tasks have yet been recorded for the vehicle, (2) planned, (3) started, where one of the planned tasks has been started, and (4) completed, once all tasks are performed [57, p. 147]. An agent's transport request is received by DVRP's optimizer that then dispatches an available driver to said agent by adjusting that driver's schedule and by using least-cost path routing.

With that, DVRP provides the basic elements for on-demand transport services such as taxis, autonomous shuttles, and—eventually—for the modelling of UAM services. First MATSim-based UAM modelling approaches were presented by Balać *et al.* [9] and Rothfeld *et al.* [78]. These early developments were further developed and later packaged into what has been named MATSim-UAM [72], the UAM-extension. This extension was used in UAM transport and demand analysis studies for Sioux Falls, United States ([7]), Zurich, Switzerland ([26]), and Munich, Germany ([24], [82]), before being used recently for the comparative UAM travel time savings study [3] which compares potential UAM implementations in Munich Metropolitan Area, Île-de-France, and San Francisco Bay Area. The following describes the functioning and usage of MATSim-UAM [72], while providing additional analyses and discussions.

3 UAM Modelling Framework

The development of the UAM-extension for MATSim began as a collaboration between Bauhaus Luftfahrt e.V., the Eidgenössische Technische Hochschule Zürich, and the Technical University of Munich and has since been published as an open-source project under GPL-3.0 license [72]. The main contributors are Raoul Rothfeld, Miloš Balać, and Aitan Militão. The following feature discussion and documentation refers to MATSim-UAM v2.1 as of September 2020 made available via GitHub [72]. For archival purposes, a compressed ZIP file of this version's source code is attached to this document[1].

3.1 Requirements & Implementation

Both, the extension's requirements and their implementations have been identified and developed in an iterative process, allowing for frequent changes and adaptions. Even though the modelling approach remained unchanged, most implementations have been revised or amended since the UAM-extension was first described by Rothfeld *et al.* [78] in 2018.

3.1.1 System Requirements

In accordance with MATSim's mesoscopic approach and UAM's infrastructure-based operation, the UAM-extension was conceptualised with the requirement of providing the following four aspects: (1) stations, (2) flight paths, and (3) vehicles in combination with (4) an on-demand operational model.

Stations. Dedicated stations for VTOL operation constitute the main ground infrastructure requirement for an UAM transport system. These UAM stations provide an interface between ground-based (i.e. walk, bike, car, and PT) and aerial modes of transportation. Thus, they must allow agents to change to and from UAM as a mode, which in itself might take a certain amount of time—regardless of whether one considers potential passenger processes, such as security checks. Each station's primary property, however, is its location and connection to, both, the road and flight path networks. Especially, since a UAM station's accessibility is primarily defined by its network centrality for car access, the density and proximity of public transport stations for PT access, and the

[1] Accessing the attached file might require dedicated PDF software that supports attachments. For security reasons, most PDF suites require manual white-listing of ZIP attachments before being able to access them.

density and proximity of trip origins and destinations for soft mode (i.e. walk, bike) access.

Flight paths. A dedicated flight path network—connecting all UAM stations—defines the possible, traversable routes for simulated agents. While low-altitude, short-range flights—as expected for UAM flights—are often performed using Visual Flight Rules (VFR), routed flight plans using Instrument Flight Rules (IFR) are the convention for commercial aviation. Thus, besides beeline flight connections, i.e. Euclidean shortest paths, UAM flight paths are also required to enable routed flight plans. With that, UAM flight paths must provide a combination of waypoints and connecting paths. While waypoints merely require a location, paths are defined by a flight level and which waypoints are being connected. Further, measures for vertical and horizontal aircraft separation must be provided.

Vehicles. Next, UAM vehicles are required that operate to and from the above-described stations using those just-mentioned flight paths. Each vehicle is assumed to be VTOL-capable with at least two distinct flight phases: (1) vertical take-off/landing and (2) cruise flight. For all phases, different travel speeds have to be provided. Further, each UAM vehicle must provide a maximum passenger capacity and durations for vehicle-specific processes, such as (de)boarding and Turnaround Time (TAT) (i.e. the time required between landing and being ready to take-off again). Since an aircraft's operational range is a fundamental property, UAM vehicles are also required to provide a maximum distance for singular legs.

On-demand operation. Finally, an on-demand operational model combines UAM stations, flight paths, and vehicles as to provide UAM as a mode of transportation. UAM being operated on-demand indicates that UAM vehicle are only dispatched upon passenger transportation being requested—in contrast to, say, scheduled services where vehicles are dispatched and provide transportation regardless of whether the service is being used by passengers. For UAM, on-demand operation implies the availability of estimated total travel time and cost for potential passengers before making a UAM transport request as to allow for meaningful mode choice decisions or calculations during agent-based simulation. Upon receiving a transport request, a suitable UAM vehicle is reserved for said request and, if necessary, dispatched to the passenger's origin UAM station. There, the passenger can board the UAM vehicle and be flown to the passenger's requested destination station. After landing and passenger deboarding, the UAM vehicle awaits further requests.

3.1.2 Operational Modelling & Functioning

The different operational aspects of the developed UAM system can be subdivided into four main parts: UAM passenger (1) routing and (2) process and waiting times, and UAM vehicle (3) flight segments and (4) dispatching.

Routing. Within the UAM-extension, routing describes the process of providing the following items to a UAM passenger request: a UAM origin station, a (routed) path thereto with a respective access mode, a UAM destination station, a (routed) flight path thereto, and a (routed) path from said destination station to a passenger's final destination with a respective egress mode. The current, default UAM intermodal routing implementation[2] does this with cached, i.e. pre-calculated, flight paths. Instead of re-identifying the least-cost paths for all origin and destination station pairs per request, all possible flight connections are being routed once at the beginning of the MATSim simulation and stored for later use. For the current implementation, the cost of a route is defined as its total travel time.

Route caching saves significant computation time but leads to all flights between two stations always taking the same path—regardless of potential congestion on any given flight link. This trade-off, between computation time and within-day re-routing, can be made if one assumes aerial en-route congestion to be too rare of an occurrence to warrant the inclusion of its impacts. An alternative implementation[3] provides within-day re-routing for the price of higher computational requirements and would have to be manually enabled within the UAM routing module provider[4]. Both provided routers are parallelized, i.e. multiple instances can be run simultaneously to make use of multi-core computers and drastically reduce computation time. By using this routing module provider, additional routers can be developed and used for simulation given that those also implement MATSim's own routing module interface.

Once a plan contains a UAM leg, either predefined or appointed via MATSim's mode choice module, the UAM intermodal router splits the leg into multiple stages, as illustrated in Figure 3.1. An initial plan only defines the leg's mode as UAM. The UAM router first creates three sub-legs with an access, a flight, and an egress leg. The access and flight legs are spatially connected at a to-be-selected origin station. Similarly, the same applies for the flight and egress legs being joined at the destination station. In compliance with MATSim's plan definition, which requires activities and legs to occur alternately, the final routed UAM plan additionally inserts UAM interactions between the different sub-legs. Those interactions represent the agent (de)boarding a UAM vehicle. Based on a user-selected routing strategy, the intermodal router provides the required combination of access mode, origin station, destination station, and egress mode. Currently, four routing strategies are provided that can be utilised as shown in Listing 3.4 (see page 39):

- Total travel time minimisation
- Access and egress travel time minimisation
- Total distance minimisation
- Access and egress distance minimisation

[2] See net/bhl/matsim/uam/router/UAMCachedIntermodalRoutingModule.java; this and all following file paths refer to MATSim-UAM v2.1 available via GitHub [72].
[3] See net/bhl/matsim/uam/router/UAMIntermodalRoutingModule.java
[4] See net/bhl/matsim/uam/router/UAMRoutingModuleProvider.java

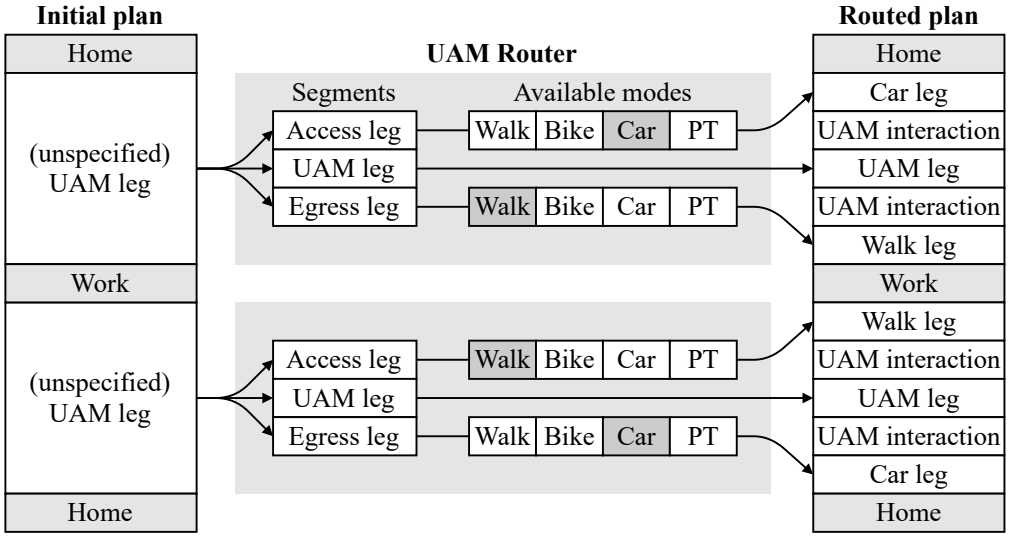

Figure 3.1: Plan modification by UAM-extension's intermodal router, inspired by Rieser [58, p. 88], based on Rothfeld *et al.* [78].

During simulation, the chosen strategy is then provided by the strategy router[5]. Dependent on the strategy's goal, the optimum combination of accessible origin and destination stations and available access and egress modes is identified per UAM request.

Accessibility to potential origin and destination stations is defined by whether their Euclidean distance to the agent's actual origin and destination, respectively, is equal to or less than a predefined search radius. This behaviour is described as using a static search radius, as the radius is always of the same size regardless of the underlying trip's distance. Additionally, the search radius can be set dynamically, where—instead of a fixed distance as radius—a ratio can be provided. This ratio then defines the maximum percentage that the access and egress distance—each independently—might have, when compared to the trip's total Euclidean distance. A similar dynamic UAM search radius behaviour was initially described by Pukhova [20, pp. 34] and later adapted, implemented, and used by Rothfeld *et al.* [3].

Availability of UAM access and egress modes is defined via the scenario configuration. The user has to explicitly list the modes that are supposed to be available for UAM station access and egress. An configuration file example is shown with Listing 3.4. Further, both access and egress mode selections are conducted independently from each other as well as from later UAM trips made by the same agent. That is to say that the selected access mode has no impact on the selection of an egress mode—also not for otherwise chain-based based modes—and may be inconsistent over, e.g., an agent's round-trip. The assumption has been made, that UAM might be accessed primarily via shared, on-demand mobility services such as bike-sharing and ride-hailing which allows for such freedom in access/egress mode selection. While the current intermodal routers

[5] See net/bhl/matsim/uam/router/strategy/UAMStrategyRouter.java

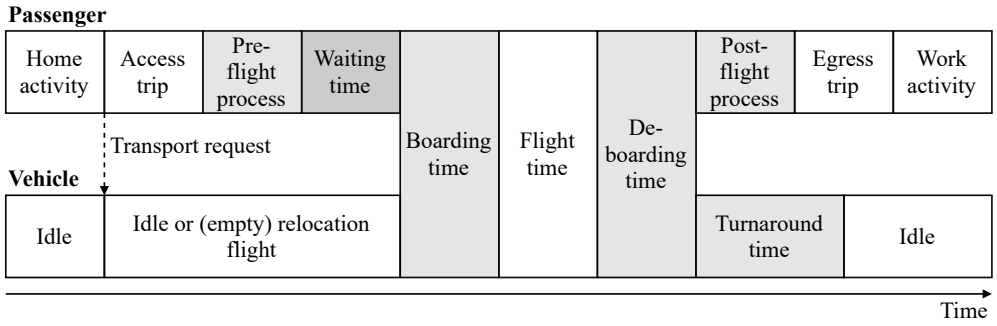

Figure 3.2: Time sequence of passenger and on-demand vehicle processes, including static times (i.e. pre-flight, boarding, deboarding, post-flight) with pre-defined durations and potential dynamic waiting time, based on Rothfeld *et al.* [82].

allow walk, bike, car, and PT as UAM access/egress modes, these modes—especially car—should be understood as representing the general transport mode more than private ownership. Lastly for access and egress mode selection, if walk is an available access/egress mode and the Euclidean access/egress distance to/from a UAM station is less than a predefined threshold, only walking will be available as access/egress modes to/from said stations.

Additionally to the before-mentioned strategies, a so-called predefined option exists as well, which disables extension-internal routing but utilizes routing information that needs to be provided within each agent's plan. See Listing 3.10 on page 45 for an example on how to provide said information within a plans file. Finally, if no predefined routing is given or a selected strategy fails to provide a UAM route, e.g. because no stations are within the search radius, the UAM intermodal router defaults to a non-UAM walking trip. In this case, the agent is expected to deselect the unfulfilled UAM plan in later MATSim iterations.

Process & waiting times. As mentioned, a routed UAM plan consists of an access, a flight, and an egress leg—each separated by UAM interactions which represent passenger (de)boarding a UAM vehicle. For UAM vehicles, there is one more static process time, TAT as illustrated in Figure 3.2, which represents the time required to, e.g., re-fuel, re-charge, or clean the vehicle before it can take off again. All static process times are defined via MATSim user input with Listing 3.3 providing an example thereof.

In addition to (de)boarding, UAM passengers undergo additional statically-defined processes before and after flights, i.e. pre- and post-flight process times. Both pre- and post-flight processes are solely modelled with predefined durations. They are intended to be used for representing the time passengers needs from reaching their origin UAM stations until they are able to board a vehicle for pre-flight times and vice versa for the post-flight equivalent. Thus, those process times can be used to represent time required for the passenger to walk through the station or to pass a security screening. Since the

security requirements for actual UAM flights have yet to be defined, the modelled process time definitions remain purposefully vague.

The sole process time that is dynamically calculated, rather than statically defined, is the passenger's potential waiting time. Passengers have to wait, if—during simulation—they arrive at their origin stations and complete their pre-flight process time before a UAM vehicle becomes available at their station. This waiting time is being tracked per station and averaged in time bins over all previous iterations of the same simulation. For UAM waiting time bin size, MATSim's core time bin size for travel time calculations is used. The default travel time bin size is 900 seconds (i.e. 15 minutes). Bin size can be changed, though, via the travel time bin size parameter, which is one of travel time calculator's settings within the conventional MATSim input configuration. These stored waiting times[6] then influence future iterations' travel time predictions. Since there can be no waiting data from previous iterations during simulation initialisation (i.e. the zeroth iteration), a default waiting time can be defined which is used in this case.

Except for boarding, flight, and deboarding, the passenger and UAM vehicle agents move independently from each other within the simulation. For example, the vehicle can still be undergoing its TAT while the passenger already embarks on their egress leg as shown in Figure 3.2. From the beginning of boarding until the end of deboarding, however, the passenger and the respective UAM vehicle are synchronised—representing the passenger sitting within the vehicle. Until the passenger debarks the UAM vehicle, only the vehicle is being simulated within MATSim and undergoes the various flight phases.

Flight segments. The four above-listed strategies (see page 29) all strive to minimise either distance or travel time. Both distance and travel time minimisations are based on the routed access, egress, and flight paths. All UAM travel times are based on the routed path's link distances and speeds are calculated by a dedicated UAM link speed calculator[7]. This dedicated speed calculator ensures correct UAM vehicle speeds according to the vehicle's current flight segment and the links maximum speed (i.e. MATSim's so-called freespeed). Since each UAM vehicle has its own maximum cruise and VTOL speeds (see Listing 3.3), the UAM link speed calculator returns the maximum allowed UAM travel speed based on the the link's and vehicle's flight segment-specific speed limits, i.e. returns the lowest one. Currently, two flight segments are modelled:

- Vertical flight: Representing both vertical take-off and landing.
- Horizontal flight: Representing level cruise flight.

Figure 3.3 illustrates how those two flight segments can be used to model a simplistic flight profile. However, there is no pre-defined or required order of vertical and horizontal flight segments. Thus, using alternating flight segments allows for more elaborate flight profiles to be modelled in order to, e.g., model flight level changes or airspace restrictions.

[6] See net/bhl/matsim/uam/data/WaitingData.java
[7] See net/bhl/matsim/uam/qsim/UAMLinkSpeedCalculator.java

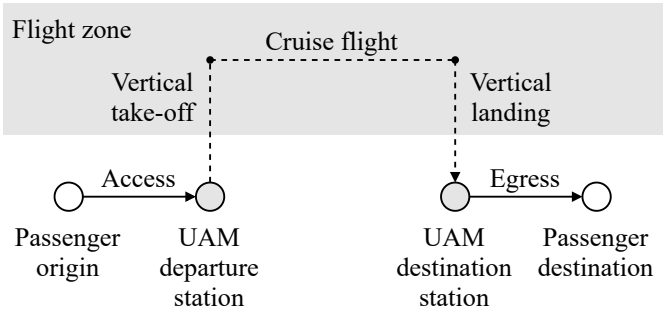

Figure 3.3: Side view of an exemplary UAM trip with access leg, flight segments, and egress leg, based on Balać *et al.* [26].

Listing 3.9 on page 43 illustrates how to define UAM links for either flight type. Additionally, all available flight segments are defined by and accessible via a flight segment container[8]. These flight segments can be extended to contain any number of flight phases, such as climb or descent with links of their own types.

Dispatching. In contrast to routing, which provides the passenger's UAM-including trip with station selection and access and egress modes, dispatching denotes the allocation and—if necessary—sending out of vehicles for passenger requests. The implemented UAM vehicle dispatcher makes use of MATSim's so-called Dynamic Vehicle Routing Problem (DVRP) contribution, created by Maciejewski [57]. With the DVRP extension, each UAM vehicle acts as an agent following a schedule that is dynamically created and altered during the simulation, i.e. throughout the simulated day, by a central vehicle manager[9]. By making use of within-day re-scheduling of vehicles, these vehicles can respond to dynamic passenger transport requests even though the underlying functioning of those vehicles is schedule-based. Based on DVRP, five possible schedule tasks have been defined for UAM vehicles, which can also be seen in Figure 3.2:

- Stay task: The default task with which each UAM vehicle's schedule is initialised and instructs the vehicle to remain idle at the current location.
- Pick-up task: Instructs the vehicle to shortly remain idle at an origin station for passenger boarding to occur.
- Fly task: Instructs the vehicle to fly from one UAM station to another, with passengers or without (relocation flight).
- Drop-off task: Instructs the vehicle to shortly remain idle at a destination station for passenger deboarding to occur.
- Turnaround task: Instructs the vehicle to remain idle at a destination station after passenger deboarding.

[8] See net/bhl/matsim/uam/router/UAMFlightSegments.java
[9] See net/bhl/matsim/uam/dispatcher/UAMManager.java

The currently implemented default UAM vehicle dispatcher[10] allocates vehicles based on pooling possibility, temporal availability, vehicle type suitability, and spatial proximity in the presented order. Passenger requests are recorded once an agent begins their trip towards a UAM station, i.e. departs from a previous activity with the intent to use UAM, as indicated in Figure 3.2. This request mainly provides the passenger's origin and destination UAM stations and the estimated time of arrival at the origin station. Upon receiving a request, the vehicle managers coordinates the provision of a suitable vehicle or, in case no suitable vehicle is available, defers the request—in order to retry fulfilment at a later point in time when suitable vehicles might, once again, be available.

For each request, the mentioned default dispatcher first queries for vehicles that allow flights to be pooled, i.e. for vehicles that are already reserved by other passengers for the same combination of origin and destination UAM stations and have capacity for more passengers. If such a reservation is found, the passenger requests are combined for a pooled, i.e. shared, UAM flight. Else, all currently idle vehicles, of vehicle types that have sufficient range for the given passenger request (i.e. whose defined range is equal to or greater than the summed distance of VTOL and horizontal flight segments), are available. Out of those, the closest vehicle, based on the vehicle's Euclidean distance to the requested origin station, is allocated to fulfil the respective passenger's request. In case the allocated vehicle is not already at the requested station, the vehicle is dispatched on an empty relocation flight towards said origin station. In conclusion, the first-available, closest vehicle with sufficient range is selected if no other vehicle is already reserved for the same itinerary.

An alternative dispatcher[11] differs to the before-mentioned order of vehicle selection in that it checks for the possibility of creating a pooled flight only if no currently unreserved vehicle is available. In other words, the default dispatcher prefers pooling passengers over providing individual non-shared flights, while the latter does the opposite in this regard. Additional or alternative dispatchers can be developed using the UAM-dispatcher interface[12] and can be provided within the UAM-extension's QSim module[13].

3.2 Documentation & Usage

The following section describes how to retrieve, use, and configure the MATSim-UAM [72] extension (v2.1). To best understand the input formats and usage description, having a solid understanding of base MATSim and its input/output file formats and structures is strongly recommended. See Horni *et al.* [54] in general and Rieser *et al.* [77] in particular for guidance on the basics of using MATSim.

[10] See net/bhl/matsim/uam/dispatcher/UAMClosestRangedPreferPooledDispatcher.java
[11] See net/bhl/matsim/uam/dispatcher/UAMClosestRangedPooledDispatcher.java
[12] See net/bhl/matsim/uam/dispatcher/UAMDispatcher.java
[13] See net/bhl/matsim/uam/qsim/UAMQsimModule.java

3.2.1 Installation

The default approach for using MATSim-UAM [72] is cloning it from its online GitHub repository in order to have an up-to-date local copy of its source code. Alternatively, as has been done by Ploetner *et al.* [24], MATSim-UAM [72] can also be integrated in existing programming projects using the online project dependency management tool, Apache Maven [83]. MATSim and the UAM-extension also use Maven for internal management of their own dependencies to other third-party programmes and libraries. The dependencies of any Maven project are specified within its Project Object Model (POM) file in Extensible Markup Language (XML) format. The Apache Software Foundation [84] provides more information on the purpose and structure of POM files.

```
1     <repository>
2     <id>jitpack.io</id>
3     <url>https://jitpack.io</url>
4     </repository>
```

Listing 3.1: Required repository information to be added to a Maven project's POM file to allow for MATSim-UAM [72] usage.

For using MATSim-UAM [72] within a Maven project, the repository information as shown in Listing 3.1 must be added to the POM's repositories section. JitPack, as mentioned in Listing 3.1, is a web service that automates the provision of GitHub repositories as Maven dependencies. Once JitPack is listed as a repository, MATSim-UAM [72] itself can be added as one of the dependencies as shown in Listing 3.2. Calling upon the so-called `master-SNAPSHOT` version will retrieve the latest version of MATSim-UAM [72]. If a specific (former) version is desired, then the version can be changed to any of the tagged versions, such as `v2.0` or `v1.1`.

```
1 <dependency>
2  <groupId>com.github.BauhausLuftfahrt</groupId>
3  <artifactId>MATSim-UAM</artifactId>
4  <version>master-SNAPSHOT</version>
5 </dependency>
```

Listing 3.2: Required dependency information to be added to a Maven project's POM file to allow for MATSim-UAM [72] usage.

Once the repository is either cloned or provided via Maven, it can be used to run MATSim simulations or travel time calculations including UAM as a mode of transportation.

3.2.2 UAM-specific Input Files

A base MATSim scenario consists of, at a minimum, its configuration, its network, and its population—as described by Rieser *et al.* [77]. Further MATSim data containers for input

information on, e.g., facilities or person attributes are also described by Rieser *et al.* [85]. All MATSim data containers adhere to the same XML file type and general, hierarchical structure. Thus, all UAM input parameters, stations, and vehicles are defined using a similar structure. A UAM-enabled MATSim scenario must include (1) a dedicated UAM stations and vehicles file in XML format, (2) a UAM module within the MATSim configuration, and (3) links that list UAM as an allowed mode within the MATSim network.

UAM stations & vehicles file. As listed in the system requirements (Section 3.1.1), the UAM-extension must allow for the definition of UAM stations and vehicles. For this purpose, a dedicated XML file has been introduced, which is being parsed by a specifically designed XML reader[14]. The content of such a UAM stations and vehicles XML file—called UAM file in short—must be structured according to the accompanying Document Type Definition (DTD) file[15]. The DTD file lists all required and optional XML elements and defines their hierarchy.

Following an initial definition of the XML document type, version, encoding, and DTD path, any UAM XML file must provide a single parent `uam` element which contains one `stations`, one `vehicleTypes`, and one `vehicles` element. Each of those three sub-elements of `uam` can contain any number—also none—of their own respective sub-elements. An example UAM file is shown with Listing 3.3 on page 38. The `stations` element can contain `station` elements, which require (or allow) the following parameters in any order:

- Station identifier (name: `id`, type: `String`): Unique, usually short, identifier.
- Station link (name: `link`, type: `String`): Unique identifier of a network link at which the station is spatially located. The respective link must allow UAM as a mode.
- Pre-flight time (name: `preflighttime`, type: `double`): Static time needed by passengers from arriving at the station until they are ready for boarding in seconds.
- Post-flight time (name: `postflighttime`, type: `double`): Static time needed by the passengers from after deboarding until they leave the station in seconds.
- Default waiting time (name: `defaultwaittime`, type: `double`): Static, initial average waiting time for passengers at the given station in seconds. This default waiting time is being included in UAM trip duration estimations when no recorded waiting times are available from previous iterations (e.g. in the first, i.e. zeroth, iteration).
- Station name (name: `name`, type: `String`): Usually longer station name for easier identification or relation to points of interest within a scenario. Station names are not used during simulation and, thus, are optional.

[14] See net/bhl/matsim/uam/infrastructure/readers/UAMXMLReader.java
[15] See resources/dtd/uam.dtd

The `vehicleTypes` element can contain `vehicleType` elements, which require the following parameters in any order:

- Vehicle type identifier (name: `id`, type: `String`): Unique, usually short, identifier.
- Vehicle range (name: `range`, type: `double`): UAM vehicle's maximum flight range in the MATSim scenario's Coordinate Reference System (CRS) distance unit—usually metres or feet.
- Vehicle capacity (name: `capacity`, type: `int`): UAM vehicle's maximum passenger capacity, i.e. the vehicle's number of seats.
- Vehicle cruise speed (name: `cruisespeed`, type: `double`): UAM vehicle's cruise flight speed, used for horizontal flight segments in the scenario's CRS distance unit per second—usually metres or feet per second.
- Vehicle vertical speed (name: `verticalspeed`, type: `double`): UAM vehicle's vertical flight speed, used for vertical flight segments, i.e. take-off and landing, in the scenario's CRS distance unit per second.
- Vehicle boarding time (name: `boardingtime`, type: `double`): Static time needed before take-off for passengers to enter the UAM vehicle in seconds.
- Vehicle deboarding time (name: `deboardingtime`, type: `double`): Static time needed after landing for passengers to exit the UAM vehicle in seconds.
- Vehicle turnaround time (name: `turnaroundtime`, type: `double`): Static time needed after deboarding for the UAM vehicle to be available for, e.g., another boarding in seconds.

The `vehicles` element can contain `vehicle` elements, which require the following parameters in any order:

- Vehicle identifier (name: `id`, type: `String`): Unique, usually short, identifier.
- Vehicle type (name: `type`, type: `String`): Unique identifier of the respective vehicle type.
- Vehicle initial station (name: `initialstation`, type: `String`): Unique identifier of the respective UAM station at which the vehicle is placed at the beginning of each simulation's iteration.
- Operation start time (name: `starttime`, type: `String` in `hh:mm:ss` format): Time of day after which the vehicle is allowed to operate.
- Operation end time (name: `endtime`, type: `String` in `hh:mm:ss` format): Time of day up to which the vehicle is allowed to operate.

With that, it is evident that the exemplary UAM file, as shown by Listing 3.3, defines two stations, `A` and `B`, that differ in their defined pre- and post-flight process times, the default waiting time, and their location within the MATSim network. Station `A`, for example, is defined with a pre-flight time of 15 minutes and a post-flight time of 5 minutes.

```
1  <?xml version="1.0" encoding="UTF-8"?>
2  <!DOCTYPE uam SYSTEM "src/main/resources/dtd/uam.dtd">
3
4  <uam>
5   <stations>
6    <station id="A" name="Alpha" preflighttime="900" postflighttime="
         ↪ 300" defaultwaittime="0" link="station_A_link"/>
7    <station id="B" name="Bravo" preflighttime="600" postflighttime="
         ↪ 120" defaultwaittime="480" link="station_B_link"/>
8   </stations>
9   <vehicleTypes>
10   <vehicleType id="S" capacity="2" range="60000" cruisespeed="33.3"
         ↪ verticalspeed="10" boardingtime="30" deboardingtime="30"
         ↪ turnaroundtime="120"/>
11   <vehicleType id="L" capacity="4" range="30000" cruisespeed="22.2"
         ↪ verticalspeed="8" boardingtime="60" deboardingtime="60"
         ↪ turnaroundtime="300"/>
12  </vehicleTypes>
13  <vehicles>
14   <vehicle id="S-A" type="S" initialstation="A" starttime="00:00:00"
         ↪  endtime="24:00:00"/>
15   <vehicle id="S-B" type="S" initialstation="B" starttime="00:00:00"
         ↪  endtime="24:00:00"/>
16   <vehicle id="L-A" type="L" initialstation="A" starttime="05:00:00"
         ↪  endtime="21:00:00"/>
17   <vehicle id="L-B" type="L" initialstation="B" starttime="05:00:00"
         ↪  endtime="21:00:00"/>
18  </vehicles>
19 </uam>
```

Listing 3.3: Exemplary UAM stations and vehicles XML file.

This exemplary UAM file also provides two vehicles types, `S` and `L`, with type `S` representing a smaller (i.e. lower capacity), faster (i.e. higher cruise and vertical speed), and further flying (i.e. higher range) UAM vehicle type. Assuming a metre-based MATSim scenario, then this `S` vehicle type is defined with a 60 km range at roughly 120 km/h cruise flight speed. Further, the small vehicle type also requires less time for (de)boarding (i.e. 30 seconds each) and turnaround (i.e. two minutes). Vehicle type `L`, on the other hand,

represents a larger vehicle type with higher passenger capacity but shorter range, slower flight speeds, and longer process times. Finally, per vehicle type, two UAM vehicles are defined, with each type's vehicles being uniformly distributed over the two UAM stations. Assuming that the simulation is defined to simulate 24 hours, then both vehicles of type `S`, i.e. vehicles with identifiers `S-A` and `S-B`, are operational for the whole simulated day. Both vehicles of type `L`, on the other hand, are operational only for a restricted time frame between 5 a.m. and 9 p.m. While two stations and one vehicle of one vehicle type are the minimum requirements for UAM to be operational, there is no upper limit for the number of stations, vehicle types, or vehicles.

UAM-enabled configuration. Following the UAM vehicle input file, two types of additions to the base MATSim configuration are required for using UAM: the addition of (1) a UAM module and (2) defining parameters for UAM-related activities and modes. Firstly, a novel UAM configuration module[16] has been defined and must be added to a non-UAM configuration. This UAM module is used to define the main behaviour and settings of UAM as a transportation mode within a MATSim simulation, such as the available modes for accessing UAM stations or the routing strategy. An exemplary UAM module is shown in Listing 3.4.

```
1  <module name="uam">
2   <param name="inputUAMFile" value="uam.xml" />
3   <param name="availableAccessModes" value="car,walk" />
4   <!-- available modes: car, pt, bike, walk -->
5   <param name="routingStrategy" value="mintraveltime" />
6   <!-- available strategies: mintraveltime, minaccesstraveltime,
        ↪ mindistance, minaccessdistance, predefined -->
7   <param name="parallelRouters" value="8" />
8   <!-- optional, default: 2 -->
9   <param name="staticSearchRadius" value="true" />
10  <!-- optional, default: true -->
11  <param name="searchRadius" value="100000" />
12  <!-- optional, default: 5000 -->
13  <param name="walkDistance" value="300" />
14  <!-- optional, default: 500 -->
15  <param name="ptSimulation" value="true" />
16  <!-- optional, default: true -->
17 </module>
```

Listing 3.4: Exemplary UAM configuration module as part of a MATSim configuration file.

The UAM module, as part of a larger MATSim configuration file, requires (or allows) the following parameters:

[16] See net/bhl/matsim/uam/config/UAMConfigGroup.java

- Input UAM file (name: `inputUAMFile`, type: `String`): Starting from the configuration file itself, relative path to the input UAM vehicles and stations XML file.

- Available access and egress modes (name: `availableAccessModes`, type: `String`): Comma-separated list of non-UAM modes available for access to and egress from UAM stations, as described in Section 3.1.2. The desired option(s) must be one or more of the available modes shown in Listing 3.4: `car`, `pt`, `bike`, and/or `walk`.

- Routing strategy (name: `routingStrategy`, type: `String`): Goal of the routing optimization towards, e.g., minimizing overall travel time, as described in Section 3.1.2. The desired option must be one of the available ones shown in Listing 3.4 (case-insensitive): `mintraveltime` (i.e. minimize overall trip's travel time), `minaccesstraveltime` (i.e. minimize access and egress legs' travel times), `mindistance` (i.e. minimize overall trip's routed travel distance), `minaccessdistance` (i.e. minimize access and egress legs' routed travel distance), or `predefined` (i.e. use input routing, see Listing 3.10 on page 45).

- Number of parallel routers (name: `parallelRouters`, type: `int`): Defines the number of parallel UAM path-finding routers, which must be larger than zero and is recommended to be equal to the number of threads used for the MATSim simulation in general, i.e. the number of available CPUs, cores or logical processors. If not provided, defaults to two.

- Use static search radius (name: `staticSearchRadius`, type: `boolean`): True or false switch for using static or dynamic search radii, respectively, as described in Section 3.1.2. If not provided, defaults to true.

- Search radius (name: `searchRadius`, type: `double`): If static search radii are used, then search radius defines the size (i.e. radius) of the circular area around agents' origins and destinations for UAM stations look-up in the MATSim scenario's CRS distance unit. If not provided, defaults to 5000. Else, if dynamic search radii are used, then search radius defines the ratio of the maximum-allowed access and egress Euclidean distance over the overall trip Euclidean distance—though, both access and egress are considered separately, as described in Section 3.1.2.

- Default-to-walking distance (name: `walkDistance`, type: `double`): If walk is an available access/egress mode, then walk will be the sole available access/egress mode for any given UAM station where the Euclidean access/egress trip distance is below this defined threshold distance in the MATSim scenario's CRS distance unit. If not provided, defaults to 500.

- Use PT simulation (name: `ptSimulation`, type: `boolean`): True or false switch for using simulated or teleported public transport, respectively. If not provided, defaults to true. Both, simulated and teleported PT are schedule-based but non-simulated PT cannot experience congestion and may reduce computational load. If

PT simulation is disabled, a parameter set for teleported PT must be provided as shown in Listing 3.5 below, else, if PT simulation is enabled, such a PT teleported mode parameter set must not be provided.

```
<module name="uam">
 <param name="inputUAMFile" value="uam.xml" />
 <param name="availableAccessModes" value="car,walk,bike,pt" />
 <param name="routingStrategy" value="mintraveltime" />
 <param name="ptSimulation" value="false" /> <!-- default: true -->
</module>
<!-- ... -->
<module name="planscalcroute">
 <parameterset type="teleportedModeParameters">
  <param name="mode" value="pt" />
  <param name="teleportedModeSpeed" value="10.0" />
  <param name="beelineDistanceFactor" value="1.0" />
 </parameterset>
</module>
```

Listing 3.5: Excerpt of a MATSim configuration file with UAM module that specifies PT to use schedule-based teleportation instead of actual simulated and the then required teleportation parameters for PT.

Besides the before-mentioned UAM module, a MATSim configuration also requires the definitions of UAM-related activities (i.e. UAM interactions) and modes (i.e. access/egress modes) as explained in Section 3.1.2. MATSim requires each occurring activity to be defined by activity parameters, even if an activity is not to be used for plan scoring. Thus, an activity parameter set has to be included in a configuration's plan score calculation module. A non-scoring example thereof is giving with Listing 3.6.

```
<parameterset type="activityParams">
 <param name="activityType" value="uam_interaction" />
 <param name="scoringThisActivityAtAll" value="false" />
</parameterset>
```

Listing 3.6: Example of non-scoring activity parameter set for UAM interaction.

Further, with the exception of PT, each possible access and egress mode requires dedicated mode parameter sets within the same plan score calculation module. Listing 3.7 shows two example non-scoring—i.e. all values are zero—parameter sets for access and egress by walking. These parameter sets have to be included for each mode that is available for station access/egress as defined in the UAM module (see Listing 3.4), except for PT. Non-zero values have to be inserted in each access/egress mode's parameter set to make meaningful use of MATSim's scoring functionality.

```
<parameterset type="modeParams" >
 <param name="constant" value="0.0" />
 <param name="marginalUtilityOfDistance_util_m" value="0.0" />
 <param name="marginalUtilityOfTraveling_util_hr" value="0.0" />
 <param name="mode" value="access_uam_walk" />
 <!-- provide also for: access_uam_car, access_uam_bike -->
 <param name="monetaryDistanceRate" value="0.0" />
</parameterset>

<parameterset type="modeParams" >
 <param name="constant" value="0.0" />
 <param name="marginalUtilityOfDistance_util_m" value="0.0" />
 <param name="marginalUtilityOfTraveling_util_hr" value="0.0" />
 <param name="mode" value="egress_uam_walk" />
 <!-- provide also for: egress_uam_car, egress_uam_bike -->
 <param name="monetaryDistanceRate" value="0.0" />
</parameterset>
```

Listing 3.7: Non-scoring example of mode parameter set for UAM access mode via walk.

Finally, for UAM access and egress trips via car to be simulated—and with that potentially be affected by congestion—car's access and egress modes must be included in the configuration's QSim module as main modes, as shown in Listing 3.8. Listing UAM car access/egress as main modes is not required, however, if omitted, agents would then be teleported instead of simulated on the road network. Thus, for more realistic (i.e. congestion including access/egress trips), it is recommended to include both UAM access and egress via car as QSim main modes.

```
<module name="qsim">
 <!-- ... -->
 <param name="mainMode" value="car,access_uam_car,egress_uam_car"/>
</module>
```

Listing 3.8: Non-scoring example of mode parameter set for UAM access mode via walk.

This concludes the required changes to enable a MATSim configuration to be used with MATSim-UAM [72]. These changes do not have to be made manually though; utility scripts are provided and discussed in Section 3.2.3.

UAM-enabled network. After providing a UAM stations and vehicles file and performing the required configuration changes, only the MATSim network remains to be updated to allow UAM movements. The UAM-extension makes use of MATSim's default network structure of property-defined nodes and links, as explained by Rieser *et al.* [77, pp. 14]. Links that allow UAM as an operating mode require UAM to be defined as

one of a link's modes (requirement of base MATSim) and require a type attribute specifying the link's UAM flight segment (requirement of MATSim-UAM [72]). As described in Section 3.1.2, currently two flight segment are implemented with `uam_vertical` (i.e. take-off and landing) and `uam_horizontal` (i.e. cruise flight). Listing 3.9 provides an example of UAM links with the required type attribute and conventional non-UAM links.

```
1  <link id="L1-2" from="N1" to="N2" length="250" freespeed="13.89"
       ↪ capacity="60.0" permlanes="1.0" oneway="1" modes="car">
2  </link>
3  <link id="L2-3" from="N2" to="N3" length="1" freespeed="35" capacity
       ↪ ="999" permlanes="1.0" oneway="1" modes="car,uam">
4   <attributes>
5    <attribute name="type" class="java.lang.String">uam_vertical</
         ↪ attribute>
6   </attributes>
7  </link>
8  <link id="L3-4" from="N3" to="N4" length="600" freespeed="35"
       ↪ capacity="999" permlanes="1.0" oneway="1" modes="uam">
9   <attributes>
10   <attribute name="type" class="java.lang.String">uam_vertical</
         ↪ attribute>
11  </attributes>
12 </link>
13 <link id="L4-5" from="N4" to="N5" length="5000" freespeed="35"
       ↪ capacity="999" permlanes="1.0" oneway="1" modes="uam">
14  <attributes>
15   <attribute name="type" class="java.lang.String">uam_horizontal</
         ↪ attribute>
16  </attributes>
17 </link>
```

Listing 3.9: Exemplary UAM links with flight segment type definition.

Combined, the links shown in Listing 3.9 illustrate how to integrate a UAM network into a conventional, i.e. base MATSim, network. Since there is no difference between conventional and UAM nodes, they are omitted from the above listing. Link `L1-2`, connecting node `N1` to node `N2`, represents a conventional car link. The following link though, i.e. Link `L2-3`, allows usage by both UAM and car and, since it allows UAM usage, must provide the `type` attribute. Link `L2-3` represents the bridge between car-only and UAM-only network parts (as illustrated in Figure 3.4). In this regard, link `L4-5` continues on from link `L3-4` with type `uam_horizontal`, intended for cruise flight.

These example links represent the recommended approach for the integration of a UAM network into a base MATSim network, as illustrated in Figure 3.4. To enable transitions from car-usage to UAM, at least one link is required that connects car and UAM links

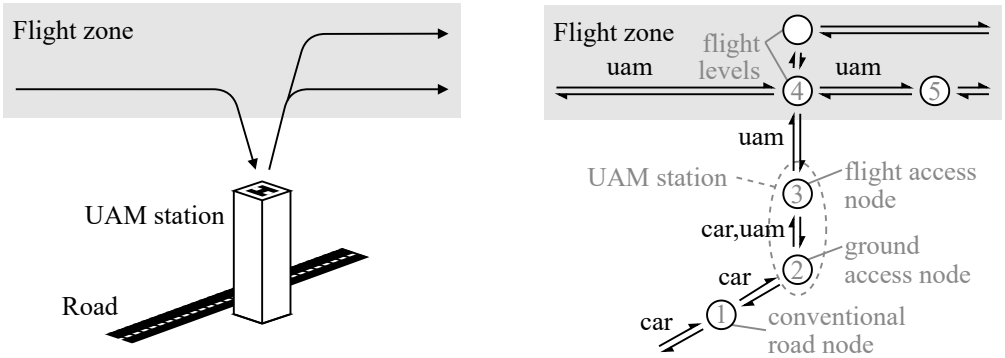

(a) Physical representation. **(b)** Network model.

Figure 3.4: Illustration of current UAM network encoding from physical representation to MATSim network model with exemplary nodes and directed links, adapted from Rieser [58, p. 71], based on Rothfeld *et al.* [78].

by allowing both modes. It is recommended to use these bridging links as the placement links for UAM stations within UAM XML files, as shown in Listing 3.3. Since MATSim is somewhat ambiguous with the start and end of trips, since trips originate from and end at links rather than nodes, it is recommended to purposefully make UAM station links short. Their sole purpose is providing an interface between UAM and non-UAM transport and should not be a substantial part of any UAM flight. After the UAM station link (i.e. link `L2-3`), a vertical take-off link (i.e. link `L3-4`) follows. Its length represents the flight level height, i.e. the vertical distance travelled during take-off. Subsequently, the flight segment transitions into cruise flight with link `L4-5`. Assuming a metre-based CRS, the listed exemplary flight level would be at 600 m height (see `length` attribute of link `L3-4`).

While MATSim does allow for three-dimensional 3D networks, by providing network nodes with `x`, `y`, and `z` coordinates, use of 3D networks for MATSim scenarios is uncommon and—even for MATSim-UAM [72]—not required. By providing links with their 3D-calculated length, a 2D projection of 3D flight paths suffices as a proxy network without falsifying flight lengths or requiring provision of `z` coordinates for all network nodes. In terms of functionality, the UAM-extension does not benefit from using 3D over 2D MATSim networks. Again, utility scripts, which semi-automate such pseudo-3D network creation, are provided and discussed in Section 3.2.3.

Predefined UAM plans. As mentioned in Section 3.1.2, routing can be disabled if UAM routing information, i.e. access/egress modes and origin/destination stations, is provided via agents' input plans. This is especially useful when using the UAM-extension in combination with external mode choice tools, as has been done by Ploetner *et al.* [24] when integration MATSim-UAM [72] into the Microscopic Transportation Orchestrator (MITO) [86]. The required input information needs to be set as attributes of each UAM

leg within agents' plans. Listing 3.10 provides an example of how to provide routing information via attributes of a leg.

```
<person id="0">
 <plan selected="yes">
  <activity type="home" link="1" x="0" y="0" end_time="08:00:00">
  </activity>
  <leg mode="uam" dep_time="08:00:00" trav_time="01:00:00">
   <attributes>
    <attribute name="accessMode" class="java.lang.String">car</
        ↪ attribute>
    <attribute name="originStation" class="java.lang.String">A</
        ↪ attribute>
    <attribute name="destinationStation" class="java.lang.String">B<
        ↪ /attribute>
    <attribute name="egressMode" class="java.lang.String">walk</
        ↪ attribute>
   </attributes>
  </leg>
  <activity type="work" link="2" x="6000" y="0" start_time="09:00:00
      ↪ " end_time="17:00:00">
  </activity>
  <!-- ... -->
 </plan>
</person>
```

Listing 3.10: Example XML representation of a MATSim plan with predefined UAM routing.

Access mode, egress mode, origin station, and destination station are provided using attributes named `accessMode`, `egressMode`, `originStation`, `destinationStation`, respectively, in any order. Each attribute's value is either one of the available access/egress modes, i.e. car, PT, bike, or walk, or the identifier of a UAM station. In the listed example, the agent would plan to access station `A` via car in order to fly to station `B` and egress by walking. While the intermodal router of the UAM-extension would still calculate and provide the access, egress, and flight paths, it would skip route optimization, e.g. by trying to minimise travel time.

3.2.3 Scenario Preparation

In order to facilitate UAM-conversion of base MATSim scenarios, a number of utility scripts are provided within MATSim-UAM [72]. Primarily, two UAM-scenario creation scripts semi-automate the creation of UAM-scenarios using either beeline (i.e. Euclidean) or routed flight paths. The core functionality of UAM-enabling an input MATSim con-

figuration and network is provided by the routed UAM scenario creation script[17], with the beeline scenario creation script[18] merely providing a simplified interface as actual scenario creation is handled by the more elaborate routed version.

Besides the MATSim XML input, the UAM scenario creation scripts use programme arguments (i.e. command line arguments) and Comma-separated Values (CSV) files with information on the to-be-created UAM stations, flight paths, and vehicles. Especially with regards to UAM network implementation, both creations scripts create an array of access and station links as previously illustrated by Figure 3.4 on page 44. All CSV input files are being parsed based on column position, in contrast to being based on named indexes. That is, the column order of CSV input files must not be changed, though the column names in the CSV files' first rows can freely be adjusted—especially, as the first row of all to-be-parsed CSV files is always assumed to be a descriptive header and, thus, ignored.

Beeline scenario creation. The beeline UAM scenario creation script[18] converts a base MATSim scenario into a UAM scenario in which all stations are connected to each other via direct, Euclidean, bi-directional flight paths. For that, the script requires at least four, and allows for up to five, programme arguments in a predefined order: (1) path to the to-be-converted base MATSim configuration file, (2) path to a stations CSV file, (3) maximum speed for all UAM flight links, (4) maximum hourly capacity of UAM flight links, and—optionally—(5) path to a vehicles CSV file.

As the first required programme argument, a relative or absolute path to a valid, conventional MATSim configuration file has to be provided that—in itself—correctly points to a non-UAM network. Secondly, a relative or absolute path has to stations CSV file is needed. Station CSV files are expected to provide information on the to-be-placed UAM station with information, such as identifier, name, coordinates, and process times, as shown in the required order in Table 3.1, filled with exemplary stations' data. Each row represents one UAM station, with the exception of the first row, the header. An actual example stations CSV file[19] is provided within the MATSim-UAM [72] source code.

Table 3.1: Exemplary stations CSV file input for UAM scenario creation.

Id	Name	x	y	z	d_{vtol}	c_{ga}	v_{ga}	c_{fa}	v_{fa}	t_{pre}	t_{post}	t_{wait}
A	Alpha	6020	500	0	600	999	35	999	35	900	300	0
B	Bravo	6020	-500	0	600	999	35	999	35	600	120	480
C	Charlie	14020	500	0	600	999	35	999	35	300	60	0
D	Delta	14020	-500	0	600	999	35	999	35	150	30	300

where:

[17] See net/bhl/matsim/uam/scenario/RunCreateUAMRoutedScenario.java
[18] See net/bhl/matsim/uam/scenario/RunCreateUAMBeelineScenario.java
[19] See examples/uam-scenario-creation/stations.csv

- x, y, and z are the desired UAM station coordinates. A dedicated station link will be created at the given coordinates on which the UAM station is then placed. The z coordinate is ignored unless the network creation script is explicitly set to include z coordinates via an in-class variable[20].

- d_{vtol} is the VTOL distance, i.e. flight level height, in the MATSim scenario's CRS distance unit—usually metres or feet.

- c_{ga} and v_{ga} are the ground access links' hourly capacity and max. speed in the scenario's CRS distance unit per second—usually metres or feet per second.

- c_{fa} and v_{fa} are the flight access links' hourly capacity and max. speed in the scenario's CRS distance unit per second.

- t_{pre}, t_{post}, and t_{wait} are the station's respective pre-flight, post-flight, and default waiting times in seconds.

The third and fourth programme arguments are maximum speed and hourly capacity for all created station-connecting Euclidean UAM flight links. As discussed in Section 3.1.2, UAM vehicle are restricted by their vehicle type's and the link's maximum flight speed. If no flight speed restriction via links' maximum speeds is desired, it is strongly recommended to set the links' maximum speeds equal to or just above the cruise flight speed of the fastest flying UAM vehicle type, instead of setting it to an arbitrary high number. In contrast to UAM vehicle movement during simulation, routing is based solely on links' maximum speeds. If all UAM links' maximum speeds are unrealistically high, the router—in trying to minimize, e.g., over travel time—will produce suboptimal itineraries as, in terms of travel time, there is little to no difference between trips with similar distances. Travelling, say, five or six kilometres at the speed of sound, for example, results in a less-than-three second travel time difference. For UAM links' hourly capacities, the inverse (i.e. very small capacities) require some elaboration. For all MATSim links, insufficient link capacities correctly lead to congestion, thus also for UAM links. In contrast to cars, however, having UAM vehicles hovering mid-air until the flight path clears might be an unrealistic and, thus, undesired vehicle behaviour. In general, except if certain restricted UAM are desired, it is recommended to set links' maximum speeds as low as possible without restricting the vehicles' flight speeds and to provide ample capacity. Compare, for example, the link speeds as defined listed in Table 3.2 with the vehicle types' cruise speeds from Listing 3.3 on page 38. To facilitate later UAM network identification, the applied maximum link speed is listed as a network attribute near the top of the resulting UAM network file.

Direct flight paths' lengths are based on multiplying the station pair's Euclidean distance, calculated based on the scenario's CRS, with a detour factor, which—by default—is set to one (i.e. no distance alteration). This in-class variable[21] can manually be changed in order to include the impact of real-life flight deviations from direct flight paths. For

[20] See net/bhl/matsim/uam/scenario/RunCreateUAMRoutedScenario.java: useZCoordinate
[21] See net/bhl/matsim/uam/scenario/RunCreateUAMRoutedScenario.java: detourFactor

example, by setting the detour factor to 1.2, a 20% increase in flight path length could be achieved. Again, to facilitate later network identification, the used UAM detour factor is also listed as a UAM network attribute.

Lastly, a vehicles CSV file can be provided. If not provided, i.e. by omitting the fifth programme argument, a UAM-enabled configuration and UAM-including network will be created but no UAM stations and vehicles XML file, which itself is required for UAM simulation. As with the stations CSV file, the vehicles CSV file requires a predefined order of input parameters with one vehicle type being defined per row, with the exception of the header row. Table 3.2 provides information on two exemplary vehicle types with all required inputs. Again, an actual example vehicles CSV file[22] is provided within the MATSim-UAM [72] source code.

Table 3.2: Exemplary vehicles CSV file input for UAM scenario creation.

Id	V/S	tod_{start}	tod_{end}	d_{range}	c_{pax}	v_{cr}	v_{vtol}	t_b	t_{db}	t_{tat}
S	2	00:00:00	24:00:00	60000	2	33.3	10	30	30	120
L	2	05:00:00	21:00:00	30000	4	22.2	8	60	60	300

where:

- V/S is the number of vehicles to be placed at each UAM station. Uniformly distributing all vehicles over all stations is the default behaviour of the scenario preparation scripts. However, there are no requirements for vehicles' initial stations to be distributed uniformly or in any particular pattern. Thus, the resulting UAM XML file can manually be changed to achieve any desired vehicle distribution.
- tod_{start} and tod_{end} are the operation start and end times in time of day in `hh:mm:ss` format, i.e. hours, minutes, and seconds since simulation start at midnight.
- d_{range} is the vehicle type's flight range, i.e. maximum possible flight distance in the MATSim scenario's CRS distance unit.
- c_{pax} is the vehicle type's maximum passenger capacity.
- v_{cr} and v_{vtol} are the cruise and VTOL flight speeds in the scenario's CRS distance unit per second.
- t_b, t_{db}, and t_{tat} are the boarding, deboarding, and turnaround times in seconds.

```
1 java -cp matsim-uam-2.1.jar:libs/* net.bhl.matsim.uam.scenario.
      ↪ RunCreateUAMBeelineScenario ./non-uam-scenario/config.xml ./
      ↪ stations.csv 35 999 ./vehicles.csv
```

Listing 3.11: Exemplary use of beeline UAM scenario creation script via Linux command line.

[22] See examples/uam-scenario-creation/vehicles.csv

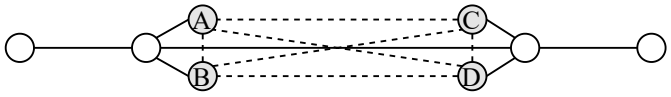

Figure 3.5: Top view of an example UAM scenario with labelled UAM stations, Euclidean (i.e. beeline) flight paths (dashed lines), and conventional roads (solid lines).

Using the beeline UAM scenario creation script[18] with provided example input files of a non-UAM scenario[23], the listed stations CSV file[19] (see Table 3.1), and the listed vehicles CSV file[22] (see Table 3.2) results in a runnable UAM scenario with partly-adjusted configuration XML file and newly-generated, GZip-compressed UAM stations and vehicles XML file and UAM-enhanced network. Listing 3.11 provides an exemplary execution of said beeline scenario creation setup for a Linux-based operation system, assuming the usage of MATSim-UAM [72] via a Java Archive (JAR) file. Figure 3.5 illustrates the resulting, exemplary network with Euclidean UAM links. As illustrated, all four defined stations have been connected to each other via direct connections.

Routed scenario creation. The functioning of the routed UAM scenario creation script[17] mirrors the that of the beeline script[18] with one exception: the user is required to specify flight nodes and links, that replace direct Euclidean flight paths which would automatically be created between all UAM stations. With regards to the difference in script usage, the routed scenario creation script requires a CSV list of flight nodes and another of flight links as the third and fourth programme arguments, i.e. in the positions where the beeline script had all links' maximum flight speeds and capacities. Thus, the routed UAM scenario creation script requires at least four (and allows for up to five) programme arguments in a predefined order: (1) path to the to-be-converted base MATSim configuration file, (2) path to a stations CSV file, (3) path to a flight nodes CSV file, (4) path to a flight links CSV file, and—optionally—(5) path to a vehicles CSV file. Other than that, the internal functioning of both scripts is identical and, thus, the same recommendations apply.

As with the previous input CSV file, the flight nodes CSV file requires a predefined order of input parameters with one flight node being defined per row, with the exception of the header row. Table 3.3 provides information on exemplary flight nodes with all required inputs, where x, y, and z are the UAM station coordinates, with z representing the flight level height in the MATSim scenario's CRS distance unit. Again, an actual example flight nodes CSV file[24] is provided within the MATSim-UAM [72] source code.

Similarly, the flight link CSV file also requires a predefined order of input parameters with one flight link being defined per row, with the exception of the header row. Table 3.4 provides information on exemplary flight links. An actual example flight links CSV file[25] is also provided. It is important to note that for flight link input, bi-directional are not automatically being created. Thus, if bi-directional links are desired, both directions

[23] See examples/uam-scenario-creation/non-uam-scenario
[24] See examples/uam-scenario-creation/flight-nodes.csv
[25] See examples/uam-scenario-creation/flight-links.csv

Table 3.3: Exemplary nodes CSV file input for routed UAM scenario creation.

Id	x	y	z
0	6020	500	600
1	6020	-500	600
2	7515	250	600
3	12525	-250	600
4	14020	500	600
5	14020	-500	600

must be listed within the flight link CSV file, as shown in Table 3.4. The flight link CSV file does not include link lengths. Those are, again, calculated based on the Euclidean distance between a link's from and to nodes and multiplied with the script's internal detour factor[21].

Table 3.4: Exemplary links CSV file input for routed UAM scenario creation.

From id	To id	c_l	v_l
0	2	999	35
1	2	999	35
2	3	999	35
3	4	999	35
3	5	999	35
2	0	999	35
2	1	999	35
3	2	999	35
4	3	999	35
5	3	999	35

where:

- From id and to id are the link's origin and destination node identifiers.
- c_l and v_l are the link's hourly capacity and max. flight speed in the scenario's CRS distance unit per second.

```
1    java -cp matsim-uam-2.1.jar:libs/* net.bhl.matsim.uam.scenario.
         ↪ RunCreateUAMRoutedScenario ./non-uam-scenario/config.xml
         ↪ ./stations.csv ./flight-nodes.csv ./flight-links.csv ./
         ↪ vehicles.csv
```

Listing 3.12: Exemplary use of routed UAM scenario creation script via Linux command line.

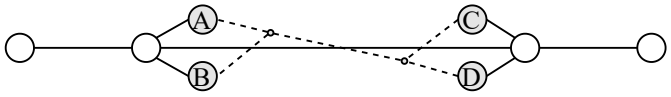

Figure 3.6: Top view of an example UAM scenario with labelled UAM stations, routed flight paths (dashed lines) along waypoint nodes, and conventional roads (solid lines).

Using the routed UAM scenario creation script[17] with provided example input files of a non-UAM scenario[23], the listed stations CSV file[19] (see Table 3.1), the listed flight nodes CSV file[24] (see Table 3.3), the listed flight links CSV file[25] (see Table 3.4), and the listed vehicles CSV file[22] (see Table 3.2) results in a routed UAM scenario. Listing 3.12 provides an exemplary execution of this routed scenario creation setup, again assuming a Linux-based operation system. Comparing Figure 3.6 to the previous figure, Figure 3.5, illustrates the difference in the resulting UAM flight paths.

Configuration conversion. Both UAM scenario creation scripts include the generation of a partly-adjusted configuration XML file by making use of auxiliary configuration functions[26]. If desired, however, the configuration conversion can also be run stand-alone, i.e. independently of the UAM scenario creation scripts. For that, the main method of the configuration functions class[26] can be used if provided with the following programme arguments in fixed order: (1) path to a non-UAM configuration XML file, (2) path to a UAM file, and (3) desired access/egress modes. Routing strategy is set to minimize total travel time with all optional UAM module parameters being set to their default values, as described in Section 3.2.2, that can be changed manually within the resulting UAM-enabled configuration.

It is important to note that any configuration conversion, be it run stand-alone or when run within the scenario creation scripts, does add all required modules and parameter sets that MATSim-UAM [72] requires for simulation, yet does not automatically add UAM as a mode of transportation to any of MATSim's replanning strategies (see Horni and Nagel [81, pp. 38] for more information). Thus, UAM is not automatically added to any mode choice strategies, e.g. change leg mode or sub-tour mode choice. If UAM is desired to be included in any (mode choice) strategy, UAM has to be manually added to the desired strategy—otherwise, agents will be unable to switch to this newly-introduced mode.

3.2.4 Scenario Simulation

Running MATSim-UAM [72], i.e. starting the simulation, is done using the run UAM scenario class[27], with the same programme arguments as used by base MATSim: the path to a UAM scenario's configuration XML file. Listing 3.13 shows how to start an exemplary UAM simulation via command line on a Linux-based operating system, using

[26] See net/bhl/matsim/uam/scenario/utils/ConfigAddUAMParameters.java
[27] See net/bhl/matsim/uam/run/RunUAMScenario.java

MATSim-UAM [72] via a JAR file. In contrast to base MATSim, though, no dedicated Graphical User Interface (GUI) is provided.

```
1 java -cp matsim-uam-2.1.jar:libs/* net.bhl.matsim.uam.run.
    ↪ RunUAMScenario ./uam-test-scenario/uam_config.xml
```

Listing 3.13: Exemplary MATSim-UAM [72] simulation start via Linux command line.

For a first MATSim-UAM [72] simulation, a UAM test scenario[28] is provided with the extension's source code with a ready-to-use UAM-enabled configuration XML file. The provided test scenario represents the routed UAM scenario as described in Section 3.2.3 (see Figure 3.6 and Tables 3.1, 3.2, 3.3, and 3.4). The provided example population already includes UAM legs, thus the created configuration does not have to be adjusted in order to include UAM in innovative replanning strategies, i.e. mode choice strategies, as explained in Section 3.2.3. Since there are no replanning strategies involved in the test scenario, it only runs for the zeroth iteration for simulating the pre-planned car and UAM travel itineraries. To facilitate UAM analyses, MATSim-UAM [72] creates a auxiliary UAM demand CSV file for each iteration. For the test scenario, such a UAM demand file is also created for the zeroth iteration and provides quick insight into the usage of UAM within the simulated scenario. This UAM demand file lists each passenger trip individually with additional information, such as origin/destination, take-off and landing times, and the serving vehicle. Empty, i.e. relocation, flights are not recorded in this list. Also, pooled passengers remain listed individually, yet they can be identified and grouped by matching the serving vehicle, origin and destination stations, and take-off time.

After running the test scenario, the UAM demand file, as partly shown by Table 3.5, lists all UAM passenger trips. Each UAM-using agent makes two flights and all—except for one agent—share their flight with at least one other agent, based on the passenger vehicles' capacities (cf. Table 3.2). With two vehicles of each type per station, there is sufficient UAM supply at the origin station that no vehicle relocation is required. In total, six flights serve all 18 passenger trips. Based on the applied UAM routing strategy, i.e. travel time minimisation, all flights occur between stations `B` and `D`—since this station pair provides the fastest left-right connection in terms of process times (cf. Table 3.1). By comparing the agents' arrival times with the vehicles' take-off times, waiting times for the earlier arriving passengers of shared flights can be observed (keep in mind the stations' pre-flight times and vehicle types' boarding times, see Tables 3.1 and 3.2 receptively, that occur between agent arrival and take-off).

3.2.5 Travel Time Calculation

Besides using MATSim-UAM [72] for its main purpose, i.e. traffic simulation, it additionally provides utility scripts for travel time calculations[29]. The individual scripts for

[28] See examples/uam-test-scenario
[29] See net/bhl/matsim/uam/analysis/traveltimes

Table 3.5: Excerpt of the exemplary UAM demand CSV file for the zeroth iteration of the test scenario, with each row representing one passenger trip and individual flights being separated by horizontal lines.

Agent id	Origin station id	Destination station id	Vehicle type id	Agent arrival time of day	Take-off time of day
PAX 1	B	D	L	06:07	06:24
PAX 2	B	D	L	06:09	06:24
PAX 3	B	D	L	06:11	06:24
PAX 4	B	D	L	06:13	06:24
PAX 5	B	D	L	06:17	06:34
PAX 6	B	D	L	06:19	06:34
PAX 7	B	D	L	06:21	06:34
PAX 9	B	D	L	06:23	06:34
PAX 10	B	D	S	06:25	06:36
PAX 1	D	B	L	10:07	10:17
PAX 2	D	B	L	10:09	10:17
PAX 3	D	B	L	10:11	10:17
PAX 4	D	B	L	10:13	10:17
PAX 5	D	B	L	10:17	10:27
PAX 6	D	B	L	10:19	10:27
PAX 7	D	B	L	10:21	10:27
PAX 9	D	B	L	10:23	10:27
PAX 10	D	B	L	10:25	10:29

car, PT, and UAM travel times provide parallelized routing and expected travel times for a list of predefined origin and destination coordinates at a given time of day. Each script, though, calculates travel times on a different basis. The car travel time script calculates trip travel times based on the scenario's network. The script for PT travel times uses, in addition, PT schedule information, while the UAM version combines the functioning and requirements of car and PT (for access and egress) with its own requirement for UAM stations and vehicle information. All three travel time calculation scripts do take the same required input programme arguments, though, with: (1) path to a MATSim configuration file, (2) path to a trips CSV file (see Table 3.6 for an example), and (3) path and name of the desired output CSV file. While the UAM script automatically provides additional information besides the travel times themselves, such as origin and destination UAM stations, the car and PT scripts only provide additional information of a fourth, optional, boolean parameter is provided on whether descriptive information should be written to the output CSV file. By default, this descriptive information, i.e. routing information for both car and PT, is given but may lead to large file sizes when calculating travel times for a multitude of trips. Table 3.6 provides exemplary trips information which can be used with the previously-mentioned example scenario[28], with the actual input trips CSV file[30] being provided within MATSim-UAM [72].

Table 3.6: Exemplary trips CSV file input for travel time calculation scripts.

From x	From y	To x	To y	tod_{start}
0	0	20040	0	06:00
20040	0	0	0	07:08:09

where:

- From and To x and y are the trips origin and destination coordinates, respectively.
- tod_{start} is the trip's start time of day in either `hh:mm` or `hh:mm:ss` format, i.e. hours, minutes, and—optionally—seconds since midnight.

Using these scripts allow travel time calculations with substantially reduced computational cost when compared to running full simulations (see Section 3.2.4). Congestion levels and dynamic UAM vehicle usage—some of the main outcomes of MATSim simulations—however, cannot be derived from these pure travel time calculation scripts. Once a full simulation has been run, though, its results can be included in travel time calculation in order to include the effects of congestions—especially for car usage, be it individually or for UAM access/egress. For this, time-dependent MATSim networks can be used. Rieser *et al.* [85, pp. 55] explain their purpose and the required configuration changes for including post-simulation congestion levels in networks. For this, together with the network file itself, a so-called network change events file must provided which lower links' maximum speeds to the observed speeds during simulation. To facilitate the

[30] See examples/uam-traveltimes-input/trips.csv

use of congestion-including travel time calculations, a utility class for generating such network change events XML files is included with the travel time scripts themselves[29]. The required input programme arguments for change events generation are: (1) path to a network XML file, (2) path to a respective events XML file, and (3) path and name of the resulting output network change events XML file. This methodology of calculating congestion-including travel times for car, PT, and UAM has seen heavy use in studies such as Rothfeld *et al.* [3].

3.2.6 Limitations & Known Issues

Despite many development cycles and multiple versions of MATSim-UAM [72], certain limitations do remain with the current iteration (i.e. v2.1). The following paragraphs outline main functional limitations for transparency and documentation and provide potential mitigation measures.

Limited distinction of vehicle types during dispatching. The provided UAM vehicle dispatchers (see Section 3.1.2) distinguish multiple UAM vehicles types solely based on range. Other than dismissing available vehicles of types whose maximum range is lower than a requested trip, dispatcher make no deliberate distinction between vehicle types based on, e.g., cruise flight speed. In line with the current dispatcher's behaviour of taking the first-available, closest vehicle of any type, if, e.g., a slower-flying vehicle is available, it is reserved rather than a faster-flying vehicle that would have to be relocated—even if, including relocation, the later option would eventually yield lower total travel times. Thus, rather than including multiple vehicle types within one simulation, it is recommended to run multiple simulations with one vehicle type each by alternating UAM vehicle files in order to allow for analyses of variations in vehicle properties.

Required initialisation of UAM departure handler. As described at the end of Section 3.2.2 and illustrated with Listing 3.8 (see page 42), for UAM access and egress via car to be simulated, both access/egress modes must be registered as QSim main modes. If they are, due to the way departure handling is implemented in MATSim with the default vehicular departure handler resolving any main mode departures, UAM transport requests are only registered once agents, that use a main mode for UAM access, arrive at their UAM station instead of as soon as they depart their original location. With that there is limited to no time for other agents to be pooled onto the same flight. A dedicated UAM departure handler[31] has been implemented to resolve this issue. However, the departure handler only gets initiated once a non-main mode departure has occurred, e.g. by a walking, biking, or UAM flight. Only after initiation will main mode access departures be registered without delay. In the rare case, though, were there are only main mode departures within a simulation before the first UAM flight occurs, the first flight cannot be shared amongst multiple passengers. All following flights will be handled as expected. In terms of a large-scale simulation and, especially, with smaller vehicle

[31] See net/bhl/matsim/uam/qsim/UAMDepartureHandler.java

capacities this behaviour will only minimally impact simulation results. For specialised scenarios, though, it might be advisable to ensure at least one non-main mode departure occurs before the first main mode UAM access departure (cf. first agent of the provided UAM test scenario's[28] population file).

Further, no maximum waiting time for shared flights has been implemented. Given a UAM vehicle with ample seat capacity combined with a relatively long station access trip time and—by chance—evenly spaced out passenger requests for the same origin-destination pair, it might happen that the early-arriving passengers have to wait a substantial amount of time until their vehicle departs. Surely, by using MATSim's plan scoring functionality, the use of UAM will then be less attractive to those long-waiting agents, yet this behaviour might not necessarily be desired by all MATSim-UAM [72] users.

Independence of UAM vehicle range & payload. Currently, UAM vehicles have a fixed, predefined range regardless of a flight's Seat Load Factor (SLF). For real-life flights, the trade-off of payload and range requires substantial consideration. In order to somewhat represent the effect of longer ranges with less or no payload, empty UAM relocation flights are not bound to the vehicle's maximum range. For studying the impacts of different vehicle ranges, it might be helpful to not restrict the vehicles' ranges within the simulation but leave it unconstrained and analyse the flights that would not have been possible—given a constraint maximum range—within the post-simulation results.

Missing UAM vehicle acceleration. As with all vehicular agents within MATSim, UAM vehicles also do not experience acceleration. Rather, all vehicles immediately travel at their own or the link's maximum speed if there is no congestion. Despite UAM vehicles having substantially higher travel speeds than, say, cars, the impact of missing acceleration is believed to have little impact. If the effects of acceleration on UAM travel times are desired, though, they could already be included by, e.g., reducing the maximum speeds of flight links to the average speeds that actual flights (with acceleration) would experience or by segmenting longer flight links into smaller segments with gradually increasing/decreasing maximum link speeds.

Brute-force approach to route optimisation. The approach for finding optimized UAM routings (see Section 3.1.2) is achieved by brute-forcing all possible combinations of access/egress modes and origin/destination stations within a given radius around an agent's location and desired destination. The strategy implementations for minimum travel time and distance cycle calculate the required variable with nested for-loops, which is highly inefficient as its computation time increases cubically, i.e. $O(n^3)$, with the number of available options. Scenarios, with a great number or density of UAM stations and/or an expansive search radius setting, will require a substantial routing effort. For large-scale scenarios, it is recommended to use relatively small search radii, limit the number of available access/egress modes, and/or change the routing strategy to access time or distance minimization in order to reduce computation time.

Difficulty of down-scaling UAM vehicle capacities. Lastly, UAM operations are difficult to scale down. As usual for MATSim simulations, the scenarios are set up with a fraction of the actual number of trips observed in real-life (see, e.g., a study by Llorca and Moeckel [87] on the impact of different sample sizes on MATSim results). Sample sizes usually vary substantially based on the number of actual daily trips within any given study area. Synthetic populations of 1%, 5%, and—especially—10% are very common. Road and parking capacities within MATSim are adjusted accordingly to match infrastructure supply to this scaled-down demand. Vehicles' seat supplies, however, are more difficult to scale down accordingly. While it is not a UAM-specific issue—PT services are similarly affected—it is evident that the supplied seat capacity of a UAM vehicle with, say, two seats is near impossible to meaningfully scale-down to, e.g., 10%. Thus, samples size of 25%, 50%, or even 100% are recommended for scenarios that are heavily restricted in terms of their UAM supply. If the available computational resources do not allow for high sample size simulations, it might be useful to split the analysis into two, subsequent simulations. A first down-scaled simulation run in order to derive network congestion levels via, e.g., network change events. By pre-processing the population and only simulating a pre-selected subpopulation that is deemed likely to be using UAM, e.g via proximity to UAM stations, a second, non-scaled down—but still less computational expensive—simulation can be run that includes actual congestion levels by implementing a time-dependent network with the congestion information of the first simulation.

3.3 Alternative Applications

The UAM-extension for MATSim can, in principle, be used for simulating any station-based, on-demand, passenger-transporting mode and is neither restricted to short-range nor aerial missions. Two exemplary alternative applications of the UAM-extension are presented with regional aviation and the hyperloop concept.

The open Germany scenario for MATSim, created by Nagel *et al.* [88] (code published under GPL-2.0 license, scenario files published under CC BY 4.0), has been utilised for the creation of two illustrative scenarios for both alternative UAM-extension applications. The open scenario provides car and PT networks and PT schedules for past and present years. The scenario's synthetic population has not been published, though. Thus, artificial illustrative populations have been created per alternative application.

3.3.1 Regional Aviation

For the example of regional aviation, four travel itineraries have been chosen: (1) Hamburg to Berlin, (2) Leipzig to Hanover, (3) Kassel-Calden to Frankfurt-Hahn, and (4) Munich to Erlangen; representing potential cross-regional travel origins and destinations. For each origin-destination pair, 20 agents have been created that have the respective itinerary set as their travel plan with the agents being split into two halves regarding their predefined mode of transportation being either car or regional aviation. Close to each origin/destination, an airport—some international (e.g. in the case of Munich), some

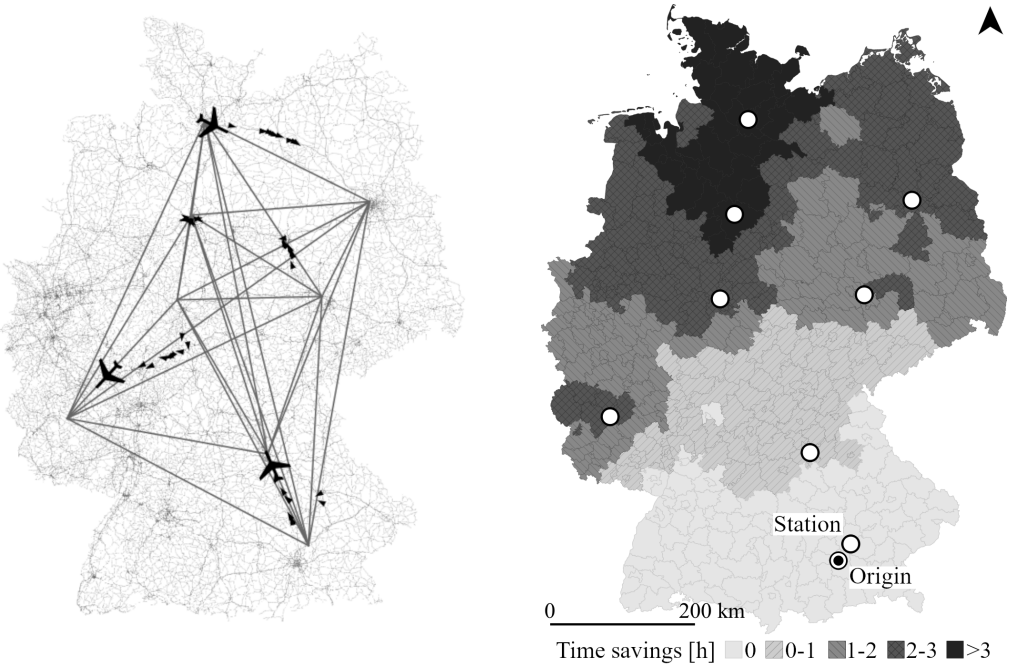

(a) Example of regional aviation, visualised with Simunto Via.

(b) Travel time savings of regional air usage over car departing from Munich.

Figure 3.7: Illustration of UAM-extension MATSim results for the Germany scenario for an exemplary regional aviation system between eight German airports.

regional (e.g. Nuremberg)—has been made available for regional aviation and provides one exemplary regional aircraft. These aircraft have been set to a passenger capacity of 19 seats and a cruise flight speed of 300 km/h.

As illustrated in Figure 3.7a, the following airports have been included and connected via direct Euclidean flight routes: Munich, Nuremberg, Berlin-Tegel, Hamburg, Kassel-Calden, Hanover, Frankfurt-Hahn, and Leipzig/Halle airport. Cars, represented by black triangles pointing in the direction of travel, can be seen following roads and highways—depicted by grey background lines—towards their destination. Black aircraft icons indicate regional aircraft flying in-between two airports along direct Euclidean flight routes.

With only one aircraft per origin region and each aircraft providing ample passenger capacity, the UAM-extension's default vehicle dispatcher, as described in Section 3.1.2, pooled each regions' regional aviation-using agents into one aircraft departure. This dispatcher behaviour stems from the example scenario's setting of multiple agents having similar origins and destinations with their departure being within a narrow time frame. Due to the spatial and temporal proximity of transport requests, they can dynamically be pooled, in contrast to a scheduled service. Upon completion of the last passenger's access leg and pre-flight process time, the aircraft takes off towards the passenger's joint destination airport. Car-using agents do not have to wait for additional passengers, nor have to complete pre-flight processes. Thus, they could be observed to remain ahead of

their regional aviation-using counterparts per route up to the point where the regional aircraft take off and—due to their cruise flight speed—overtake the ground-based drivers. Though, regional aviation users are also required to complete post-flight processes and their egress leg.

Figure 3.7b illustrates the travel time savings of using the described regional aviation system over car usage without congestion, when travelling outwards from Munich to each of Germany's NUTS3 regions (based on each region's geometric centroid). As expected, the travel time savings increase with distance and, notably, are most distinct when in proximity of one of the provided regional airports. For this exemplary application with pre- and post-flight process times of five and two minutes, respectively, travel time savings can be observed beginning from Nuremberg northwards. Travel times from Munich to Hanover or Hamburg would be shortened by more than three hours in this scenario.

3.3.2 Hyperloop

For the exemplary application of the UAM-extension for the hyperloop concept, Munich and Hamburg have been chosen as the sole two hyperloop stations, being connected via a direct Euclidean tunnel. Again, for the travel itinerary of Munich to Hamburg, 20 agents have been created, half of which are set to be using cars with the other half being predefined to be using the hyperloop system for their trip. This fictional hyperloop implementation is defined to be travelling at the speed of sound, i.e. with up to 1,235 km/h. Figure 3.8a illustrates the hyperloop connection between Munich and Hamburg in light blue, with the hyperloop shuttle currently being beyond halfway on its trip to Hamburg. Black triangles represent the car-using agents on the same route, nearly having reached Nuremberg in the same amount of time.

Similarly to the regional aviation example, the spatial and temporal proximity of the artificial agents allowed the dispatcher to pool all transport requests into one hyperloop shuttle departure, awaiting all ten agents to arrive and complete the pre-flight, or rather pre-departure, process time. Figure 3.8b again illustrates the potential travel time saved by using, in this case, the hyperloop system instead of car for an outwards trip starting from Munich. With the presented, exemplary hyperloop stations in Munich and Hamburg, the travel time from Munich towards northern Germany could be reduced by more than four hours around Hamburg and still up to two hours to Berlin (without Berlin having a hyperloop station). The same pre- and post-departure times as before have been chosen, i.e. five and two minutes respectively. While an actual realization of the hyperloop concept could well be imagined to be operated on a scheduled basis, this on-demand modelling approach allows the analysis of various dispatching algorithms in order to strike a balance between maximum passenger waiting times until departure, vehicle utilization, and the seat load factors per trip.

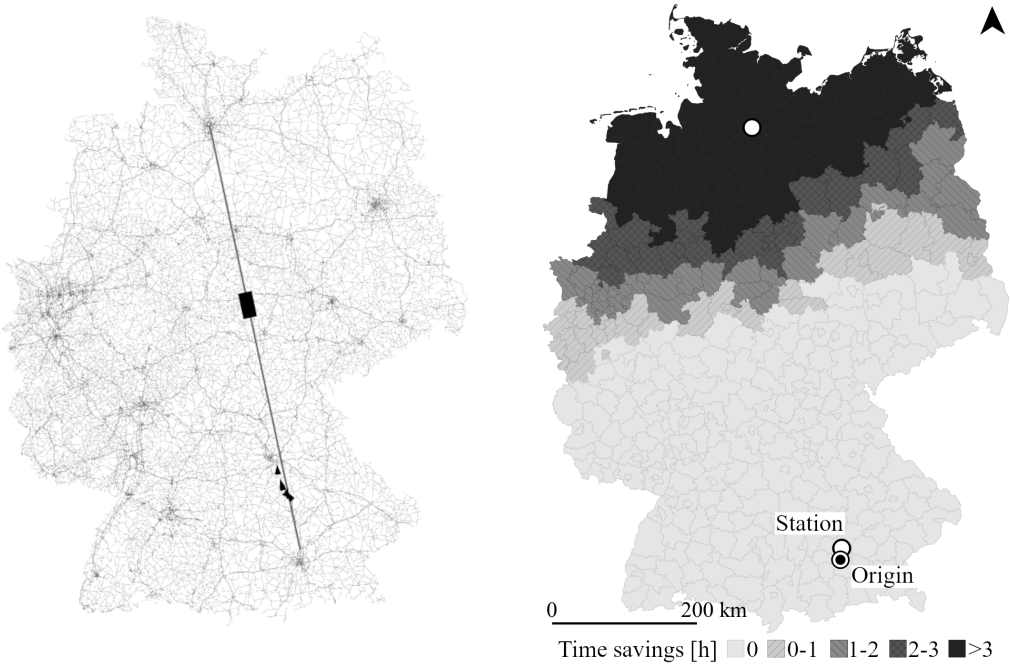

(a) Example of hyperloop, visualised with Simunto Via.

(b) Travel time savings of hyperloop usage over car departing from Munich.

Figure 3.8: Illustration of UAM-extension MATSim usage and results for Germany for an exemplary hyperloop connection between Munich and Hamburg.

4 UAM Travel Times & Transport Performance

While a detailed analysis of UAM travel times—on the examples of Munich Metropolitan Region (centered around Munich) (MUC), Île-de-France (centered around Paris) (PAR), and San Francisco Bay Area (centered around San Francisco) (SFO)—is presented by Rothfeld *et al.* [3], the following sections provide additional information on the study's foundations, comparative analyses with prior studies (e.g. [1], [24]), and considerations of additional topics such as pooling potential and accessibility. In contrast to the initial analysis [3], however, this chapter will focus exclusively on MUC.

4.1 Scenario Preparation

While Rothfeld *et al.* [3] does provide a short summary of how the scenarios were prepared for analysis, the following expands on said explanation for the reasons of transparency and reproducibility.

4.1.1 Automated Zoning

For reasons of visualisation and to aide with spatial analyses, sub-dividing a study area into smaller zones can very helpful. Often-times, using administrative boundaries perfectly suit this purpose as, e.g., shown in Figure 3.8b, where Germany is presented by its rural districts. In some cases, however, available administrative borders might be unsuitable for the required analysis. A common reason for this is in cases where the spatial resolution, of said boundaries, is too coarse. Moeckel and Donnelly [89] elaborate on this and provide the basis the following zoning approach. For the travel time analysis [3], the available administrative boundaries where too large as well as too varied in their scopes, since most countries follow their own, individual guidelines for the definition of administrative districts.

Thus, study areas are sometimes divided into equally-sized shapes (most-commonly squares or hexagons). While creating zones of equal size can quickly be achieved, if used for transportation modelling, those zones may be overly detailed in very rural areas and—at the same time—too coarse in urban settings; hence the use of a gradual rasterization [89] that results in finer zones for densely-populated areas. As the first step, the study area (Figure 4.1a) is divided into initial, coarse square zones (b) (10-km spacing). For MUC, population was used as the weight with a threshold set to 1% of the study

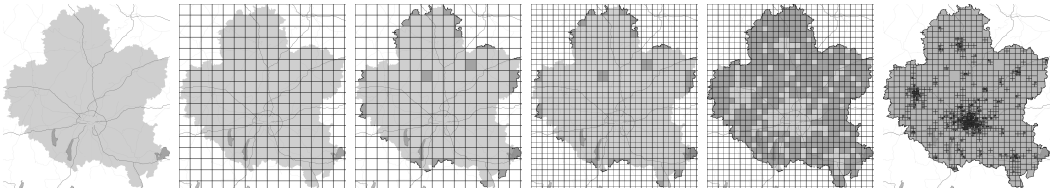

(a) Without zones. **(b)** Initial, 1^{st} grid. **(c)** Excluded zones. **(d)** Halved, 2^{nd} grid. **(e)** Excluded zones. **(f)** Resulting zones.

Figure 4.1: Employed rasterization approach on the example of MUC.

area's total population. As Moeckel and Donnelly [89, p. 15] state in their introduction, "[d]efining the most suitable level of spatial resolution in modeling often is considered to be more art than science." In line with that statement, the 1% threshold has been defined after multiple exploratory attempts to achieve the desired mix of coarse and fine zones. Each zone that already contains less the defined threshold was fixed, i.e. excluded from further division (c) (shown in dark grey). In an iterative process, the grid size is halved, dividing non-excluded zones into four smaller, equally-sized zones (d), before all those smaller zones, that fall below the threshold, are also excluded from further division (e). This process was repeated for six iterations, resulting in 2,714 zones for MUC, after removing zone fragments at the study area's borders with less than $0.05\,\mathrm{km}^2$ in size.

4.1.2 Flight Path Detour

As used by Rothfeld *et al.* [3] and first mentioned by Rothfeld *et al.* [82], a ground infrastructure-based approach was proposed for UAM flight routing in order to approximate real-life VFR flight routes instead of direct Euclidean flight paths. In this approach, road and rail infrastructure is categorized according to their throughput and capacity. Higher capacity infrastructure is given a lower weight (i.e. cost) than low-capacity infrastructure so that a least-cost path finding algorithm can be applied to derive UAM flight paths predominantly following high capacity (i.e. high noise) ground infrastructure. Three categories of infrastructure have been defined: "(1) regional and high-speed rail, motorways, and primary roads, (2) secondary and tertiary roads, and (3) all remaining road and rail infrastructure" [3], based on the OpenStreetMap classifications as listed and illustrated in the OpenStreetMap Wiki [90]. The different categories' weights, which are relative to each other, are derived by using a weight factor (wf) that is multiplied with the previous category's weight. The first category always has a weight of one. As a preparation for applying least-cost path algorithms to derive routed flight paths in-between all stations of a scenario, the categorized layers (i.e. OpenStreetMap road and rail) needs to be combined, intersected with itself (to allow flight paths to make use of road/rail intersections, where in real-life there would be no intersection, e.g. because of an underpass), and categorized into the above-mentioned three groups from high to low capacity.

Figure 4.2a illustrates the least-cost path for uniform weighting by using a weight factor of 1. The three categories all use the same weight resulting in shortest ground

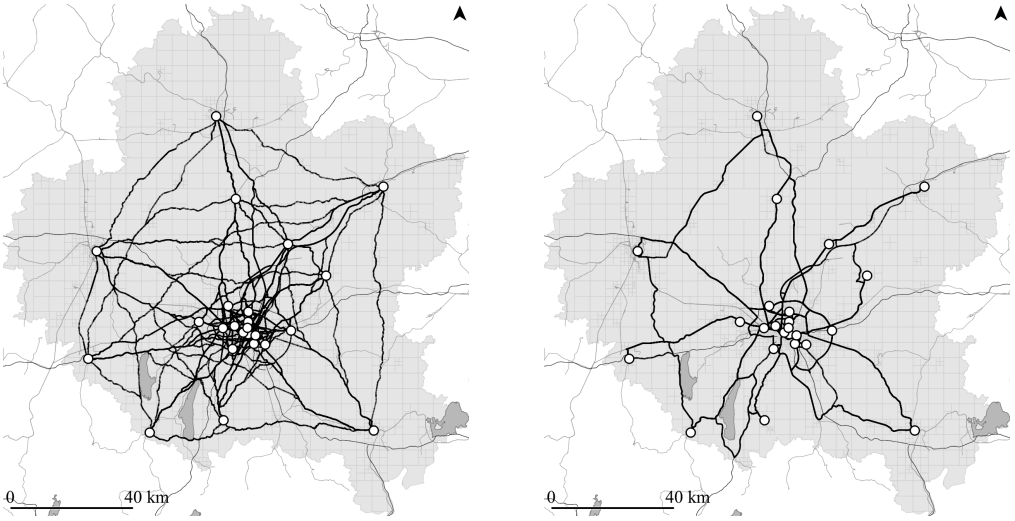

(a) Flight paths with $wf = 1$.

(b) Flight paths with $wf = 5$.

Figure 4.2: UAM least-cost path routings using the weight factors of 1 and 5 for MUC.

infrastructure-based paths. Figure 4.2b shows the least-cost paths for a weight factor of 5 (i.e. $wf = 5$), i.e. weight of 1 for category (1), weight of 5 for category (2) and weight of 25 for category (3). By comparing Figures 4.2a and 4.2b, the difference in routing is obvious with Figure 4.2b heavily emphasising the use of highways over smaller, but more direct, roads. This difference in routing can be quantified by analysing each weight factor's mean detour factors when comparing the distances of these resulting routes to direct, Euclidean flight paths.

Figure 4.3a illustrates the mean detour factor for various weight factors ranging from 1 to 5 for all station-to-station flight routes in MUC with all station number variations (i.e. 4, 8, 24, 76, and 130 [3]). For a weight factor of 1, i.e. shortest path, a mean detour factor of $M_1 = 1.10$ ($SD = 0.04$) can be derived with the minimum and maximum observed detour factors being 1.03 and 1.29, respectively. With increasing weight factors, the mean detour factor increases accordingly with means of $M_{1.5} = 1.25$ ($SD_{1.5} = 0.11$), $M_2 = 1.31$ ($SD_2 = 0.22$), $M_3 = 1.33$ ($SD_3 = 0.23$), $M_4 = 1.34$ ($SD_4 = 0.23$), $M_5 = 1.34$ ($SD_5 = 0.23$) for weights factors of 1.5, 2, 3, 4, and 5, respectively. At the maximum weight factor of 5, the minimum and maximum observed detour factors are 1.09 and 2.42. It is evident that the increase in mean detour factor drastically slows beyond a weight factor of 3—in fact, most change in mean detour factor occurs between factors 1 and 2. After initial sensitivity analyses, a weight factor of 3 has been used within the travel time savings study [3] as it strikes a good balance of predominantly following high-capacity infrastructure with shortest-paths within high-density areas such as city centres.

When continuing the analysis of detour factors with $wf = 3$, it is evident that the detour factor is also heavily dependent on any given station-to-station distance, as illustrated by Figure 4.3b. There are substantial differences in the distribution of mean detour factors when taking distance into account, with longer flight paths having lower detour

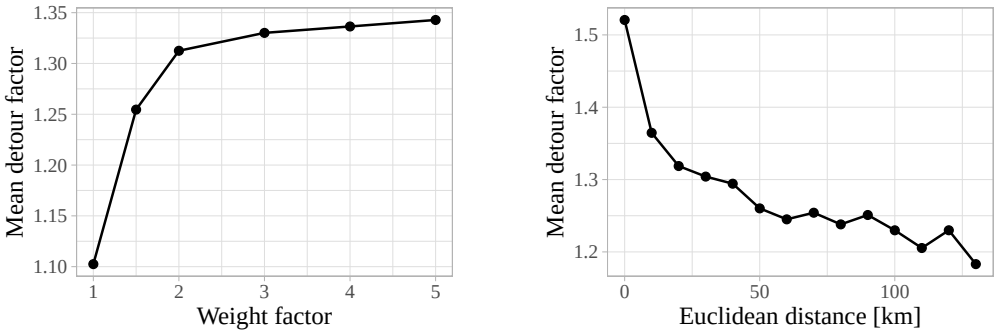

(a) Mean detour factors using different weight factors.

(b) Mean detour factors over Euclidean distance for $wf = 3$.

Figure 4.3: Impact of weight factor and Euclidean distance on mean detour factors in MUC.

factors when compared to shorter ones. While the detour factor for Euclidean station-to-station distances of below 10 km averages $M = 1.52$ ($SD = 0.35$), the mean detour factor for the distance band 130–140 km yields $M = 1.18$ ($SD = 0.05$), highlighting the reduction of mean detour factor but also the reduction in standard deviation. For distances of 50–60 km, the mean detour factor is $M = 1.26$ ($SD = 0.15$). As generating flight paths using shortest path algorithms does require substantial computational resources, this detour factor analysis should allow future research to use Euclidean station-to-station distances with relatively detailed detour corrections—avoiding having to apply least-cost path finding.

4.2 Operational and Market Aspects

Advancing on the analyses presented by Rothfeld *et al.* [3], the following sub-sections take up the topics of passenger pooling and the sensitivity of required travel time savings. The former, in particular, is frequently mentioned as a field of research that warrants further investigation and prove to be essential for the feasibility and/or sustainability of UAM.

4.2.1 Potential for Passenger Pooling

Even though the original analysis [3] purposefully did not include passenger-pooling, based on the non-simulation approach of the study and the difficulty of scaling down UAM vehicle capacity (see Section 3.2.6), a results-based analysis of pooling potential can still be provided. Given the above-mentioned UAM trip demand within MUC for base-case assumptions, the percentage of combinable trips should give an indication of whether UAM pooling might be viable. The base case, in this case, was defined to be a UAM system with 24 stations, 15 minutes process time, and 180 km/h cruise flight speed (see [3, p. 9] for further specifications). Similarly to the functioning of the current dispatching algorithms (see Section 3.1.2 on page 34), any given trip's flight is deemed shareable if at least one other trip is occurring within a given time frame (e.g. 15 min) that

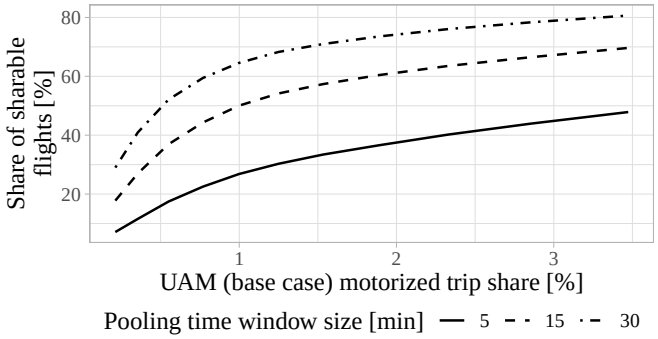

Figure 4.4: Percentage of UAM trips in MUC under UAM base-case assumptions that could be combined with at least another trip within a given time frame.

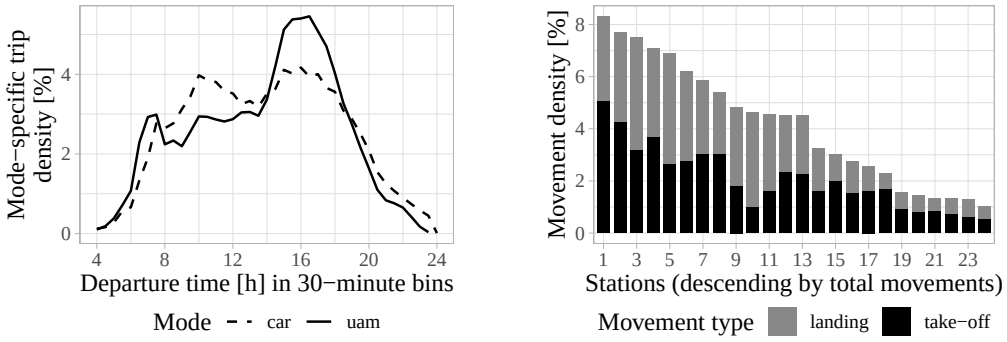

(a) Trip departure time distribution over time of day in 30-minute bins.

(b) UAM station utilization, ordered by number of movements.

Figure 4.5: UAM trip distribution in MUC under base-case assumptions for minimum travel time savings ratio of zero.

has matching origin and destination UAM stations. Figure 4.4 illustrates the percentage of shareable flights over UAM trip share. UAM motorized trip share ranges up to 3.47% in MUC (see [3]).

Comparing the three different pooling time window sizes of 5, 15, and 30 minutes, it is evident that the percentage of shareable flights increases with the time window size. At a UAM motorized trip share of 1% for example, the percentages of shareable flights are 28%, 50%, and 65%, respectively for 5-, 15-, and 30-minute time windows. Further, with higher UAM motorized trip shares (i.e. more UAM trips), the potential for passenger-pooling also increases. While—at a motorized trip share of 0.2%—only 7% (5 min), 18% (15 min), and 29% (30 min) of trips have shareable flights, whereas 48% (5 min), 70% (15 min), and 81% (30 min) can be observed for a motorized trip share of 3%. Thus, given sufficient demand (e.g. above 0.5% motorized trip share) and passenger's willingness to share flights with a potentially prolonged waiting time, great potential for UAM passenger-pooling can be observed within MUC.

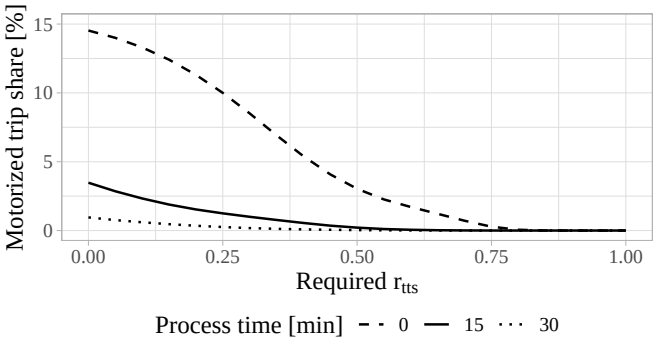

Figure 4.6: Sensitivity of UAM motorized trip share with increasing minimum required r_{tts} for different process times.

The relatively high potential for passenger-pooling is aided by the non-uniform distribution of UAM trips over the observed day and stations, as illustrated by Figures 4.5a and 4.5b. The more UAM trips are concentrated within peak-times and from and to only few, high-demand stations, the higher the change to find combinable trips. Given the requirement for matching origin and destination stations, increasing the number of stations within a study area without a corresponding increase in overall UAM trips would lead to a decrease in the percentage of shareable flights. This could drastically be influenced by introducing en-route passenger pick-up and drop-off, as is being done with ground-based shared ride-hailing. In contrast to ground-based ride-hailing, however, each take-off and landing operation for UAM vehicles take up a substantial part of overall travel time and, more importantly, of the vehicle's stored energy reserve. A further addition to pooling could be the introduction of pooling-including passenger routing strategies. Meaning, routing strategies (see Section 3.1.2 on page 29) which actively select origin and destination UAM stations to increase the share or likelihood of combinable trips.

4.2.2 Motorized Trip Share Sensitivity

The initial analysis [3] assumes every motorized trip, for which UAM does save travel time, as a potential UAM trip. The saving, though, could be a miniscule difference that, in actual transport behaviour, would most likely not led to a change in mode. Increasing the required travel time saving of UAM over the respective ground-based mode could provide an insight on the UAM's motorized trip share if additional factors, like pricing, would be included. Figure 4.6 illustrates the sensitivity of UAM motorized trip share based on an increasing the minimum travel time savings ratio r_{tts} that is required—in contrast to the static requirement of $r_{tts} > 0$ applied previously (see [3]). The travel time savings ratio describes the relative travel time savings that UAM provides over the original transport mode, i.e. a ratio of zero means UAM is just competitive to the original travel time, while a ratio of, say, 0.5 indicates that UAM provides a 50% time saving.

Figure 4.6 shows how UAM motorized market share for MUC develops as the minimum required travel time savings ratio increases from zero to one with variations in process

time—i.e. the combined passenger waiting, pre- and post-flight, and (de-)boarding times. Especially for a minimum required r_{tts} of zero, the impact of shorter process times is immense. Without process time, nearly 15% of motorized trips would see UAM travel time savings—against 3% with 15 minutes process time. Assuming a 50% travel time saving ($r_{tts} > 0.5$) is required before a mode change to UAM would occur, the overall share and, with it, the difference between process times diminishes with 3% motorized trip share without process times and below 1% for 15 minutes. No other analysed variable—be it cruise flight speed, number of UAM stations, or flight path routing—has such an immediate impact on potential shares as process times.

4.3 Spatial Analyses

While the impacts of UAM on travel times has been discussed (see [3]), the spatial distribution have not yet been analysed. For UAM though, particular local circumstances and topography might be a major factor in whether UAM could be feasible. For example, Rothfeld *et al.* [3] note that "more localized analyses of the study areas' ground infrastructure and topography might lead to particular flight connections that prove to be useful despite being, e.g., short-range." The following provides further detail on the distribution of time savings benefits within MUC.

4.3.1 Accessibility Impact

Introducing UAM into the study area of MUC is expected to impact the study area's internal accessibility. Based on Geurs and Wee [91] and similar to Arellano [17], each zone's accessibility has been calculated using the following potential accessibility measure (see Equation 4.1):

$$A_i = \sum_{j=1}^{n} D_j e^{-\beta c_{ij}} \tag{4.1}$$

where, according to [91], "A_i is a measure of accessibility in zone i to all opportunities D in zone j, c_{ij} the costs of travel between i and j, and β the cost sensitivity parameter." The study area's combined number of unique facilities (e.g. home, work, and shopping locations) provided the number of opportunities per zone. Travel times between all zones' centroids (i.e. geographical centres) have been used as the cost parameter, with the cost sensitivity parameter being set to $\beta = 0.2$, which—according to Arellano [17]—is "consistent with several other studies." Travel times from each zone to each other zone has been calculated for modes car, PT, and UAM. First, each zone's base accessibility was calculated using the lowest ground-based mode's (i.e. car or PT) travel time as cost. Secondly, each zone UAM-including accessibility resulted from repeating the calculation using UAM's travel time as cost if it time was lower than the ground-based one. Finally, the increase in accessibility has been derived by dividing the accessibility difference by the base accessibility.

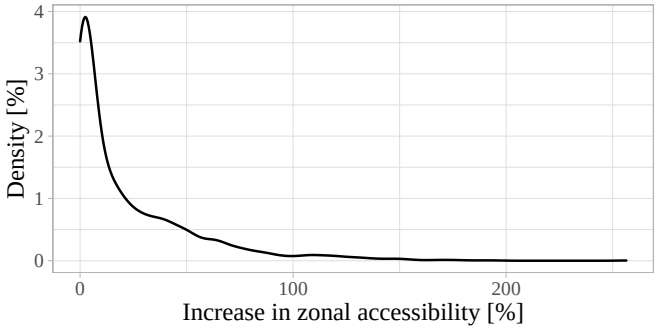

Figure 4.7: Density of change in accessibility per zone in MUC.

Figure 4.7 illustrates the distribution of zonal accessibility increase within MUC after the introduction of UAM under base-case assumptions (i.e. 14 stations, 180 km/h cruise speed, 15 min process time; [3, p. 9]). While 97% of all zones ($N = 2714$) in MUC do experience an increase in accessibility, the majority of zones' accessibilities increase by less than 10%; a median accessibility increase of 9.5% could be observed. The third quartile with $Q_3 = 34.3\%$ and the maximum zonal accessibility increase of 256.5% indicate that there are some zones whose accessibility benefits greatly from the introduction of UAM.

The spatial distribution of this observed accessibility increase, as illustrated by Figure 4.8a, naturally reflects the distribution of mean travel time savings ratios as presented by Rothfeld *et al.* [3, Figure 10a]. Naturally, since the number of opportunities has not changed with the introduction of UAM, leaving only travel time as the impacting factor—of which the travel time savings ratio is a descriptive representation. The areas benefiting the most in terms of accessibility by UAM can be found on the outskirts of Munich, around UAM stations north-east of the city, and at the south-western border of the study area. The four larger cities surrounding Munich (i.e. Rosenheim, Augsburg, Ingolstadt, and Landshut) experience only limited increases in overall accessibility.

4.3.2 Time Savings Distribution

Figure 4.8b illustrates the percentiles of mean travel time savings ratio of originating UAM trips per zone for MUC under UAM base-case assumption, in order to identify regions that would benefit most in terms of UAM travel time savings. For each zone, all travel time savings ratios (r_{tts}) of originating UAM trips, under base-case assumptions, have been averaged and put into relation with the remaining zones. Divided into four percentile categories, the first, second, third, and fourth quarter, Figure 4.8b shows whether a zone's mean ratio is, for example, above or below average (i.e. 50^{th} percentile) or expected to benefit greatly (i.e. above 75^{th}) or very little (i.e. below 25^{th}) from the introduction of UAM in terms of travel time savings.

Evidently, the zones, that would see the most time saving benefit through UAM, are the fringe zones of the study area. In particular, the areas north of Augsburg, west of Landshut and Rosenheim, and east of Augsburg. One additional aspect attracts atten-

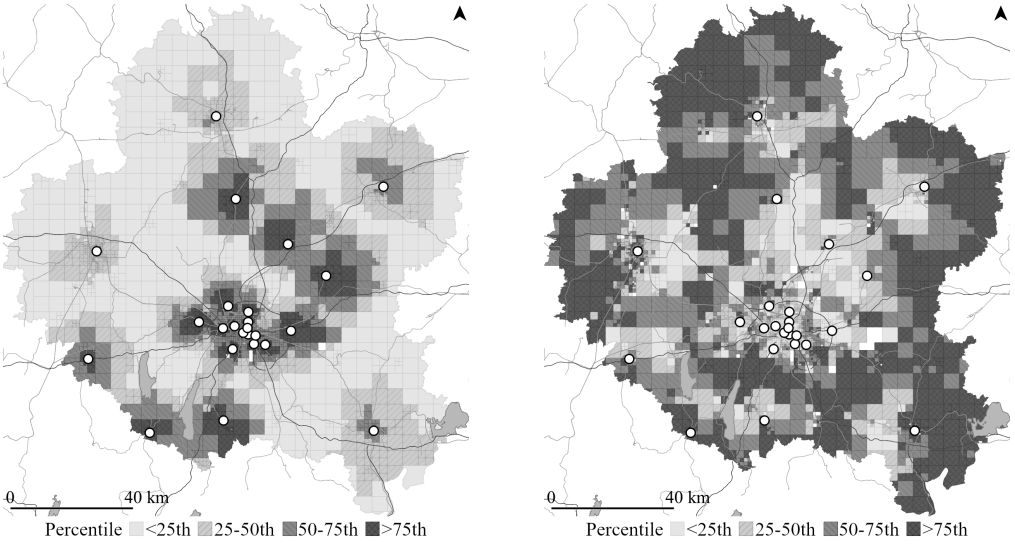

(a) Accessibility increase. **(b)** Zones' median r_{tts}.

Figure 4.8: Distributions of accessibility increase and median travel time savings ratios at UAM base-case assumptions per zone in MUC.

tion, though: on average, the more rural areas—the ones where no stations have been places—represent most of the upper percentile zones. This provides a stark contrast to the previously-discussed distribution of accessibility improvement shown in Figure 4.8a, which is heavily concentrated around Munich city-near and rural UAM stations. The primary factor for this contrast is the difference in what both indicators are based on. While accessibility only includes travel time improvements and that for all zone-to-zone combinations, mean travel time savings are naturally weighted by the number of trips and are heavily influences by the majority of trips for which UAM would result in longer travel times (i.e. negative savings ratios). This could indicate that the more rural, station-distant zones have substantial higher shares of trips that would see UAM travel time savings, despite also being the zones that see a lesser impact on travel times compared to station-near zones. Naturally, the more densely-populated zones also contain high shares of very short, UAM-unsuitable trips. Based on this, it might be advisable to not place stations using number of trips-based weights, but to include trip distances and speeds, if the goal of a potential UAM implementation is time savings maximisation.

4.3.3 Points of Interest Isochrones

In addition to overall accessibility and savings ratios, travel times to main Points of Interest (POIs) within MUC allow a less abstract evaluation. Main POIs are assumed to be the study area's most-populated Central Business District (CBD) and its primary international airport. A comparison of ground-based modes' POIs access speeds proceeds an evaluation of UAM's impact.

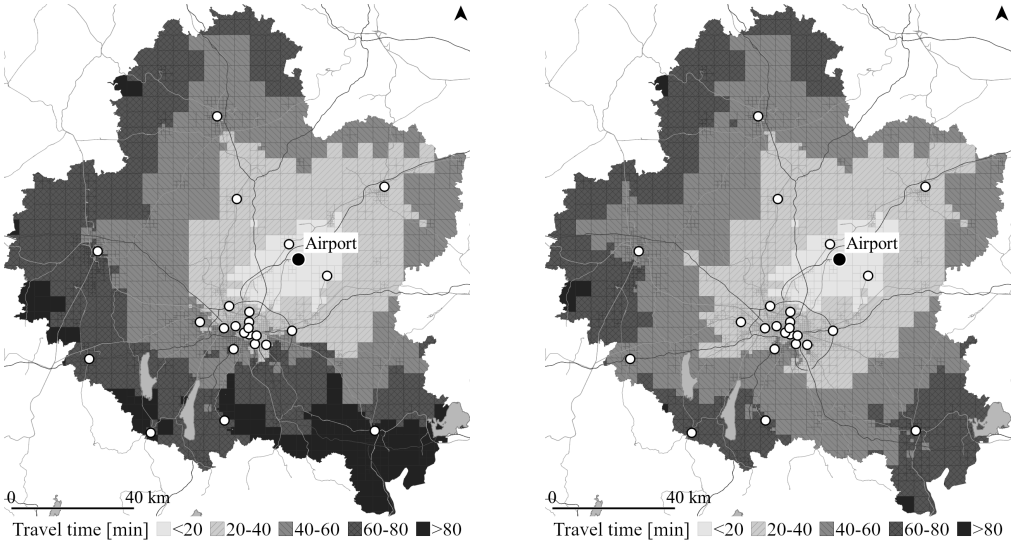

(a) Peak airport access times. **(b)** Off-peak airport access times.

Figure 4.9: Access travel times to MUC's airport via car during peak and off-peak hours.

Ground-based Modes. Travel times from each zone's centroid to the two POIs, i.e. CBD and MUC airport, have been been calculated. Figure 4.9a, for example, illustrates each zone's car travel time towards MUC airport at peak hour (i.e. at 17:00). Clearly, travel times increase with increasing distances to the destination. Also, non-circular shapes of travel time bands can be observed, which follow along existing car infrastructure; highways in particular. Figure 4.9b, in contrast to Figure 4.9a, depicts off-peak car travel times (i.e. at 12:30). When comparing the two figures, the travel time difference is especially noticeable along the south, i.e. for zones whose airport access route has to pass through or around the city of Munich itself.

The difference between peak and off-peak travel times is minimal when comparing the travel time difference between car and PT for MUC, as illustrated by Figure 4.10 with visualisation of car and PT travel times per zone towards Munich's CBD. While car access times are semi-concentric along the highways, PT access times drop sharply with increasing distance to urban centres. Apparently, Munich and surrounding cities, such as Augsburg, Ingolstadt, and Landshut have adequate PT connections towards the city centre. The highest access times can be observed in the more rural areas in-between the mentioned urban centres.

Using these calculated travel times towards POIs in MUC, a simplified linear regression for estimating travel speeds can be established as presented in Table 4.1. The linear regression model for estimating car and PT travel speeds in km/h for accessing POIs in MUC (Equation 4.2) can be written as:

$$\hat{v_{car/pt}} = \beta_1 ln(d_e) + \beta_2 mode_{pt} + \beta_3 destination_{cbd} + \beta_4 ln(d_e) * destination_{cbd} + \beta_5 mode_{pt} * destination_{cbd} + \alpha \tag{4.2}$$

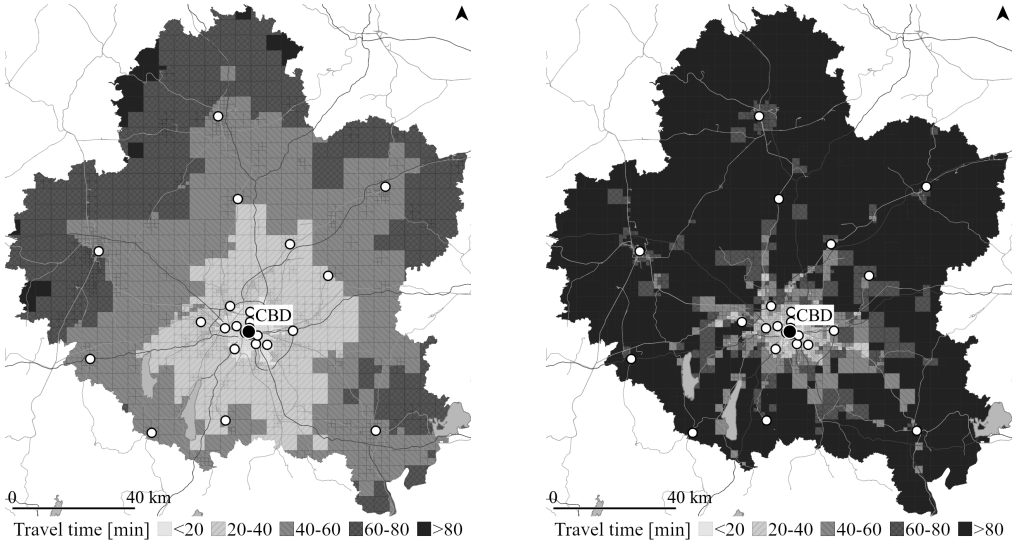

(a) Car access times. **(b)** PT access times.

Figure 4.10: Access travel times to MUC's CBD via car and PT.

where:

- $ln(d_e)$ is the natural logarithm of Euclidean travel distance in kilometres
- $mode_{pt} = 1$ corresponds to PT as the mode of transportation and $mode_{pt} = 0$ to car usage
- $destination_{cbd} = 1$ corresponds to the destination locations being MUC's CBD and $destination_{cbd} = 0$ to the destination being MUC's airport.
- *alpha* is the constant (or interception point)

The regression allows to estimate car and PT access travel speeds towards MUC's airport or CBD. Regression models for airport access speeds for Munich and other European cities have been presented by an earlier study [1, Table 3]. Since this previous study used Google Maps data, a comparison between the models' estimates might highlight the similarity or difference of both, Google Maps' and the MATSim MUC scenario's estimations. Figure 4.11 plots the access speed estimations of Table 4.1 against the same estimations of variation (2) by Rothfeld *et al.* [1, Table 3]. Both models do not distinguish by time of day but, primarily, by Euclidean trip distance and mode.

Evidently, the Google Maps-based model [1, Table 3, variation (2)] estimates higher access speeds when compared to the access speed estimation of the before presented model (Table 4.1) for car usage. This might stem from the exclusion of time of day since the Google Maps-based models include trips that have been gathered throughout all times of day, including night time where, usually, no congestion is experienced. The simulation-based model, however, was estimated using only two times of day, i.e. peak

Table 4.1: Access travel speed regression model towards POIs (i.e. airport or CBD) in MUC via car and PT.

Coefficient	Notation	*Dependent variable:*
		speed [km/h]
$ln(d_e)$ [km]	β_1	4.62***
		(0.51)
$mode_{pt}$	β_2	13.41***
		(0.13)
$destination_{cbd}$	β_3	−6.91***
		(0.75)
$ln(d_e)$ [km]:$mode_{pt}$	β_4	−5.24***
		(0.19)
$mode_{pt}$:$destination_{cbd}$	β_5	3.30***
		(0.37)
Constant	α	4.62***
		(0.52)
Observations		10,255
R^2		0.76
Adjusted R^2		0.76
Residual Std. Error		8.71
Degrees of Freedom		10,249
F Statistic		6,565.10***
Note:		*p<0.1; **p<0.05; ***p<0.01

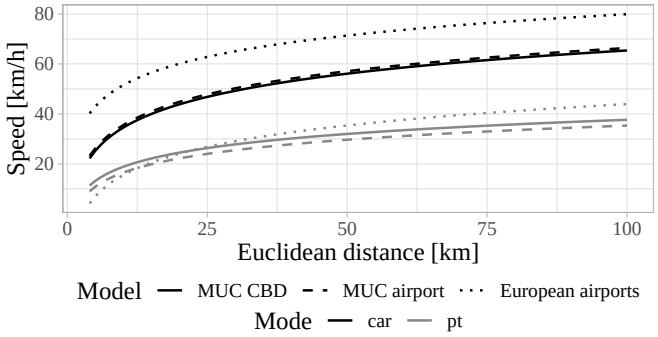

Figure 4.11: Access speed estimation comparison between models from simulated trips in MUC with access trips to the city's CBD and airport and from Google Maps travel time calculations presented by Rothfeld *et al.* [1, Table 3].

and off-peak—while off-peak time at 12:30 still resembles average traffic volumes. For PT travel speeds, though, the simulation-based estimates are close to the Google Maps-based ones.

Impact of UAM Introduction. For evaluating the impact of UAM on the accessibility of POIs, the travel time savings of UAM, under base-case assumptions [3, p. 9] of passengers experiencing process times of 15 minutes in total with a UAM vehicle cruise speed of 180 km/h, over car usage are evaluated. Figure 4.12 illustrates time saved from each of MUC's zones towards Munich's CBD when using UAM with four, 24, and 130 stations. The figures illustrate that, both, the coverage as well as the range of travel time savings increase with an increasing number of stations. While 17% of MUC's zones experience time savings with four stations, 36% and 50% of zones experience UAM time savings for 24 and 130 stations, respectively. For those travel time savings, the median and maximum time savings of UAM over car usage are -19 and 18 minutes for two stations. With 24 stations, the median and maximum are -5 and 21 minutes, increasing to one minute and 32 minutes with 130 stations. Interestingly, the maximum achievable travel time savings towards the city centre are relatively constant over the various number of stations around 20–30 minutes.

For all numbers of stations, from four to 130, the utilised UAM station placement algorithm [3, pp. 5] always placed a station near Munich's CBD. Having accessible origin and destination UAM stations heavily impacts the expected UAM travel time. Figure 4.13 illustrates zonal travel time savings ratios for accessing Munich's airport, where the nearest UAM station—in contrast to Munich's CBD—is not located directly at the actual destination. This shows with there only being few zones that would benefit from the introduction of a four-station UAM system in terms of travel time savings. At four stations, the nearest station to the airport is within Munich's CBD, 27 km away. At four stations, 9% of MUC's zones experience travel time savings ($median = -27min$, $max = 12min$). With 24 stations, 30% of zones have travel time savings with median

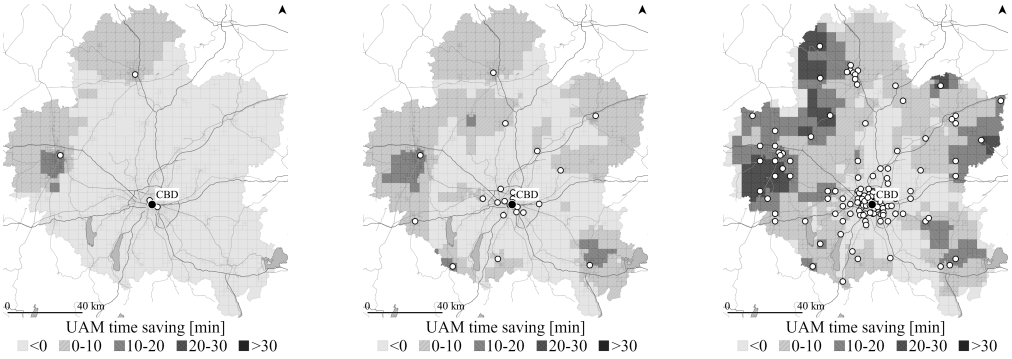

(a) Difference with four stations.

(b) Difference with 24 stations.

(c) Difference with 130 stations.

Figure 4.12: Travel time savings of UAM (base case) over car-usage in minutes per zone in MUC for various station numbers towards Munich's CBD.

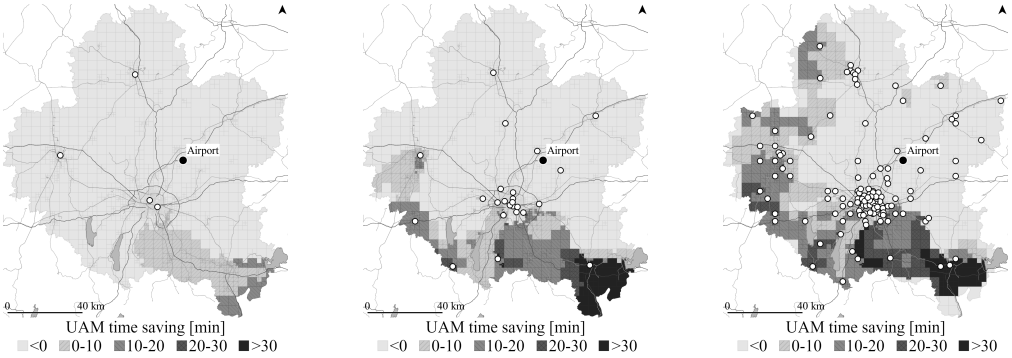

(a) Difference with four stations.

(b) Difference with 24 stations.

(c) Difference with 130 stations.

Figure 4.13: Travel time savings of UAM (base case) over car-usage in minutes per zone in MUC for various station numbers towards Munich's airport.

and maximum of -8 and 49 minutes. For 130 station, it is a 45% zone coverage with median and maximum savings of -2 and 56 minutes.

For airport access, the study area regions that were previously identified as having high access times along the south of the study area benefit most from the introduction of UAM. Again, those are the zones from which one has to pass through or around the city of Munich for accessing the airport. Without a widespread UAM station network, such as 130 stations, time savings by UAM only seem realisable for specific pre-defined routes which have dedicated, close, and well-connected UAM stations. To make main POIs accessible via UAM while providing travel time savings over ground modes requires UAM stations in direct proximity of said POIs.

4.4 Station Placement & Throughput

As seen from the isochronic maps of POIs, the importance of UAM station placement for achieving travel time savings can not be overstated. The following elaborates further on station placement and adds a new aspect to the analysis, that of station throughput and space requirement.

4.4.1 Placement Comparison

Regarding the study area of MUC, two further studies provided precise station locations. Ploetner *et al.* [24] used local experts to qualitatively place UAM stations within MUC based on their judgment, while Arellano [17] used a multi-layered, quantitative approach. Arellano gathered expert judgement within a Delphi process—combined with the Analytic Hierarchy Process (AHP)—in order to create an artificial, normalised, and densified location suitability weight; advancing the earlier UAM station suitability study by Fadhil [15]. Arellano's location suitability weight combined factors such as population density, median income, existence of major transport nodes, and pre-existing noise levels. When comparing the experts' individual weights, however, one can observe limited consistency in-between the experts. Even more so, when also consulting the proceeding AHP-Delphi study [15], where low levels of agreement on factor's weighting in-between the experts could also be observed. Thus, this process was simplified by using the density of trip origins and destinations as the sole factor for station placement suitability in the impedance-minimization station-allocation algorithm that has been developed jointly with Arellano [17] and re-applied in the appended travel time savings analysis [3]. A further difference to the station placement procedure of Arellano lies in the combination of points along a evenly-spaced grid as well as manually-placed points for potential UAM station locations.

Figure 4.14a shows 24 stations placed by Ploetner *et al.* [24] over the same number of stations allocated by the revised impedance-minimization algorithm [3]. The hand-placed stations can be categorised roughly into four categories: transportation, attractions, companies, and communities. For example, stations labelled 1–6 are transportation related with station (1) and (2) being Munich's Ost- and Hauptbahnhof. Station (3) is located at Augsburg Hauptbahnhof, station (4) at the rail station Ingolstadt Nord, station (5) is near Landshut Hauptbahnhof, and station (6) has been placed at Munich's airport. Stations 7–9 are located in proximity to attraction such as the Dachau concentration camp (7), and football stadiums (8,9). Companies are covered by stations such as the ones labelled (10–13); station (10) has been placed at the premises of MTU Aero Engines AG, stations (11) and (12) both being Airbus SE properties, and station (13) being located at the Audi AG facilities near Ingolstadt. Finally, further communities and cities have been considered by Ploetner *et al.* [24]. Stations, such as (14) at Rosenheim, (15) at Starnberg, or (16) at Landsberg am Lech represent this fourth category. Similarities between the hand-placed network and the revised algorithm-produced one lie specifically in the coverage of Munich's city centre and the larger cities surrounding Munich, such as Augsburg, Ingolstadt, Landshut, and Rosenheim—though, the computer-placed sta-

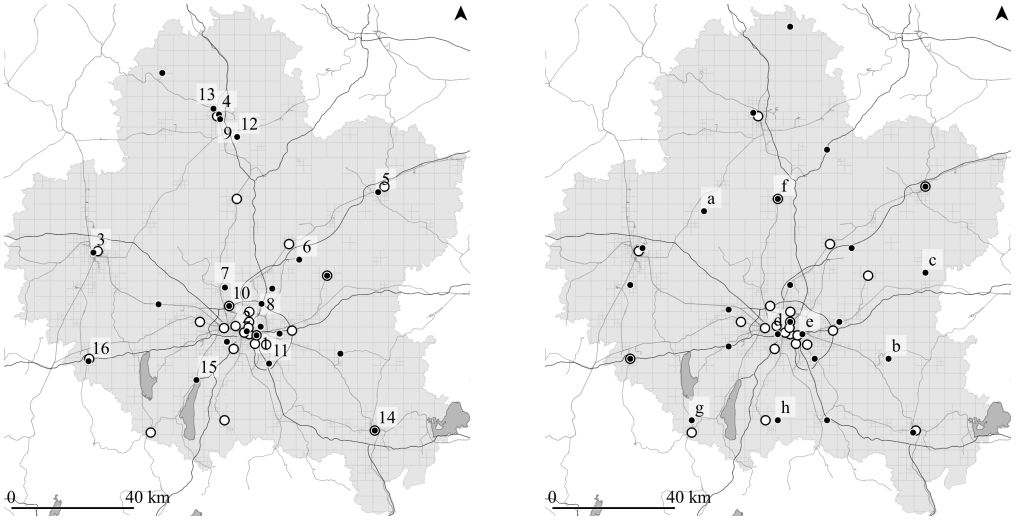

(a) Stations by Ploetner *et al.* [24] (black points) over those by Rothfeld *et al.* [3] (white circles).

(b) Stations by Arellano [17] (black points) over those by Rothfeld *et al.* [3] (white circles).

Figure 4.14: Station placement comparison for 24 station within MUC.

tions usually gravitate more towards the city centres rather than be placed at the city's respective main stations. Differences can be observed in the expert's consideration of attractions and companies. The computer-generated network did not result in stations placed near the before-mentioned memorial site or sport arenas. Also, with the exception of the MTU Aero Engines AG station (10), the computer-placed UAM stations do not seem to cover particular companies' production facilities. Overall, however, when comparing both networks' station placements, a similar distribution can be observed.

Figure 4.14b shows the difference in station placement for 24 stations between the initial impedance-minimization algorithm by Arellano [17] and the revised, simplified re-application [3]. Arellano's stations form semi-concentric rings around Munich by combining—by now—common station locations such as Augsburg, Ingolstadt, Landshut, and Rosenheim with more rural station locations, such as, for example, stations (a), (b), and (c). Arellano's approach of combining multiple data layers into a weighted average led to a wider spatial distribution of stations which also shows in the difference in Munich city centre station density. While, both, the manual [24] and simplified algorithm-based [3] station placements led to many stations being in/around Munich itself, Arellano's station placement provides fewer station within Munich. Stations (d) and (e) cover the west and east parts of Munich's CBD, yet are not located at or near major transportation nodes such as Munich's main station. As Arellano [17] exclusively used evenly-spaced points on a grid as potential station-allocation locations, it would be chance if those regular points would align with POIs, e.g. train stations. In contrast to the manual stations [24], both algorithm-based networks share, for example, a station (f) in-between Ingolstadt and Munich and two stations (g,h) being located at the southern study area

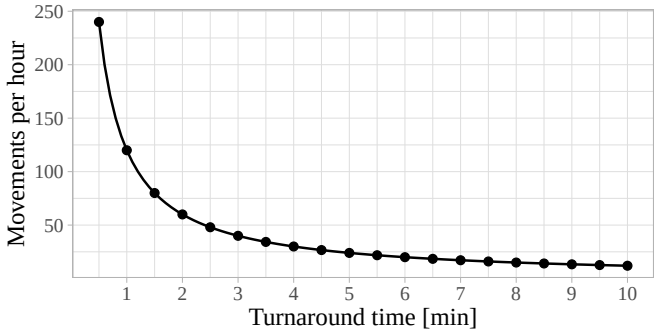

Figure 4.15: Number of possible movements per landing pad occupation time, inspired by Vascik [92, p. 145].

border, east and west of lake Starnberg. Still, when comparing all three discussed networks, Arellano's deviates from the other two with a lesser focus on Munich's city centre and placing more station in rural areas.

4.4.2 Throughput & Requirements

So far, UAM market studies have mostly focused on potential trip shares from a demand-side perspective. UAM infrastructure restrictions, in particular the capacities of UAM stations, have rarely been considered. Rothfeld *et al.* [3] also estimate infrastructure-unrestricted potential UAM demands; though, a post-result analysis does allow to gauge the required station infrastructure where the estimations to be realized.

The examined MUC scenario was used with a 25% sample size that included 3.8 million trips [3, p. 4]. Thus, 15.2 million trips are expected to occur within the non-sampled study area of which 67% are motorized trips [3, p. 7]—resulting in 10.2 million motorized trips within MUC for an average day. Now, assuming UAM motorized trip shares of up to 3% [3, pp. 9], would result in around 300,000 UAM trips per day. Each one of these trips denotes one take-off and one landing movement, resulting in a total of 600,000 movements. Given UAM base-case conditions [3, p. 9], up to 8.3% of all movements were operated at MUC's busiest UAM station (see Figure 4.5b). Over the course of one day, this station would serve up to 25,000 take-off and/or landing movements in total. If we combine this with the busiest hour in terms of UAM movements in MUC, in which 5% of movements occur, this station would have to allow for the operation of 1,250 movements within 60 minutes.

Any take-off, processing, and landing operation occupies any given UAM station's landing pad for a given duration, similar to aircraft's TAT. Figure 4.15 illustrates the number of movements (i.e. take-off or landing) over the assumed TAT for UAM's—i.e. the UAM vehicle's occupation time of said landing pad. This TAT comprises two movements, an initial landing and a following take-off, separated by passenger (de-)boarding. Vascik [92, pp. 144], for example, assumed a five minute TAT for UAM. One landing pad would then allow for 24 movements. Given the 1,250 movements to be operated, MUC's busiest station would need to provide 52 independent UAM take-off and landing pads.

Assuming a circular landing pad with a diameter of 18.75 meters [15, Table 2.3], these 52 pads alone would require an area of up to six hectares. In comparison, an ordinary football field requires between 0.7–1 ha. Granted, the selected station at peak times represent an edge case. Assuming a UAM motorized trip share of 1%, at the median station with 4.5% of overall movements during the median hour (2.6% of daily movements) results in 120 movements within 60 minutes. For a station with one landing pad, the TAT would have to be equal to or below one minute. If we remain with the assumption of a TAT of five minutes, the station would require five independent pads for the off-peak number of trips and a minimum of 0.6 ha.

4.5 Interpretation & Discussion

Beginning with the just-mentioned space requirements for UAM stations of only medium size, it seems that station capacity will be a highly limiting factor for UAM. Often-discussed rooftop stations might not be able to provide substantial throughput that allows for more than just occasional VTOL operations. Similarly, Straubinger *et al.* [8, p. 10] conclude that "UAM might complement existing mobility system, but due to probable capacity constraints at vertiports, UAM will likely not fully substitute them." In addition to the space requirements, noise emissions and safety considerations might lead to fewer stations being provided in a given area and those stations being placed in less-densely populated areas. Both, fewer and less-accessible stations, would increase access/egress trip times and, thus, reduces the viability of UAM as an alternative transport mode compared to ground-based ones.

Combining UAM infrastructure constraints with the low share of motorized trips that—with regards to travel time—would benefit from UAM must lead to the conclusion that UAM as an on-demand air taxi will not be able to provide mass transport; even before discussing a potential price for using UAM. Arguably, the passenger cost of UAM hinges on novel VTOL aircraft being fully autonomous to allow for a drastic reduction in cost compared to conventional helicopters–yet, even then, it remains questionable whether autonomous UAM operations can reach the same price levels as also-autonomous ground-based ride-hailing. Most likely, UAM will serve specific niche markets where UAM provides substantial time savings over ground-based modes due to, for example, a certain topography or a destination being hard to reach from the ground.

The development of such novel, electrified VTOL vehicles should be somewhat separated from the concept of UAM. While potentially enabling UAM, their possible fields of application exceed the idea of air taxis. If their manufacturers' promises of providing cheaper, safer, and—in terms of noise and greenhouse gas emissions—more sustainable alternatives to helicopters, then surely, electrified VTOL vehicles could and should partly take over and expand the areas of application of conventional helicopters such as for medical emergencies, time-critical deliveries, sightseeing flights, or traffic surveillance. While potentially desirable, these VTOL vehicle usages will not be the desired aide in dealing with current transportation challenges.

As stated in an earlier study, "UAM is aimed at reducing problems facing the growing demand for mobility in an increasingly crowded environment, such as congestion, pollution, and scarcity of urban space" [2, p. 268]. Now, given relatively marginal trip shares and high station capacity constraints, UAM would be unable to alleviate any congestion, significantly reduce transport-related emissions, or decrease inner-city transport-related land use. In select cases, UAM might be a viable option for increasing accessibility of remote or especially rural areas, where passenger pooling could be of great benefit to decrease cost for passengers that already are not excessively time-sensitive.

Despite all, there remains the possibility that UAM does establish itself as an on-demand air taxi for inter- and intra-city transport for a small, select, affluent, and exclusive group of customers—just as is the case with today's on-demand helicopter operation. The provocative questions arises whether we—as a society—desire expanding such air taxi services. Beyond being exciting, allowing inner-city UAM operation might substantially increase local transport-related noise emissions and, arguably, amplify societal inequality [2, Section 4]. While the near future of transportation surely includes electrification, widespread use of UAM—as in commercial, on-demand, inner-city VTOL passenger transport—might, for now, remain science fiction.

5 Limitations & Directions for Future Research

The following can be categorised into two groups: (1) limitations (i.e. desired improvements) of MATSim-UAM [72] and (2) additional UAM-related studies that might be independent of the UAM-extension. While the former focuses on framework additions or changes within the extension's code, the later provides ideas for additional analyses that warrant further investigation.

5.1 Further Development of UAM-extension

MATSim as a mesoscopic transport simulation framework combines the modelling of multiple transportation modes and vehicle types, such as walking, cars, PT, SAVs, and UAM. It is in the best interest of any framework that combines wide facets of functionality that the detail of each subpart remains comparable, in balance, with the others. The following topics offer ideas for further UAM-extension development.

Dispatching & relocation:

- Include en-route UAM vehicles in dispatching, based on their estimated time of arrival. Currently, only idle vehicles are considered during dispatching. Waiting for an exemplary en-route UAM vehicle might be preferable over ordering an empty relocation flight in terms of system efficiency, waiting time, and/or sustainability.
- Include active relocation of UAM vehicles during idle or off-peak hours. Currently, idle vehicles remain at their last passenger trip's destination station. Steering relocation flights based on expected demand might reduce passenger's waiting times.
- Include the ability to distinguish between various UAM vehicle types within the dispatching algorithm. Currently, vehicle types are only considered in terms of mission range; no active decision is being taken to pair passenger transport requests with the, e.g., most efficient vehicle type for said request. See also the relevant paragraph in Section 3.2.6 on page 55.
- Allow for passenger request rejections in line with other on-demand MATSim studies (e.g. by Militão [67]). Currently, all passenger requests are being fulfilled even

if the overall UAM system efficiency suffers greatly from, e.g., far-away transport requests.

- Implement maximum waiting times for UAM vehicles or other pooled passengers. Even though no such waiting time limits are currently implemented, agents do change their chosen route/mode in following MATSim iterations if they experienced long waiting times. Still, including a pooling time window might provide a more realistic modelling of shared UAM flights.
- Allow for en-route pooling and pooling-focused UAM routing, as discussed at the end of Section 4.2.1 on page 64.

Station & vehicle modelling:

- Enhance station modelling with capacity constraints. Currently, there are only rudimentary measures for a station's vehicle in- and outflow through the capacities of the network's links. Stations could be modelled with fixed number of gates, landing pads, taxiways, and queues for passenger processes. Since infrastructure capacity constraints have been identified as a potential bottleneck of UAM operation, their inclusion might enrich the results gained from using MATSim-UAM [72].
- Include energy storage/usage and payload-range trade-off for UAM vehicles. Currently, vehicle types have a fixed maximum range, regardless of a flights payload or previous the vehicle's previous flight or the time in-between them. Vehicles could be extended by having energy storage which deplete over usage time and are refilled while being idle. This might be specifically interesting when comparing the transport performance of vehicles with different types of energy storage, e.g. batteries versus hydrogen tanks. See also the relevant paragraph in Section 3.2.6 on page 56.
- Introduce additional flight phases, such as climb and descent and vehicular acceleration. Currently, UAM flight is modelled using vertical take-off, horizontal cruise, and vertical landing with fixed speeds. Additional, diagonal flight phases and a gradual increase in vehicle speed might provide more accurate UAM travel time estimations. See also the relevant paragraph in Section 3.2.6 on page 56.
- Introduce holding patterns. Currently, en-route congestion for UAM is handled in the same manner as for cars: vehicles remain on any given link until capacity on the subsequent link becomes available. Even though UAM vehicles are VTOL-capable, flying in holding patterns instead of hovering in place might offer a more realistic representation of en-route UAM congestion.
- Enhance the capabilities for vertical and horizontal in-flight UAM vehicle separation. Currently, vertical separation is done via pre-defined flight levels within MATSim networks, with horizontal separation being approximated by using flight links' hourly throughput capacities. Ensuring minimum distances for separation and guiding UAM flights accordingly might again impact UAM's overall system performance.

Optimization & miscellaneous:

- Provide a more time-efficient UAM routing algorithm. Currently, UAM routing, i.e. the selection of access/egress modes and origin/destination stations, is done by brute-forcing all available combinations at the beginning of each simulation. While saving computation time in comparison to re-calculating all possible connections' flight times ad-hoc, en-route congestion will not be included in flight time estimations. Cashing of, for example, intermediate routing results could be used to allow for dynamic (i.e. ad-hoc) flight time calculation without a disproportionate increase in computation time. See also the relevant paragraph in Section 3.2.6 on page 56.

- Provide an eqasim [93] interface. In terms of external mode choice models, UAM-extension currently provides an interface that allows MATSim-external frameworks to configure, start, and analyse UAM simulation; as has been done with MITO [86]. eqasim allows using MATSim with discrete mode-choice models that replace MATSim's own scoring and, when jointly usable with the UAM-extension, would broaden its applicability.

- Provide online documentation and automated testing. While Chapter 3 serves as an introduction to MATSim-UAM [72], extensive online documentation could complement the provided information. Also, automatic code testing would increase the framework's resilience and re-usability. Accessibility, usability, and reach of the UAM-extension would benefit greatly from providing both testing and documentation.

5.2 Further UAM-related Studies

The following list provides ideas or inspiration for follow-up studies in addition to the above-proposed framework enhancements and previously identified topics [3, p. 14]. It is assumed that most of the above-listed enhancements would each warrant their on study once developed; study topics directly related to these enhancements have, thus, been omitted below. However, these topic ideas are not restricted to being based on the UAM-extension—on the contrary, a vast number of UAM-related research questions require non-simulative approaches.

- Application of the UAM-extension on additional study areas. Especially on larger scenarios such Germany or Switzerland in combination with longer-range flight vehicles. UAM is estimated to provide more significant travel time savings with increasing distances (see [3]) and could be competitive with high-speed trains given sufficient flight distances.

- Analysis of UAM usage for for trips by non-locals. Most transport scenarios, so too for MUC, usually only include local population, i.e. agents whose home location lies within the given study area. Trips by non-locals, e.g. tourists or business travellers,

which originate at hotels or major transportation hubs (e.g. train stations and airports), might prove to be suitable for UAM.

- Noise analyses on vehicular and, subsequently, on a spatial level within a study area. One of the most prominent criticism of UAM usage are the expected noise emissions, even though that electrified, distributed propulsion promises noise reductions when compared to conventional helicopters. UAM vehicles' noise levels and their propagation during flight warrant further research.

- Compare on-demand with scheduled UAM operation. The current UAM-extension provides the ability to model and simulate on-demand UAM services, though for selected routes, e.g. CBD to major airports, scheduled services might provide more consistent and reliable travel times. Whether there is are different levels of demand where scheduled services are more efficient than on-demand operation could be of particular interest.

- Advance transport simulation methodology for highly capacity restricted modes. As discussed in Section 3.2.6 on page 57, transport scenarios often use down-scaled population samples as their input agents in order to reduce computational requirements. This down-scaling is then also applied to transport's supply side, which proves to be problematic with, e.g., low-capacity UAM vehicles. Novel approaches might be required to solve or alleviate this issue.

Evidently, the above is not an exclusive list. There are countless more topics yet to be covered, with whole research areas surrounding UAM left to be delved into, such as the engineering of vehicles, the architecture of stations, or the necessity for regulation.

6 Conclusion

This dissertation consolidates and accompanies the research by Rothfeld *et al.* [1] (Appendix A), Rothfeld *et al.* [2] (Appendix B), and Rothfeld *et al.* [3] (Appendix C), focusing on accessibility to and by (urban) aerial mobility. Within the context of the presented research, Urban Air Mobility (UAM) is understood as on-demand operation of novel VTOL aircraft for inter- and intra-urban passenger transport, i.e. sometimes-called air taxis. Said research identified the need for significantly increasing accessibility to conventional aerial mobility [1], documents the state of and provides outlines for UAM-related literature [2], and showed that UAM is not expected to provide significant travel time savings for a majority of daily trips [3]. In particular, this compendium serves as documentation of the functioning and usage of the self-developed, open-source UAM-extension for MATSim, called MATSim-UAM [72], while supplementing previous studies' analyses. MATSim-UAM [72] is an agent- and activity-based transportation modelling framework that enables analyses of comprehensive, multimodal study areas that—besides MATSim's core modes such as car, PT, walking, and cycling—allows the simulation of station-based, on-demand transport modes such as UAM.

High expectations have been placed on UAM for widespread travel time savings and reductions in traffic congestion, while providing a more cost-effective and sustainable transport alternative at the same time. On the basis of existing literature and self-conducted studies, however, UAM might be unable to meet some, if not most, of those promises. Even if one excludes the topic of potential UAM service pricing, UAM provides significant travel time savings only in selected cases. Combined with the limited throughput of space-constrained inner-city UAM station infrastructure, UAM is not believed to be able to provide mass transportation. However, a clear distinction must be made between the viability of these novel, mostly electrified, VTOL vehicles as technological progressions of conventional helicopters—used, for example, for medical emergencies—and their utilisation as air taxis. Though we could soon see such VTOL vehicles in operation, it remains questionable whether we, as common citizens, will be using them on-demand for day-to-day trips in the near future; given our current understanding of and assumptions about UAM. Evidently, however, more research is required in specifying viable fields of application for UAM and in identifying the extents of possible service optimizations, such as passenger pooling. The possibilities of UAM, in its mixture of various technologies and operational concepts, is far from being fully comprehended. It is, thus, hoped that the presented research and the MATSim-UAM [72] framework facilitate and encourage further studies.

Bibliography

[1] R. Rothfeld, A. Straubinger, A. Paul, and C. Antoniou, "Analysis of European airports' access and egress travel times using Google Maps", *Transport Policy*, vol. 81, no. May, pp. 148–162, 2019, ISSN: 1879310X. DOI: 10.1016/j.tranpol.2019.05.021. [Online]. Available: https://doi.org/10.1016/j.tranpol.2019.05.021.

[2] R. Rothfeld, A. Straubinger, M. Fu, C. Al Haddad, and C. Antoniou, "Urban air mobility", in *Demand for Emerging Transportation Systems*, C. Antoniou, D. Efthymiou, and E. Chaniotakis, Eds., 1st, Amsterdam, Netherlands: Elsevier, 2020, ch. 13, pp. 267–284, ISBN: 9780128150184. DOI: 10.1016/B978-0-12-815018-4.00013-9. [Online]. Available: https://linkinghub.elsevier.com/retrieve/pii/B9780128150184000139.

[3] R. Rothfeld, M. Fu, M. Balać, and C. Antoniou, "Potential Urban Air Mobility Travel Time Savings: An Exploratory Analysis of Munich, Paris, and San Francisco", *Sustainability*, vol. 13, no. 4, 2021, ISSN: 2071-1050. DOI: 10.3390/su13042217. [Online]. Available: https://www.mdpi.com/2071-1050/13/4/2217.

[4] European Commission, "Flightpath 2050 - Europe's vision for aviation", Publications Office of the European Union, Luxembourg, Tech. Rep., 2012, p. 28. DOI: 10.2777/15458. [Online]. Available: https://op.europa.eu/s/olDg.

[5] M. Urban, C Jessberger, R. Rothfeld, M Schmidt, V Batteiger, K. Plötner, and M. Hornung, "Multi-Modal Transport Hub Concept for Inner-City Airport Operation", in *DLRK - German Aerospace Congress*, Braunschweig, Germany, 2016.

[6] M. Shamiyeh, J. Bijewitz, and M. Hornung, "A Review of Recent Personal Air Vehicle Concepts", in *Aerospace Europe 6th CEAS Conference*, Bucharest, 2017, pp. 1–16.

[7] R. Rothfeld, M. Balać, K. Plötner, and C. Antoniou, "Initial Analysis of Urban Air Mobility's Transport Performance in Sioux Falls", in *2018 Aviation Technology, Integration, and Operations Conference*, 2018, pp. 1–13, ISBN: 9781624105562. DOI: 10.2514/6.2018-2886.

[8] A. Straubinger, R. Rothfeld, M. Shamiyeh, K.-D. Buechter, J. Kaiser, and K. Plötner, "An Overview of Current Research and Developments in Urban Air Mobility - Setting the Scene for UAM Introduction", *Journal of Air Transport Management*, vol. 87, no. 101852, 2020. DOI: 10.1016/j.jairtraman.2020.101852.

[9] M. Balać, A. R. Vetrella, R. Rothfeld, and B. Schmid, "Demand Estimation for Aerial Vehicles in Urban Settings", *IEEE Intelligent Transportation Systems Magazine*, vol. 11, no. 3, pp. 105–116, 2019, ISSN: 19411197. DOI: 10.1109/MITS.2019.2919500.

[10] E. Lim and H. Hwang, "The Selection of Vertiport Location for On-Demand Mobility and Its Application to Seoul Metro Area", *International Journal of Aeronautical and Space Sciences*, vol. 20, no. 1, pp. 260–272, 2019, ISSN: 20932480. DOI: 10.1007/s42405-018-0117-0. [Online]. Available: https://doi.org/10.1007/s42405-018-0117-0.

[11] L. A. Garrow, P. Mokhtarian, B. German, and S.-S. Boddupalli, "Commuting in the Age of the Jetsons: A Market Segmentation Analysis of Autonomous Ground Vehicles and Air Taxis in Five Large U.S. Cities", in *AIAA AVIATION 2020 FORUM*, Reston, Virginia: American Institute of Aeronautics and Astronautics, Jun. 2020, ISBN: 978-1-62410-598-2. DOI: 10.2514/6.2020-3258. [Online]. Available: https://arc.aiaa.org/doi/10.2514/6.2020-3258.

[12] S. Roy, M. Kotwicz Herniczek, C. Leonard, A. Jha, N. Wang, B. German, and L. A. Garrow, "A Multi-Commodity Network Flow Approach for Optimal Flight Schedules for an Airport Shuttle Air Taxi Service", in *AIAA SciTech Forum*, Orlando, FL, USA, 2020. DOI: 10.2514/6.2020-0975.

[13] M. Fu, R. Rothfeld, and C. Antoniou, "Exploring Preferences for Transportation Modes in an Urban Air Mobility Environment: Munich Case Study", *Transportation Research Record*, 2019, ISSN: 21694052. DOI: 10.1177/0361198119843858.

[14] S. Rath and J. Y. J. Chow, "Air Taxi Skyport Location Problem for Airport Access", pp. 1–22, 2019. arXiv: 1904.01497. [Online]. Available: http://arxiv.org/abs/1904.01497.

[15] D. N. Fadhil, "A GIS-based Analysis for Selecting Ground Infrastructure Locations for Urban Air Mobility", Master's thesis, Technical University of Munich, 2018. [Online]. Available: http://www.msm.bgu.tum.de/fileadmin/w00bvh/www/masterThesis/fadhil{_}2018.pdf.

[16] M. Daskilewicz, B. German, M. M. Warren, L. A. Garrow, S.-S. Boddupalli, and T. H. Douthat, "Progress in Vertiport Placement and Estimating Aircraft Range Requirements for eVTOL Daily Commuting", in *2018 Aviation Technology, Integration, and Operations Conference*, Reston, Virginia: American Institute of Aeronautics and Astronautics, Jun. 2018, pp. 1–11, ISBN: 978-1-62410-556-2. DOI: 10.2514/6.2018-2884. [Online]. Available: https://arc.aiaa.org/doi/10.2514/6.2018-2884.

[17] S. Arellano, "A Data- and Demand-Based Approach at Identifying Accessible Locations for Urban Air Mobility Stations", Master's thesis, Technical University of Munich, 2020.

[18] M. Shamiyeh, R. Rothfeld, and M. Hornung, "A Performance Benchmark of Recent Personal Air Vehicle Concepts for Urban Air Mobility", in *31st Congress of the International Council of the Aeronautical Sciences, ICAS*, Belo Horizonte, Brazil, 2018, ISBN: 9783932182884.

[19] K. R. Antcliff, M. D. Moore, and K. H. Goodrich, "Silicon valley as an early adopter for on-demand civil VTOL operations", in *16th AIAA Aviation Technology, Integration, and Operations Conference*, American Institute of Aeronautics and Astronautics, Ed., ser. AIAA Aviation, American Institute of Aeronautics and Astronautics, 2016, ISBN: 9781624104404. DOI: 10.2514/6.2016-3466.

[20] A. Pukhova, "Environmental Evaluation of Urban Air Mobility Operation", Master's thesis, Technical University of Munich, 2018.

[21] A. Kasliwal, N. J. Furbush, J. H. Gawron, J. R. McBride, T. J. Wallington, R. D. De Kleine, H. C. Kim, and G. A. Keoleian, "Role of flying cars in sustainable mobility", *Nature Communications*, vol. 10, no. 1, 2019, ISSN: 20411723. DOI: 10.1038/s41467-019-09426-0.

[22] C. Al Haddad, E. Chaniotakis, A. Straubinger, K. Plötner, and C. Antoniou, "Factors affecting the adoption and use of urban air mobility", *Transportation Research Part A: Policy and Practice*, vol. 132, no. November 2019, pp. 696–712, Feb. 2020, ISSN: 09658564. DOI: 10.1016/j.tra.2019.12.020. [Online]. Available: https://doi.org/10.1016/j.tra.2019.12.020https://linkinghub.elsevier.com/retrieve/pii/S0965856419303830.

[23] A. Straubinger, U. Kluge, M. Fu, C. Al Haddad, K. Plötner, and C. Antoniou, "Identifying Demand and Acceptance Drivers for User Friendly Urban Air Mobility Introduction", in *Towards User-Centric Transport in Europe 2: Enablers of Inclusive, Seamless and Sustainable Mobility*, B. Müller and G. Meyer, Eds. Cham: Springer International Publishing, 2020, pp. 117–134, ISBN: 978-3-030-38028-1. DOI: 10.1007/978-3-030-38028-1_9. [Online]. Available: https://doi.org/10.1007/978-3-030-38028-1{_}9.

[24] K. O. Ploetner, C. Al Haddad, C. Antoniou, F Frank, M. Fu, S. Kabel, C. Llorca, R. Moeckel, A. T. Moreno, A. Pukhova, R. Rothfeld, M. Shamiyeh, A. Straubinger, H. Wagner, and Q. Zhang, "Long-term application potential of urban air mobility complementing public transport: an upper Bavaria example", *CEAS Aeronautical Journal*, vol. 11, no. 4, pp. 991–1007, Dec. 2020, ISSN: 1869-5582. DOI: 10.1007/s13272-020-00468-5. [Online]. Available: http://link.springer.com/10.1007/s13272-020-00468-5.

[25] N. Syed, M. Rye, M. Ade, A. Trani, N. Hinze, H. Swingle, J. C. Smith, S. Dollyhigh, and T. Marien, "Preliminary Considerations for ODM Air Traffic Management based on Analysis of Commuter Passenger Demand and Travel Patterns for the Silicon Valley Region of California", in *17th AIAA Aviation Technology, Integration, and Operations Conference*, 2017, p. 3082.

[26] M. Balać, R. Rothfeld, and S. Hörl, "The Prospects of on-demand Urban Air Mobility in Zurich, Switzerland", *2019 IEEE Intelligent Transportation Systems Conference, ITSC 2019*, pp. 906–913, 2019. DOI: 10.1109/ITSC.2019.8916972.

[27] A. Pukhova, C. Llorca, A. Moreno, Q. Zhang, and R. Moeckel, "Urban air mobility: another disruptive technology or just an insignificant addition", in *European Transport Conference*, Dublin, Ireland, 2019. [Online]. Available: https://www.bgu.tum.de/fileadmin/w00blj/msm/publications/moeckel/2019{_}pukhovaEtAl.pdf.

[28] R. Goyal, "Urban air mobility (UAM) market study", 2018. [Online]. Available: https://ntrs.nasa.gov/citations/20190001472.

[29] M. Gripsrud and R. Hjorthol, "Working on the train: From 'dead time' to productive and vital time", *Transportation*, vol. 39, no. 5, pp. 941–956, 2012, ISSN: 00494488. DOI: 10.1007/s11116-012-9396-7.

[30] F. S. Koppelman, "Predicting transit ridership in response to transit service changes", *Journal of Transportation Engineering*, vol. 109, no. 4, pp. 548–564, 1983, ISSN: 0733947X. DOI: 10.1061/(ASCE)0733-947X(1983)109:4(548).

[31] M. D. Uncles, M. Ben-Akiva, and S. R. Lerman, *Discrete Choice Analysis: Theory and Application to Travel Demand.* 4. Transportation Studies, 1987, vol. 38, p. 370. DOI: 10.2307/2582065.

[32] M. Fu, A. Straubinger, and J. Schaumeier, "Scenario-based Demand Assessment of Urban Air Mobility in the Greater Munich Area", in *AIAA AVIATION 2020 FORUM*, Reston, Virginia: American Institute of Aeronautics and Astronautics, Jun. 2020, pp. 1–16, ISBN: 978-1-62410-598-2. DOI: 10.2514/6.2020-3256. [Online]. Available: https://arc.aiaa.org/doi/10.2514/6.2020-3256.

[33] A. Moreno, C. Llorca, Q. Zhang, R. Moeckel, and C. Antoniou, "Modeling Induced Demand by Urban Air Mobility", in *mobil. Tum-International Scientific Conference on Mobility and Transport*, 2019.

[34] J. Holden and N. Goel, "Fast-Forwarding to a Future of On-Demand Urban Air Transportation", *San Francisco, CA*, pp. 1–98, 2016. [Online]. Available: https://www.uber.com/elevate.pdf.

[35] S. Baur, S. Schickram, A. Homulenko, N. Martinez, and A. Dyskin, *Urban air mobility The rise of a new mode of transportation*, S. Baur, S. Schickram, A. Homulenko, N. Martinez, and A. Dyskin, Eds., Roland Berger, 2018. [Online]. Available: https://www.rolandberger.com/publications/publication{_}pdf/Roland{_}Berger{_}Urban{_}Air{_}Mobility.pdf.

[36] Y. Liu, M. Kreimeier, E. Stumpf, Y. Zhou, and H. Liu, "Overview of recent endeavors on personal aerial vehicles: A focus on the US and Europe led research activities", *Progress in Aerospace Sciences*, vol. 91, pp. 53–66, 2017, ISSN: 03760421. DOI: 10.1016/j.paerosci.2017.03.001.

[37] A. Kasliwal, N. J. Furbush, J. H. Gawron, J. R. McBride, T. J. Wallington, R. D. De Kleine, H. C. Kim, and G. A. Keoleian, "Role of flying cars in sustainable mobility", *Nature Communications*, vol. 10, no. 1, pp. 1–9, 2019, ISSN: 20411723. DOI: 10.1038/s41467-019-09426-0.

[38] H. Eißfeldt, "Sustainable urban air mobility supported with participatory noise sensing", *Sustainability (Switzerland)*, vol. 12, no. 8, 2020, ISSN: 20711050. DOI: 10.3390/SU12083320.

[39] Z. Jia and S. Lee, "Acoustic analysis of Urban air mobility quadrotor aircraft", *International Powered Lift Conference 2020, IPLC 2020, Held at Transformative Vertical Flight 2020*, pp. 24–40, 2020.

[40] European Union, *Towards sustainable urban air mobility*, 2019. [Online]. Available: https://cordis.europa.eu/programme/id/H2020{_}MG-3-6-2020 (visited on 01/19/2021).

[41] Z. Trattner, *Modeling Future Mobility*, 2016. [Online]. Available: http://www.iaacblog.com/programs/modeling-future-mobility/ (visited on 01/19/2021).

[42] F. Galton, "On the Construction of Isochronic Passage-Charts", *Proceedings of the Royal Geographical Society and Monthly Record of Geography*, vol. 3, no. 11, pp. 657–658, Jan. 1881, ISSN: 0266626X. DOI: 10.2307/1800138. [Online]. Available: http://www.jstor.org/stable/1800138.

[43] E. Weiner, G. E. Gray, and L. L. Hoel, *Urban Transportation Planning in the United States: an Historical Overview Fifth Edition*, Fifth Edit. Washington, DC, 1997.

[44] R. Moeckel, N. Kuehnel, C. Llorca, A. Moreno, and H. Rayaprolu, "Agent-Based Simulation to Improve Policy Sensitivity of Trip-Based Models", *Journal of Advanced Transportation*, vol. 2020, 2020, ISSN: 20423195. DOI: 10.1155/2020/1902162.

[45] M. L. Manheim, *The Challenge of Transportation Systems Analysis*. Cambridge, MA, USA: MIT Press, 1979, pp. 10–57, ISBN: 0262131293.

[46] P. M. Jones, "A new approach to understanding travel behaviour and its implications for transportation planning", Doctoral Thesis, Imperial College London, 1983.

[47] K. W. Axhausen and T. Gärling, "Activity-based approaches to travel analysis: conceptual frameworks, models, and research problems", *Transport reviews*, vol. 12, no. 4, pp. 323–341, 1992, ISSN: 0144-1647.

[48] J. L. Bowman and M. E. Ben-Akiva, "Activity-based disaggregate travel demand model system with activity schedules", *Transportation research part a: policy and practice*, vol. 35, no. 1, pp. 1–28, 2001, ISSN: 0965-8564.

[49] B. Hillier and J. Hanson, *The Social Logic of Space*. Cambridge: Cambridge University Press, 1984, ISBN: 9780521367844. DOI: DOI:10.1017/CBO9780511597237. [Online]. Available: https://www.cambridge.org/core/books/social-logic-of-space/6B0A078C79A74F0CC615ACD8B250A985.

[50] G. E. Moore, *Cramming more components onto integrated circuits*, 1965.

[51] H Van Dyke Parunak, R. Savit, and R. L. Riolo, "Agent-Based Modeling vs. Equation-Based Modeling: A Case Study and Users' Guide BT - Multi-Agent Systems and Agent-Based Simulation", J. S. Sichman, R. Conte, and N. Gilbert, Eds., Berlin, Heidelberg: Springer Berlin Heidelberg, 1998, pp. 10–25, ISBN: 978-3-540-49246-7.

[52] A. L. Bazzan and F. Klügl, "A review on agent-based technology for traffic and transportation", *Knowledge Engineering Review*, vol. 29, no. 3, pp. 375–403, 2014, ISSN: 14698005. DOI: 10.1017/S0269888913000118.

[53] P. Davidsson, L. Henesey, L. Ramstedt, J. Törnquist, and F. Wernstedt, "Agent-Based Approaches to Transport Logistics", in *Applications of Agent Technology in Traffic and Transportation*, 2005, pp. 1–15. DOI: 10.1007/3-7643-7363-6_1.

[54] A. Horni, K. Nagel, and K. W. Axhausen, Eds., *The Multi-Agent Transport Simulation MATSim*. London: Ubiquity Press, Aug. 2016, ISBN: 9781909188754. DOI: 10.5334/baw. [Online]. Available: http://www.ubiquitypress.com/site/books/10.5334/baw/.

[55] A. Horni, K. Nagel, and K. W. Axhausen, "Introducing MATSim", in *The Multi-Agent Transport Simulation MATSim*, A Horni, K Nagel, and K. W. Axhausen, Eds., London: Ubiquity Press, Aug. 2016, ch. 1, pp. 3–8. DOI: 10.5334/baw.1. [Online]. Available: http://www.ubiquitypress.com/site/chapters/10.5334/baw.1/.

[56] F. Zwick, N. Kuehnel, R. Moeckel, and K. W. Axhausen, "PREPRINT - Agent-Based Simulation of City-Wide Autonomous Ride-Pooling and the Impact on Traffic Noise", 2020.

[57] M. Maciejewski, "Dynamic Transport Services", in *The Multi-Agent Transport Simulation MATSim*, A Horni, K Nagel, and K. W. Axhausen, Eds., London: Ubiquity Press, 2016, ch. 23, pp. 145–152. DOI: 10.5334/baw. [Online]. Available: http://www.ubiquitypress.com/site/books/10.5334/baw/.

[58] M. Rieser, "Adding Transit to an Agent-Based Transportation Simulation: Concepts and Implementation", PhD, Technischen Universität Berlin, 2010. [Online]. Available: https://svn.vsp.tu-berlin.de/repos/public-svn/publications/vspwp/2010/10-05/20100610{_}phdthesis{_}mrieser.pdf.

[59] H. Ayed, D. Khadraoui, and R. Aggoune, "Using MATSim to simulate carpooling and car-sharing trips", in *2015 World Congress on Information Technology and Computer Applications (WCITCA)*, IEEE, Jun. 2015, pp. 1–5, ISBN: 978-1-4673-6636-6. DOI: 10.1109/WCITCA.2015.7367046. [Online]. Available: http://ieeexplore.ieee.org/document/7367046/.

[60] F. Ciari, M. Balać, and K. W. Axhausen, "Modeling Carsharing with the Agent-Based Simulation MATSim: State of the Art, Applications, and Future Developments", *Transportation Research Record: Journal of the Transportation Research Board*, vol. 2564, no. 1, pp. 14–20, Jan. 2016, ISSN: 0361-1981. DOI: 10.3141/2564-02. [Online]. Available: http://journals.sagepub.com/doi/10.3141/2564-02.

[61] M. Balać, H. Becker, F. Ciari, and K. W. Axhausen, "Modeling competing free-floating carsharing operators – A case study for Zurich, Switzerland", *Transportation Research Part C: Emerging Technologies*, vol. 98, pp. 101–117, Jan. 2019, ISSN: 0968090X. DOI: 10.1016/j.trc.2018.11.011. [Online]. Available: https://linkinghub.elsevier.com/retrieve/pii/S0968090X18316656.

[62] P. Segui-Gasco, H. Ballis, V. Parisi, D. G. Kelsall, R. J. North, and D. Busquets, "Simulating a rich ride-share mobility service using agent-based models", *Transportation*, vol. 46, no. 6, pp. 2041–2062, 2019, ISSN: 15729435. DOI: 10.1007/s11116-019-10012-y. [Online]. Available: https://doi.org/10.1007/s11116-019-10012-y.

[63] J. Bischoff, I. Kaddoura, M. Maciejewski, and K. Nagel, "Simulation-based optimization of service areas for pooled ride-hailing operators", *Procedia Computer Science*, vol. 130, pp. 816–823, 2018, ISSN: 18770509. DOI: 10.1016/j.procs.2018.04.069. [Online]. Available: https://linkinghub.elsevier.com/retrieve/pii/S1877050918304290.

[64] R. Vosooghi, J. Kamel, J. Puchinger, V. Leblond, and M. Jankovic, "Robo-Taxi service fleet sizing: assessing the impact of user trust and willingness-to-use", *Transportation*, vol. 46, no. 6, pp. 1997–2015, 2019, ISSN: 15729435. DOI: 10.1007/s11116-019-10013-x. [Online]. Available: https://doi.org/10.1007/s11116-019-10013-x.

[65] D. J. Fagnant and K. M. Kockelman, "Dynamic ride-sharing and fleet sizing for a system of shared autonomous vehicles in Austin, Texas", *Transportation*, vol. 45, no. 1, pp. 143–158, 2018, ISSN: 15729435. DOI: 10.1007/s11116-016-9729-z.

[66] K. Winter, O. Cats, K. Martens, and B. van Arem, *Relocating shared automated vehicles under parking constraints: assessing the impact of different strategies for on-street parking*, 0123456789. Springer US, 2020, ISBN: 0123456789. DOI: 10.1007/s11116-020-10116-w. [Online]. Available: https://doi.org/10.1007/s11116-020-10116-w.

[67] A. Militão, "Total Cost Minimization Models for Shared Demand Responsive Transport Systems with Human Driven and Automated Vehicles", Master's Thesis, Technische Universität München, 2019.

[68] J. Bischoff and M. Maciejewski, "Simulation of city-wide replacement of private cars with autonomous taxis in Berlin", 2016, ISSN: 1877-0509.

[69] J. Kim, "Assessment of the DRT system based on an optimal routing strategy", *Sustainability (Switzerland)*, vol. 12, no. 2, 2020, ISSN: 20711050. DOI: 10.3390/su12020714.

[70] S. Hörl, "Dynamic Demand Simulation for Automated Mobility on Demand", Doctoral Thesis, ETH Zurich, 2020.

[71] M. Rieser, "Modeling Public Transport with MATSim", in *The Multi-Agent Transport Simulation MATSim*, A Horni, K Nagel, and K. W. Axhausen, Eds., London: Ubiquity Press, Aug. 2016, ch. 16, pp. 105–110. DOI: 10.5334/baw.1. [Online]. Available: http://www.ubiquitypress.com/site/chapters/10.5334/baw.1/.

[72] R. Rothfeld, M. Balać, and A. Militão, *MATSim-UAM*, 2020. [Online]. Available: https://github.com/BauhausLuftfahrt/MATSim-UAM (visited on 08/15/2020).

[73] N. Kühnel, *Applied Transport Modeling with MATSim*, Munich, 2020.

[74] D. Ziemke, K. Nagel, and R. Moeckel, "Towards an Agent-based, Integrated Land-use Transport Modeling System", *Procedia Computer Science*, vol. 83, pp. 958–963, 2016, ISSN: 18770509. DOI: 10.1016/j.procs.2016.04.192. [Online]. Available: http://dx.doi.org/10.1016/j.procs.2016.04.192.

[75] M. Rieser, K. Nagel, and A. Horni, "Generation of the Initial MATSim Input", in *The Multi-Agent Transport Simulation MATSim*, A Horni, K Nagel, and K. W. Axhausen, Eds., London: Ubiquity Press, 2016, ch. 7, pp. 61–64. DOI: 10.5334/baw. [Online]. Available: http://www.ubiquitypress.com/site/books/10.5334/baw/.

[76] A. Neumann and M. Zilske, "MATSim JOSMNetwork Editor", in *The Multi-Agent Transport Simulation MATSim*, A Horni, K Nagel, and K. W. Axhausen, Eds., London: Ubiquity Press, 2016, ch. 8, pp. 65–66. DOI: 10.5334/baw. [Online]. Available: http://www.ubiquitypress.com/site/books/10.5334/baw/.

[77] M. Rieser, A. Horni, and K. Nagel, "Let's Get Started", in *The Multi-Agent Transport Simulation MATSim*, A Horni, K Nagel, and K. W. Axhausen, Eds., London: Ubiquity Press, 2016, ch. 2, pp. 9–21. DOI: 10.5334/baw. [Online]. Available: http://www.ubiquitypress.com/site/books/10.5334/baw/.

[78] R. Rothfeld, M. Balać, K. Plötner, and C. Antoniou, "Agent-based Simulation of Urban Air Mobility", in *2018 Modeling and Simulation Technologies Conference*, 2018, pp. 1–10, ISBN: 9781624105517. DOI: 10.2514/6.2018-3891.

[79] M. Rieser, K. Nagel, and A. Horni, "QSim", in *The Multi-Agent Transport Simulation MATSim*, A Horni, K Nagel, and K. W. Axhausen, Eds., London: Ubiquity Press, 2016, ch. 11, pp. 77–80. DOI: 10.5334/baw. [Online]. Available: http://www.ubiquitypress.com/site/books/10.5334/baw/.

[80] K. Nagel, B Kickhöfer, A. Horni, and D Charypar, "A Closer Look at Scoring", in *The Multi-Agent Transport Simulation MATSim*, A Horni, K Nagel, and K. W. Axhausen, Eds., London: Ubiquity Press, 2016, ch. 3, pp. 23–34. DOI: 10.5334/baw.1. [Online]. Available: http://www.ubiquitypress.com/site/chapters/10.5334/baw.1/.

[81] A. Horni and K. Nagel, "More About Configuring MATSim", in *The Multi-Agent Transport Simulation MATSim*, A Horni, K Nagel, and K. W. Axhausen, Eds., London: Ubiquity Press, Aug. 2016, ch. 4, pp. 35–44. DOI: 10.5334/baw.1. [Online]. Available: http://www.ubiquitypress.com/site/chapters/10.5334/baw.1/.

[82] R. Rothfeld, M. Fu, and C. Antoniou, *Analysis of Urban Air Mobility's Transport Performance in Munich Metropolitan Region*, Munich, 2019. DOI: 10.13140/RG.2.2.15444.42886.

[83] The Apache Software Foundation, *Welcome to Apache Maven*, 2020. [Online]. Available: https://maven.apache.org (visited on 08/04/2020).

[84] ——, *Introduction to the POM*, 2020. [Online]. Available: https://maven.apache.org/guides/introduction/introduction-to-the-pom (visited on 08/04/2020).

[85] M. Rieser, K. Nagel, and A. Horni, "MATSim Data Containers", in *The Multi-Agent Transport Simulation MATSim*, A Horni, K Nagel, and K. W. Axhausen, Eds., London: Ubiquity Press, Aug. 2016, ch. 6, pp. 55–59. DOI: 10.5334/baw.1. [Online]. Available: http://www.ubiquitypress.com/site/chapters/10.5334/baw.1/.

[86] R. Moeckel, N. Kuehnel, C. Llorca, A. Moreno, and H. Rayaprolu, "Microscopic Travel Demand Modeling: Using the Agility of Agent-Based Modeling Without the Complexity of Activity-Based Models", in *Annual Meeting of the Transportation Research Board*, Washington, DC, 2019.

[87] C. Llorca and R. Moeckel, "Effects of scaling down the population for agent-based traffic simulations", *Procedia Computer Science*, vol. 151, no. 2018, pp. 782–787, 2019, ISSN: 18770509. DOI: 10.1016/j.procs.2019.04.106. [Online]. Available: https://doi.org/10.1016/j.procs.2019.04.106https://linkinghub.elsevier.com/retrieve/pii/S1877050919305691.

[88] K. Nagel, S. Müller, M. Zilske, M. Rieser, and J. Laudan, *Matsim-germany*, Berlin, 2020. [Online]. Available: https://github.com/matsim-scenarios/matsim-germany.

[89] R. Moeckel and R. Donnelly, "Gradual Rasterization: Redefining Spatial Resolution in Transport Modelling", *Environment and Planning B: Planning and Design*, vol. 42, no. 5, pp. 888–903, 2015, ISSN: 14723417. DOI: 10.1068/b130199p.

[90] OpenStreetMap Wiki, *Key:highway*, Jan. 2021. [Online]. Available: https://wiki.openstreetmap.org/w/index.php?title=Key:highway{\&}oldid=2099776.

[91] K. T. Geurs and B. van Wee, "Accessibility evaluation of land-use and transport strategies: review and research directions", *Journal of Transport Geography*, vol. 12, no. 2, pp. 127–140, Jun. 2004, ISSN: 09666923. DOI: 10.1016/j.jtrangeo.2003.10.005. [Online]. Available: https://linkinghub.elsevier.com/retrieve/pii/S0966692303000607.

[92] P. D. Vascik, "Systems-Level Analysis of On Demand Mobility for Aviation", Master's Thesis, Massachusetts Institute of Technology, 2017. [Online]. Available: http://seari.mit.edu/documents/theses/SM{_}VASCIK.pdf.

[93] S. Hörl and M. Balać, *Eqasim*, 2019. [Online]. Available: https://eqasim.org (visited on 09/27/2020).

A Rothfeld et al. (2019). Analysis of European Airports' Access and Egress Travel Times using Google Maps.

Reference: Rothfeld, R., Straubinger, A., Paul, A., & Antoniou, C. (2019). Analysis of European airports' access and egress travel times using Google Maps. *Transport Policy*, 81(May), 148–162. https://doi.org/10.1016/j.tranpol.2019.05.021

Transport Policy 81 (2019) 148–162

Contents lists available at ScienceDirect

Transport Policy

journal homepage: www.elsevier.com/locate/tranpol

Analysis of European airports' access and egress travel times using Google Maps

Raoul Rothfeld[a,*], Anna Straubinger[a], Annika Paul[a], Constantinos Antoniou[b]

[a] Bauhaus Luftfahrt e.V., Taufkirchen, 82024, Germany
[b] Technical University of Munich, Munich, 80333, Germany

ARTICLE INFO

Keywords:
Airport access travel time
Four hours door-to-door
Google maps route data

ABSTRACT

Door-to-kerb (*access*) and kerb-to-door (*egress*) times from and to 22 European airports are being analysed to draw conclusions on the durations of air travel chains with regard to the European Commission's Flightpath 2050 challenge of enabling four hours door-to-door intra-European air travel. This ambitious goal intends to foster a seamless European transport system, thereby increasing the travel comfort for passengers and strengthening the intermodal cooperation between different transport providers. Since air travel plays an essential role in connecting different European regions, this research focuses on analysing access and egress times to and from European airports in order to identify their potential in reducing overall door-to-door travel times. Travel durations and distances to and from airports, under varying conditions/parameters, have been gathered using the Google Maps Distance Matrix API. The received results have been mapped and utilised to establish linear regression models for European airport access and egress speeds. In multiple steps, significant variables and interaction terms have been added to improve the expressiveness of the linear regression. The analyses show great variations in airport access and egress speeds between European airports and even greater discrepancies between private (*driving*) and public (*transit*) transport. Airport access and egress times have to be reduced significantly for intra-European travel chains to converge on the European Commission's goal of four hours door-to-door air travel.

1. Introduction

The European Commission published a strategy paper on aviation research for the coming decades, Flightpath 2050, where various challenges, visions, and goals regarding the air transport sector are determined. One of the main goals, concerning societal and market needs, is that "90% of travellers within Europe [should be] able to complete their journey, door-to-door within 4 h" (European Commission, 2011a, p. 11).

The four hours door-to-door goal supports the European countries by facilitating travel and transport as well as strengthening the air transport market. This is in line with the European Union's cohesion policy, which aims to enable easier access to and from all European regions through projects like the Trans-European Transport Networks (Mączka, 2016b; Vickerman et al., 1999). Flightpath 2050, in contrast to the Trans-European Transport Networks, focuses on air traffic – which connects more remote locations and bridges longer distances. In its white paper, the European Commission (2011b) points out that the integration of all transport modes, aerial as well as ground-based transportation, is of great importance. As an example, they suggest that every airport should be accessible by (high speed) rail.

Improved connectivity between European regions reduces the importance of spatial distance. Spatial proximity leads to agglomeration effects, which have a positive impact on economic development (Fujita and Thisse, 2013). Research on wider economic benefits of transport demonstrates that efficient transport networks and high connectivity can generate economic forces, which are similar to agglomeration effects (Vickerman, 2007).

At this point in time, the goal of four hours door-to-door air travel is far from being achieved (Lehner et al., 2014; Mączka, 2016a). Yet, the potential for time savings in the air is limited, especially with regard to economic and ecological constraints. Schmitt and Gollnick (2016) show that air travel speeds have been stagnating for decades, mainly due to economic impediments. Opposing this, considering the entire door-to-door travel chain, airport access and egress times as well as airport process times are assumed to bear the potential for significant travel time reduction. Detailed analyses covering these travel segments and associated travel time reduction are therefore crucial in detecting the

* Corresponding author.
E-mail addresses: Raoul.Rothfeld@bauhaus-luftfahrt.net (R. Rothfeld), Anna.Straubinger@bauhaus-luftfahrt.net (A. Straubinger), Annika.Paul@bauhaus-luftfahrt.net (A. Paul), c.antoniou@tum.de (C. Antoniou).

https://doi.org/10.1016/j.tranpol.2019.05.021
Received 4 April 2018; Received in revised form 22 January 2019; Accepted 31 May 2019
Available online 03 June 2019
0967-070X/

levers of moving towards a more seamless and intermodal European transport system. The following research is meant to contribute to the understanding of potentials for travel time reductions in airport access and egress as well as to assess the impeding impact of these parts of the travel chain.

This research contribution consists of three main parts, starting with a literature review on airport access, egress, and process times in order to gain an understanding of how much time passengers currently spend in these travel segments (Section II). Building on this, Section III outlines the data acquisition process. In order to evaluate access and egress travel times and the potential for reduction, travel durations to and from 22 European airports via private (i.e. *driving*) and public transport (i.e. *transit*), have been calculated. The calculation was accomplished by using Google Maps data. The use of Google Maps facilitated the generation of a large travel duration dataset including the influence of road congestion. The consecutive data analysis in Section IV determines travel time maps, detailed and data-intensive access/egress travel times with a high spatial resolution, for a selection of six major European airports and travel time estimations by mode for the entire airport data set of 22 airports. Due to the enormous requirement for Google Maps data points in order to create travel time maps, the mapping approach has only been applied to a selection of the major surveyed airports. In addition to this, a linear regression models assesses the different factors influencing the speed with which passengers can get to or from the selected airports. This approach yields further insight into the potentials to reduce overall travel time. According to this, policy makers are provided with guidelines of how feasible measures can be developed and implemented in the future European transport system. Section V discusses and concludes these three main parts and highlights the way forward for policy makers in creating a more seamless and intermodal European transport system.

2. Literature review

Existing literature indicates that the four hours door-to-door goal is a challenge. Fig. 1 shows the average inner-European flight time weighted per seat. It illustrates that, currently, off-block times already take up two hours of the four hours and tend to increase even further (based on OAG[1] data). The same data reveals that the 24%-increase in flight duration from 2000 to 2016 stems from an average flight distance increase of 38% during the same period of time. This leaves 120 min for boarding, deboarding, airport processes (e.g. check-in, security), and airport access and egress. In contrast to airport and boarding processes (e.g. Koster et al., 2011; Manataki and Zografos, 2010; Schultz, 2010; Takakuwa and Oyama, 2008), little research has been conducted on airport access and egress times.

Typically, airports use and define catchment areas to describe and spatially visualise the relation between their passengers' airport access driving times and origin location or distance. However, the definition of catchment area varies greatly. Marcucci and Gatta (2011), for example, defined catchment area as everything that is accessible in a two hours' drive from the airport. In contrast, Lieshout (2012) pointed out that the airport's competition plays a significant role, so that catchment area cannot be defined solely by driving times. Lieshout underlined that for some flights more remote airports may be attractive if an interchange/stopover can be prevented and overall travel time can be reduced. Hereinafter, competitive catchment areas only play a subordinate role, as the main topics are access and egress times to individual airports. Nonetheless, it is clear, that access and egress times strongly depend on the airport's competitive environment, as for example a higher airport density in a multiple airport region leads to lower average travel times.

Literature on access times shows great variety concerning relevant travel times to and from airports. Poelman (2013) considered 90 min as an adequate time scope for airport access. By using data on roads, road network access points, and average speeds he created areas around airports from where travellers can reach the airport within 90 min by automobile. Poelman did not consider public transport because of a lack of data. By overlapping catchment areas of different airports, he obtained the number of accessible flights per day from a given location. In contrast, Lieshout et al. (2015) stated that an airport's catchment area, in some cases, can be as large as to include up to a three hours' drive, noting that other sources only see a one or two hours' drive as relevant. They criticize that remote regions near the European border, have too few airports. Therefore, the regions' inhabitants generally have longer airport access and egress travel durations.

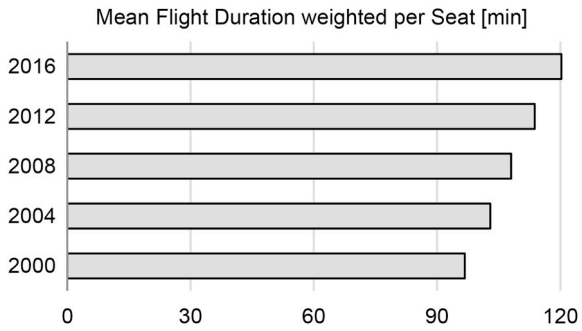

Fig. 1. Mean inner-European flight duration (based on OAG data).

Overall, recent literature distinguishes between spatial distance and temporal distance. Temporal distance is mostly seen as being more relevant. It is important to note that a small spatial distance does not necessarily lead to a short temporal distance. Sun et al. (2017) especially focused on this aspect while identifying multi-airport regions. They emphasised that the consideration of temporal, instead of only spatial, distance leads to different results. They calculated temporal distance by using open street map data in order to incorporate speed limits and road infrastructure. Similar research has been conducted by Welch et al. (2015). The goal was to compare accessibility of different airports in the Washington metropolitan area. The access travel times were calculated for peak and off-peak times by using network travel times, for private and public transport, derived from a state wide travel model. The analyses by Sun et al. and Welch et al. determine the access travel time as being one of the most important factors by which travellers choose their departure airport in a multi-airport region.

Kouwenhoven (2009) analysed airport choice and mode choice for airport access, also considering interdependencies. He stated that access mode choice differs significantly between countries and their transport policies. Furthermore, various key factors for access mode choice were determined. The most influencing factors are relative journey time advantages, city accessibility, price, and traveller characteristics.

An additional aspect that is covered by existing literature is willingness to pay for access travel time savings. Travel time savings are strongly related to the four hours door-to-door goal, as it mostly aims on decreasing the travel chain time requirements. Yet, Tsamboulas and Nikoleris (2008) showed that the willingness to pay for travel time savings is sparse. Two main reasons for this tendency were considered: (1) some passengers like to arrive at the airport early, thus, minimizing their travel time does not generate any surplus for them; (2) others might already have chosen the optimal mode for their needs and, therefore, no improvement is required.

Besides flight time and airport access and egress time, passengers have to pass a number of processes, like check-in, baggage drop-off, security screening, and baggage claim at the airport. Each process in itself is prone to variability, which urges travellers to schedule buffer time.

The first process at the airport is the passenger check-in. Joustra and Van Dijk (2001) point out that, unlike other queuing processes, the waiting time cannot be modelled via queuing theory due to strong

[1] OAG, a UK-based air travel intelligence company, provides in-depth commercial aviation flight plan schedule data.

peaks depending on the scheduled time of departure.

Takakuwa and Oyama (2008) considered all processes at the airport and found out that travellers spend 25% of their time at the airport waiting. 80% of the waiting time results from waiting for their check-in. Manataki and Zografos (2010) developed a model in which they can simulate concrete demand peaks at check-in and security screening. In their base case scenario, travellers spend a maximum of 13 min waiting for economy check-in and a maximum of 19 min for security screening.

Another decisive factor for loss of time is early arrival due to airport access and process time variability in combination with the high costs of missing a flight. Koster et al. (2011) estimated the cost of access time variability by analysing the preferred arrival time at the airport and the determinants of arrival time. Their model includes the disutility of early and late arrival and, in extreme cases, the total costs of missing a flight. They state that a good approximation for kerb-to-gate time is 25 min before desired gate arrival time. The passenger's decision is influenced by different parameters like the travel frequency, the need to check in luggage, and the size of the airport. Schultz (2010), however, calculates 74 min from airport arrival time to potential arrival at the gate. It is obvious that, even in literature, grave discrepancies exist when analysing time requirements for airport processes.

In summary, existing literature shows that the Flightpath 2050 goals are difficult to achieve. Considering merely airport processes, a time requirement of 3 h and 10 min is a conservative estimate. Assuming 25 min for check-in processes (Koster et al., 2011), 30 min for boarding (Nyquist and Mcfadden, 2008), and 120 min off-block time, the expected expenditure already adds up to 2 h and 55 min. With deboarding and baggage claim the average time spent at an airport and in the air adds up to the above mentioned 3 h and 10 min. This only leaves 50 min for airport access and egress.

In order to evaluate the current state of the four hours door-to-door target achievement, Nieße and Grimme (2014) analysed flight data, access and egress times, and airport process times. They found out that, in a theoretical setting, where a European citizen visits each region of the European Union, in only 13% (60 min transfer/stopover time) or 22% (45 min transfer/stopover time) of all cases the four hours door-to-door goal can be achieved.

There are different impeding factors concerning the four hours door-to-door goal, for which solutions are being discussed (ACARE, 2012; Piwek and Wiśniowski, 2016; Urban et al., 2016). A concrete approach to minimize airport process time and access and egress time is made by Urban et al. (2016), who have proposed building an airport on top of existing transport infrastructure like train stations. By streamlining airport processes and the airports architectural setup, all landside processes are said to be completed within 15 min. Yet, this is still a theoretical concept and far from being implemented.

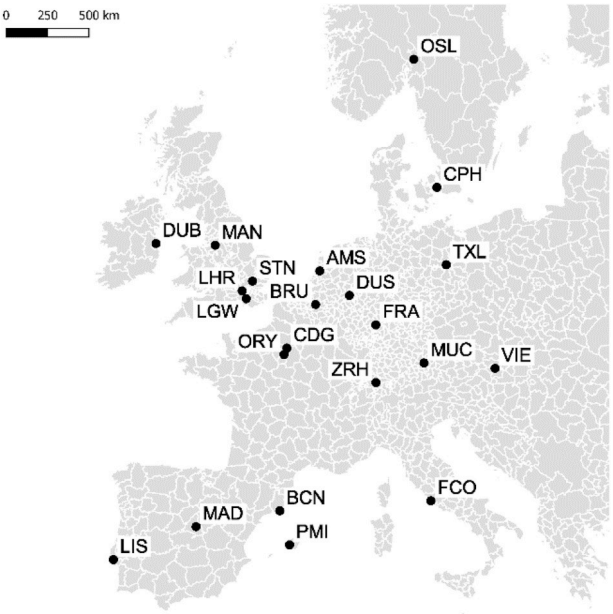

Fig. 2. Overview of the 22 queried European airports.

As indicated above, a decrease of flight time is – ecologically and economically – not feasible. Therefore, besides accelerating the airport processes, a topic of interest is increasing airport access and egress speeds. In this context, ACARE, the Advisory Council for Aviation Research and Innovation in Europe (2012), outlines future research questions in the aviation sector – mainly focusing on intermodality. The provision of more travel information and a higher level of integration of different transport modes are important goals of the European transport policy. Piwek and Wiśniowski (2016) see Small Air Transport as an inevitable development to reach the Flightpath 2050 goal. Small Air Transport shall operate on medium distances with up to 19 seats in order to supply low demand connections and avoid long ground-based travels to the next airport.

The airport access and egress times are an essential part of the travel chain and should, therefore, be evaluated further. Especially, their impact on the achievement of the four hours door-to-door goal is of interest.

3. Data acquisition

Travel times have been gathered using the Google Maps Distance Matrix API[2] (Google Developers, 2017b) for 22 large European airports (see Fig. 2) during September and October of 2016. An airport selection had to be made in order to reduce the number of required Google Maps API requests due to financial constraints and time restrictions.

The airports were primarily selected according to the number of annual seats (as of OAG, 2014) in order to achieve the highest-possible market coverage with the least number of to-be-analysed airports. Despite being highly-ranked, Turkish (i.e. IST and SAW) and Russian (i.e. SVO and DME) airports have been excluded from this analysis, as these airports are not located in EU-member states. Additionally, the airports have also been selected as to ensure a large geographical spread and to include airports from most major European countries – for example, by replacing Milan-Malpensa Airport (MXP, ranked 22nd), which is located near Rome's airport (FCO) and would be the second Italian airport included in the analysis, with Lisbon Airport (LIS, ranked 23rd), in order to include a Portuguese airport. The remaining airports – included in this analysis – are, hence, AMS, BCN, BRU, CDG, CPH, DUB, DUS, FCO, FRA, LGW, LHR, LIS, MAD, MAN, MUC, ORY, OSL, PMI, STN, TXL, VIE, and ZRH. These airports amount to 37% of all annual seats from and to European airports in 2014. For each of these airports, Google Maps has been queried with varying conditions, which can be set by providing parameters to the Google Maps API.

3.1. Google Maps Distance Matrix API and its parameters

The Google Maps Distance Matrix API provides similar functionality as the Google Maps graphical end-user interface in a web browser, as it returns the distance and time required for a specific transport mode from a pre-defined origin to a pre-defined destination. This API enables automated querying of numerous routing or travel requests, thus facilitating the accumulation of a large number of travel distances and time information for a specific city or airport. Especially, since the Distance Matrix API, in contrast to the Google Maps Directions API, allows for the definition of multiple origins and destinations at the same

[2] In the case of Google Maps, the application programming interface (API) is a web service that automatically responds to computer-generated requests. Both, requests and responses follow a pre-defined and machine-readable format.

time and returns results for all combinations. However, when using the Distance Matrix API, the exact, proposed route to be taken cannot be viewed or edited.

At the most basic level, each Google Maps Distance Matrix API request requires at least one origin and one destination in order to be able to return travel distance and duration results. Such a request can be further elaborated by the following optional parameters:

- multiple origins and destinations
- transport mode to be taken (i.e. *driving*, *walking*, *bicycling*, and *transit*)
- travel options to be avoided (i.e. *tolls*, *highways*, *ferries*, and *indoor*)
- preferred units of measurement (i.e. *metric* or *imperial*)
- preferred arrival or departure time
- preferred traffic model (i.e. *optimistic*, *best_guess*, or *pessimistic*; controls the influence of congestion on the returned results)
- preferred means of public transport to be chosen (i.e. *bus*, *subway*, *train*, and *tram*), if *transit* has been chosen as the transport mode
- preferred routing option (i.e. *less_walking* or *fewer_transfers*)), if *transit* has been chosen as the transport mode

See Google Developers (2017a) for more information.

It has to be noted, though, that the offered transport modes of *driving* and *transit* use fundamentally different methods to estimate travel distance and duration when using Google Maps. While *driving* incorporates current traffic volumes and, thus, congestion, *transit* does not and, instead, is purely based on public transport schedules – omitting potential delays within public transport systems. Additionally, when using the transport mode *transit*, the proposed route incorporates walking to/from the first/last point of access to the public transport system, while, when using the transport mode *driving*, the automobile route commences directly. The times for accessing, starting, and parking automobiles are, thus, omitted from the Google Maps results at the origin and, vice-versa, when arriving at the destination.

As mentioned, the results from Google Maps incorporate traffic congestion for the transport mode *driving*. It does so by providing each result with two different travel durations: the travel duration required to traverse the proposed route based on (1) an average traffic volume at the chosen time and day and (2) based on near real-time information about the current traffic volume. As an example, the latter (2) would include potential traffic congestion due to an unforeseen traffic incident while the former (1) would not. Unfortunately, the exact assumptions and influences on Google Maps' traffic volume calculations cannot be described. Similarly, information on Google Maps' coverage of public transport schedules and networks is sparse and non-transparent. Thus, the inclusion of all public travel options at each of the 22 airports cannot be ensured. While spot checks have been performed, Google Maps' data availability, validity, and timeliness cannot be guaranteed.

For the following analyses, extensive use has been made of the origin, destination, transport mode, and departure time parameters. *Ferries* have been set to be avoided and the *best_guess* traffic model has been chosen for all following Google Maps Distance Matrix API requests. The presented results originate from repeatedly sending requests to the Google Maps servers with alterations in the described parameters. Both, the generation of requests as well as their querying, have been performed automatically by two self-developed Python scripts. The request generation for each airport has been implemented with two different algorithms: (1) a mapping algorithm with a densely populated grid of request nodes (see Fig. 4) and (2) a circular sampling algorithm with fewer, more wide-spread request nodes (see Fig. 5).

3.2. Travel time mapping

For a detailed look at travel times in the direct vicinity of an airport, an exceedingly high density of request nodes is required. Thus, grids of nodes with total heights and widths of 70 km each, a node distance of

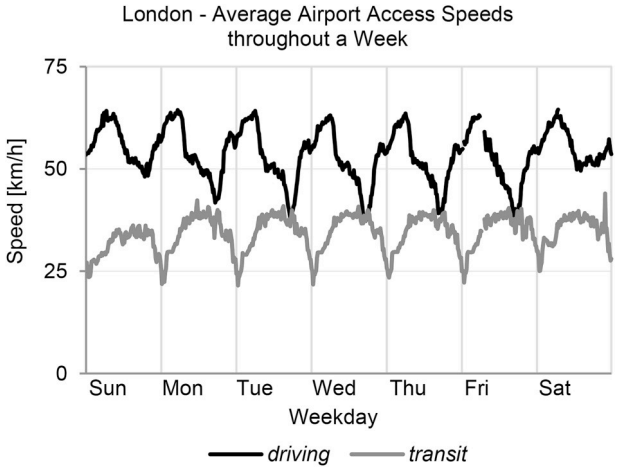

Fig. 3. Average access speeds [km/h] throughout a sample week from within Greater London to the fastest-reachable airport around London (i.e. LHR, LGW, LCY, STN, LTN).

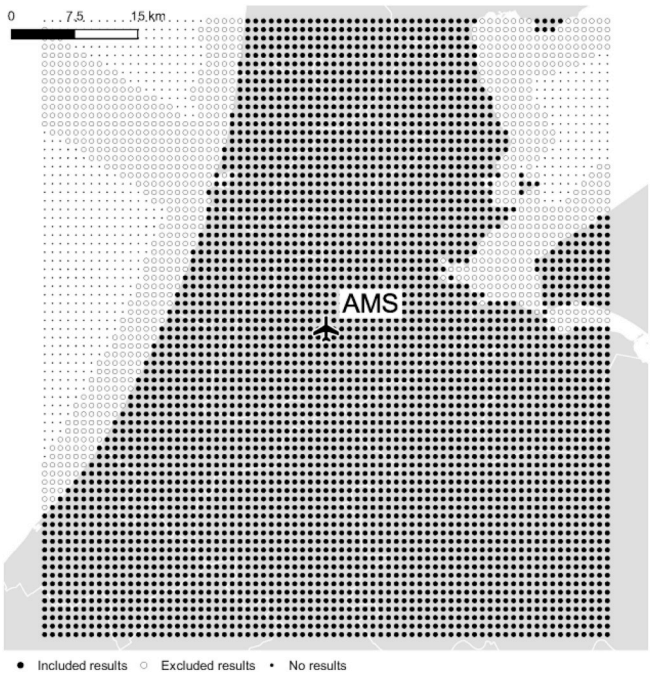

Fig. 4. Illustration of the request node grid surrounding Amsterdam Airport Schiphol (AMS) with indication for result provision and inclusion.

ca. 1 km, and with the airports as the centre points have been generated (c.f. Fig. 4). Each mapping node was used as the origin of a route to the airport and as the destination of a route from the airport in order to simulate airport access (i.e. door-to-kerb) and egress (i.e. kerb-to-door). Each mapping node was analysed for two weekdays (i.e. *Tuesday* and *Wednesday*) and two times of day (i.e. *12:00*, as an off-peak travel time, and *18:00*, as a peak travel time) in order to reduce the overall number of requests to be made. The mentioned weekdays and times of day have been chosen as they proofed to consistently be close to the overall average travel speeds during a preliminary time series analysis of London's airport access speeds (see Fig. 3).

Still, the number of airports to be mapped had to be reduced considerably. Thus, six major European hubs have been selected according to their annual offered seat market share and regional distribution. The selected airports for travel time mapping are AMS, CDG, FCO, FRA, LHR, and MAD; as Munich Airport (MUC, ranked 6th) had been replaced with Rome Fiumicino Airport (FCO, ranked 7th) for a more

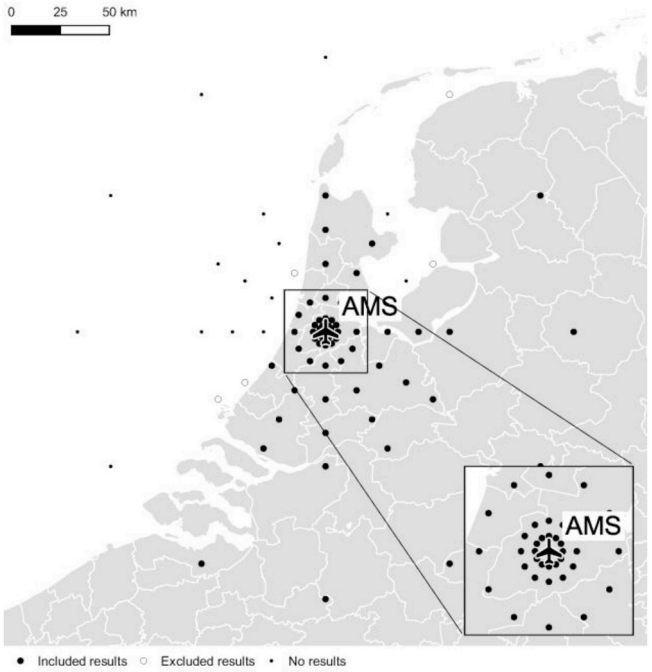

Fig. 5. Illustration of the sampling request nodes encircling Amsterdam Airport Schiphol (AMS) with indication for result provision and inclusion.

representative geographical coverage of European airports. The six airports' grids, in combination with the various permutations of travel directions, travel modes, weekdays, and times of day; required 85,248 Google Maps requests per airport and, consequently, 511,488 in total.

Not every request, however, resulted in a response with travel duration and distance given by the Google Maps servers. Responses without travel options occur, for example, when no origin street address could be found (e.g. in large bodies of water) or where no public transport access point is within walking distance. Even though the cut-off point for acceptable walking distance is not clearly identifiable, initial tests using Google Maps suggest that *transit* routes are only being proposed when a public transport access point can be found within a 2.0–2.2 km radius from the origin. For *driving*, Google Maps automatically assigns off-road locations to the nearest road, neither taking the distance nor the duration for the shift of travel origin into account. Again, the cut-off distance for road allocation has not been published and has been approximated by testing. An initial value of 5 km is assumed for the maximum distance from an origin to a road for Google Maps to be able to allocate that origin.

In order to superimpose the travel time maps with population counts, information on population distribution and density was required. Eurostat has published a comprehensive spatial population dataset, the GEOSTAT 2011 population-grid dataset (Eurostat, 2016), covering EU-member states' population densities in a 1 km^2 resolution. This enabled the calculation of an average airport access/egress time weighted by population for each of the six major European hubs.

3.3. Travel time sampling

By sampling instead of mapping the vicinity of airports, a greater number of airports and variations in accompanying variables could be requested. Thus, for each of the 22 airports, eight circles with varying radii (i.e. great circle distances of *5*, *10*, *25*, *50*, *75*, *100*, *200*, and 300 km) around the airports have been defined. On each of these circles, twelve sampling nodes have been equally distributed along the circle's circumference bearing different cardinal directions, resulting in 96 sampling nodes per airport (c.f. Fig. 5). Again, each sampling node was analysed in both travel directions (i.e. *access* and *egress*) and for both transport modes (i.e. *driving* and *transit*). Due to the reduced number of nodes per airport, each sampling node could be analysed for three weekdays (i.e. *Monday*, *Wednesday*, and *Friday*), and five times of day (i.e. *09:00*, *12:00*, *15:00*, *18:00*, and *21:00*).

These weekdays and times of day have, again, been chosen based on the preliminary time series analysis of London's airport access speeds (see Fig. 3). Even though the number of weekdays and the number of times of day are interchangeable, times of day have been emphasised as they proofed to show greater variability than day-to-day comparisons. Consequently, travel durations and distances have been gathered for all combinations of the above-listed airports, travel directions, travel modes, weekdays, and times of day; which led to 126,720 Google Maps requests in total.

In order to include an urbanisation factor, as to be able to identify travel speed differences from and to urban areas in contrast to rural ones, the GEOSTAT 2011 population-grid data has been merged with the requested sampling nodes. Each sampling node has then been classified according to two categories: (1) *urban* and (2) *rural* areas, where areas with a population density of at least 500 persons per km^2 are, according to the German Federal Statistical Office (Statistisches Bundesamt, 2000), considered to be urban. This classification has been included in order to simplify the use and increase the expressiveness of subsequent analyses.

4. Data analysis

The received results from the Google Maps servers were converted from JSON[3] into a comma-separated data format and combined into a coherent dataset. Combined with additional merged variables, the dataset provides these data columns: (1) transport mode, (2) travel duration [min], (3) travel distance [km], (4) travel speed [km/h], (5) street longitude, (6) street latitude, (7) airport longitude, (8) airport latitude, (9) travel direction, (10) weekday, (11) time of day, and (12) urbanisation; where origin and destination have been replaced by street and airport designations with the addition of the travel direction definition.

Request nodes, for which Google Maps was able to provide travel durations and distances, have still been excluded from the analysis dataset if they are located outside the European NUTS[4] regions, i.e. if the nodes are located above the surface of the sea (e.g. see Figs. 4 and 5 for excluded results around Amsterdam Airport Schiphol (AMS)). Due to Google Maps' above-mentioned mechanism of shifting travel origins to the nearest road, results can be received for request nodes off the coast. The exclusion of off-mainland request nodes also includes remaining ferry travel routes, as illustrated in Fig. 4. Numerous excluded request nodes can be seen in the top left corner of Fig. 4, straying off the Dutch coastline. Google Maps was able to return travel results by using the ferry route from Ijmuiden (Netherlands) to Newcastle (United Kingdom) for estimating travel duration and distance.

4.1. Travel time maps of six major European airports

The received results for travel time mapping of the six major European airports vary greatly in their land coverage. Google Maps only returns valid travel options and, with that, valid travel durations and distances when the Google Maps services could identify, either, a drivable road connection (in the case of *driving*) or a suitable public transport service (in the case of *transit*). Europe's dense road network in combination with Google Maps' automatism of adjusting travel origins led to virtually area-wide results for *driving*. The land coverage for *transit*, however, varies greatly between the different analysed airports. This indicates substantial differences in, either, public transport supply or Google Maps' data availability thereof for the six mapped airports.

[3] JavaScript Object Notation (JSON) is a human-readable text format commonly used for data transfer between web servers and browsers.

[4] The Classification of Territorial Units for Statistics (NUTS) is a hierarchical, geocoded standard for representing the economic territory of the EU.

Table 1
Land coverage with valid travel option results above landmass around the six airports for *driving* and *transit* within 35 km.

Airport	Result's land coverage for transport mode	
	driving	transit
AMS	100.00%	93.01%
CDG	99.98%	40.22%
FCO	100.00%	44.56%
FRA	99.91%	30.84%
LHR	99.94%	97.11%
MAD	99.98%	31.68%

Table 1 lists the percentages of landmass for which Google Maps returned valid travel options for the two transport modes: *driving* and *transit* (see Appendix A for illustrational maps of the coverage per mode and airport), for a radius of 35 km around each airport.

Due to the incomplete and varying land coverage, all mapping results were interpolated for the area around the six airports to provide full area-wide data coverage. For illustrative purposes, an average travel speed has been calculated for each mapping node – combining the received travel speeds for both travel directions, both times of day, and both weekdays per node. Each mapping node was, hence, left with an average travel speed per transport mode. These interpolated results allow a more comprehensive comparability between the six airports' maps (see Fig. 6 and Fig. 7 for travel time maps of Amsterdam Airport Schiphol (AMS) for *driving* and *transit*, respectively; see Appendix B for travel time maps of all six major European airports).

Homogeneous patterns can be observed throughout the *driving* time maps for all of the six major European airports. Despite varying ranges, all airports display a sizeable area around the airport with low travel times (e.g. below 30 min) and steadily increasing travel times as the distance to the airport grows. The airports' maximum *driving* times commonly range from 73 min (FRA) to 83 min (LHR) within the 35 km radius, with the exception of MAD – which strays off with a maximum of 111 min.

Still, each of the six airports' *driving* time maps illustrates the effect of motorways on travel times, as the areas of shorter travel time follow

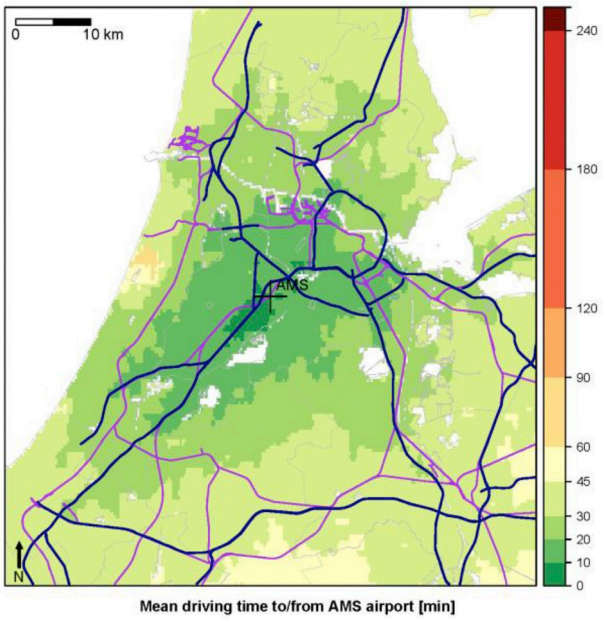

Fig. 6. *Driving* time map for Amsterdam Airport Schiphol (AMS) [min]; coloured lines represent motorways (dark blue) and rail tracks (purple). (For interpretation of the references to colour in this figure legend, the reader is referred to the Web version of this article.)

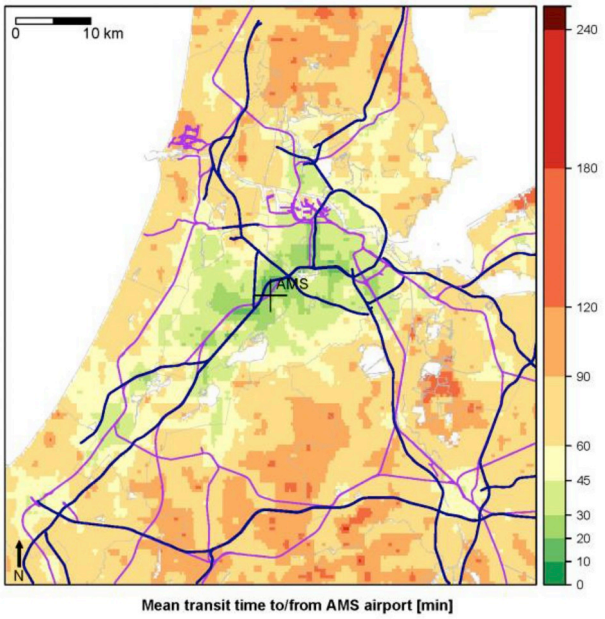

Fig. 7. *Transit* time map for Amsterdam Airport Schiphol (AMS) [min]; coloured lines represent motorways (dark blue) and rail tracks (purple). (For interpretation of the references to colour in this figure legend, the reader is referred to the Web version of this article.)

the indicated motorway infrastructure. In contrast to *driving*, reduced *transit* times can be observed along rail infrastructure. In addition, each airport's *transit* time pattern suggests faster travel connections towards each airport's adjacent city centre (c.f. Appendix E the *transit* maps for, e.g., CDG and FCO). Otherwise, however, the six airports reveal greater variations in their *transit* time patterns, compared to their *driving* time ones. AMS, FRA, and LHR demonstrate more wide-spread low *transit* travel times than CDG, FCO, and MAD.

Fig. 8 and Fig. 9 illustrate the difference in *transit* to *driving* times, i.e. how much longer or shorter travel duration would be using *transit* instead of *driving* from any given point, for AMS and LHR. In contrast to Figs. 6 and 7, these differentiation maps introduce a legend ranging into negative numbers – indicating shorter *transit* than *driving* times. However, this is rarely the case: merely LHR displays a noteworthy area coverage of 2% where *transit* times are below *driving* times. For LHR, the time benefit of *transit* to *driving* reaches up to 22 min. For all other airports, the area coverage for beneficial *transit* times is below 1‰. Even further, FCO and MAD have no cases at all where *transit* subverts *driving* time. Still, with the exception of MAD, all airports show *transit* times that can reasonably compete with *driving* times (i.e. *transit* times that are no more than 30 min longer than *driving*) for the airports' adjacent city centres.

In addition to the above comparisons, interpolation also enabled superimposing travel times with population counts. Thus, allowing to compare mean travel times per mode weighted by the number of people living within the illustrated regions around the airports. The weighted means, as shown in Table 2 (see Appendix A for the superimposed population maps of the six major European airports), show that a person living within 35 km – the common used mapping radius – of Madrid Airport (MAD) needs – on average – 24 min to/from the airport when *driving* – the lowest duration of all six airports. When using public transport (*transit*), however, people living in Madrid have the longest airport access/egress times with an average of 95 min – illustrating how severe differences in *driving* and *transit* access/egress can be at one single airport.

While the method of travel time mapping allows population-based comparisons, it is simultaneously restricted to the vicinity of a few selected airports, as the number of required data requests is significantly higher than when sampling travel times.

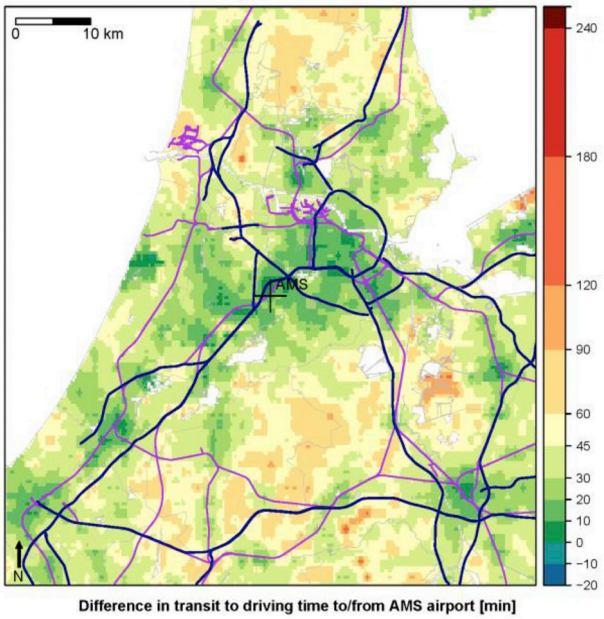

Fig. 8. *Transit* to *driving* time difference map for Amsterdam Airport Schiphol (AMS) [min]; coloured lines represent motorways (dark blue) and rail tracks (purple). (For interpretation of the references to colour in this figure legend, the reader is referred to the Web version of this article.)

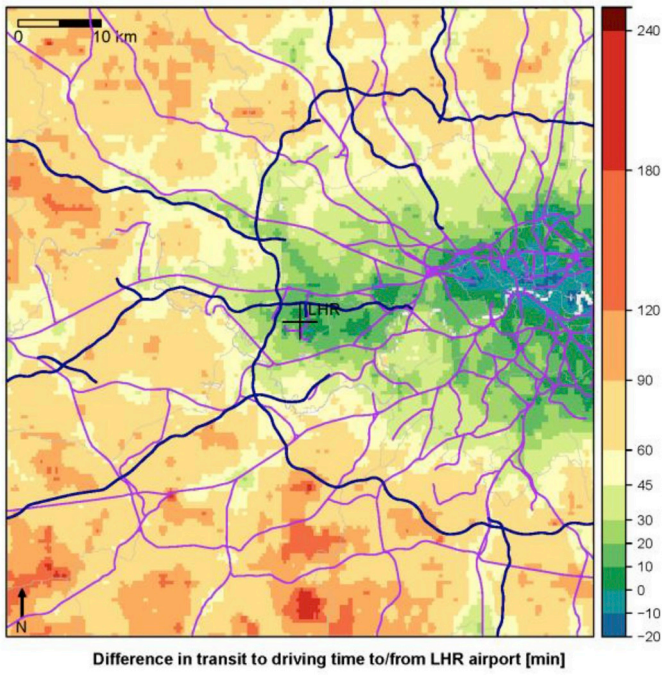

Fig. 9. *Transit* to *driving* time difference map for London Heathrow Airport (LHR) [min]; coloured lines represent motorways (dark blue) and rail tracks (purple). (For interpretation of the references to colour in this figure legend, the reader is referred to the Web version of this article.)

4.2. Travel speed analysis of 22 European airports

By sampling a larger number of European airports, a more European-wide applicability of the results should be provided. In order to simplify comparison between the 22 queried airports, travel speeds have been derived from the retrieved travel distance and duration data. Fig. 10 illustrates the unweighted mean *driving* and *transit* speeds [km/h] per airport, regardless of other factors such as time of day or weekday (see Appendix C for tabulated means and standard deviations), facilitating identification of airports that are, e.g., highly accessible by, both, car and public transport and airports that are neither. Thus, located in the top right quadrant are airports with above-average *driving* and *transit* speeds, whereas airports located in the bottom left show below-average airport access/egress speeds. Airports in the far bottom right corner strongly favour *driving* over *transit* access in terms of speed.

Table 2
Mean travel time [min] for the six major European airports weighted by population for *driving* and *transit* within 35 km.

Airport	Mean travel time [min] weighted by population for	
	driving	transit
AMS	28.73 (5.36)	55.05 (7.42)
CDG	34.52 (5.88)	75.11 (8.67)
FCO	34.12 (5.84)	88.23 (9.39)
FRA	25.57 (5.06)	60.15 (7.76)
LHR	45.94 (6.78)	75.36 (8.68)
MAD	24.28 (4.93)	95.28 (9.76)

Standard deviations in parentheses.

The airports with the fastest access/egress *driving* speeds are DUS (75 km/h), MUC (74 km/h), and MAD (74 km/h). For *transit*, the top three airports are FRA (38 km/h), ZRH (33 km/h), and AMS (33 km/h). The most severe difference between *transit* and *driving* speeds can be found at the airports MAD (55 km/h), LIS (54 km/h), and ORY (46 km/h) – supporting the previous observation of large differences for Madrid Airport (MAD). Interestingly, different airport serving the same city also show substantial differences in access/egress speeds. Paris Charles de Gaulle Airport (CDG) and Paris Orly Airport (ORY), for example, show differences of 8 km/h in mean *transit* and 6 km/h in mean *driving* speeds – both in favour of the larger airport, CDG. Similarly, London's airports (i.e. LHR, LGW, and STN; London City Airport (LCY) is not included in this study) also show a spread of average speeds – though, the spread is less severe than Paris' airports variations.

During the conversion of travel durations and distances to travel speeds, it became obvious that average speeds do not remain constant over distance. Instead, travel speeds continuously increase with increasing

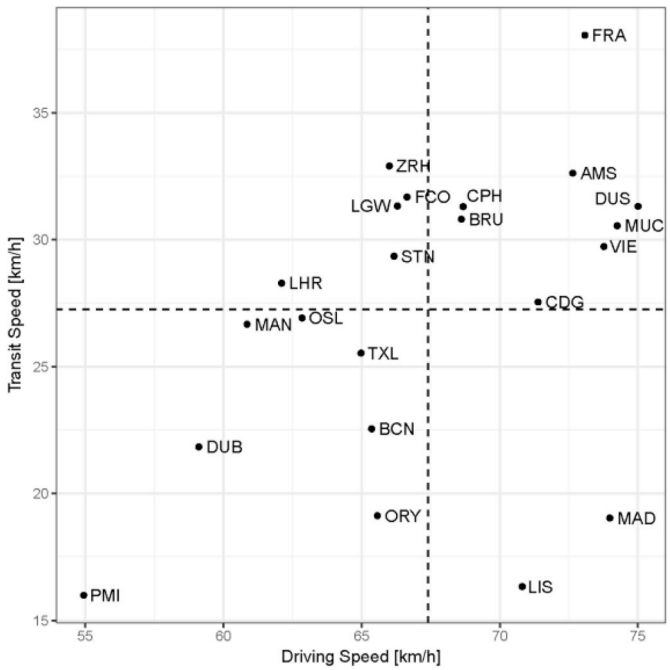

Fig. 10. Mean *driving* and *transit* speeds [km/h] of each of the 22 airports; dashed lines represent the overall mean *driving* and *transit* speeds.

travel distance. Though, the positive change in travel speed diminishes at larger distances. This effect, of shorter distances having lower average speeds than longer distances, might have contributed to Palma de Mallorca Airport (PMI) having the lowest average *transit* (16 km/h) and *driving* (55 km/h) speeds, since the available maximum distance for data to PMI was 88 km due to Mallorca being a rather small island.

4.3. Linear travel speed model for European airports

In order to generalise the results and to facilitate European airport access and egress modelling, linear regressions have been performed, using the ordinary least squares (OLS) method, on the sampled travel time and speed data. The results of four regressions, with variations in the number of variables, are being presented in Table 3. Variations (1) and (2) provide a more simplified model for estimating European airport access and egress travel times with only few required inputs, such as the transport mode. Variations (3) and (4) provide a more detailed model for European airport access and egress travel time estimation, including additional factors, such as the time of day and level of urbanisation.

The variables, transport mode, travel direction, travel distance, time of day, and level of urbanisation; have been selected subsequently to preliminary analyses on the severity and significance of their influence. Each request, combined with an appropriate and valid Google Maps travel result, provides specific information on the origin's and destination's location, time and date of the request, the distance of the proposed route, and the estimated travel duration for the requested transport mode. Thus, transport mode, travel direction (by taking the airport's location as reference), weekday, time of day, and distance are natural candidates for regression variables. In contrast to transport mode and travel direction, weekday did not show significant influence on travel speed. In order to reduce the model's complexity, weekday was omitted from the linear model.

Analyses on the influence of time of day rendered the inclusion of time of day as a quantitative variable as unfeasible due to the non-linear nature of travel speed development throughout a day (c.f. Fig. 3). Hence, time of day was categorised and included as a dummy variable. Multiple time of day distinctions, i.e. categories for each of the five times of day that have been sampled, resulted in insignificant differences between travel speeds resulting from the times of day *09:00*, *12:00*, *15:00*, and *18:00*. Results from the time of day *21:00*, however, proofed to have significant influence. Thus, time of day has been reduced to a binary variable offering the options of *day* and *night*.

With all distances being greater than zero, distance has been incorporated as a logarithmic function since the observed correlation between distance and travel speed is not linear. The inclusion of travel distance as a logarithmic function led to a significant improvement of the fit of the linear regression (c.f. Table 3, variations (1) and (2)) and was performed in accordance with (Wooldridge, 2009, pp. 197–200). It has to be noted, though, that travel – instead of great circle – distance has been included in the analysis. Based on the received sampling results, travel distances can be derived as the 1.63-multiple (i.e. detour factor) of great circle distance for *driving* and the 2.07-multiple for *transit* travel distances.

Transport mode, travel direction, time of day, and level of urbanisation each offer two options, with the available transport modes being *driving* and *transit*, travel directions being *access* and *egress*, times of day being *day* and *night*, and levels of urbanisation being *rural* and *urban*. These factors have been modelled using binary variables, as they are represented in qualitative terms. The transport mode *driving*, in combination with the travel direction *access*, time of day *day*, and urbanisation level *rural;* have been chosen as the benchmark (or base) group.

Throughout the different variations of the linear regression model, marginal variations of the coefficients and low standard errors can be observed. In addition, with the extensive size of sample data, the linear model is assumed to be relatively robust and able to provide credible estimations. An increasingly close fit (see R^2 in Table 3) can be observed from linear regression variation (1) to (4), with the inclusion of more, statistically significant variables. The relatively high R^2 values, especially for variation (2) to (4), indicate that the presented linear model closely fits the data. The best fitted variation, variation (4), will be the focus for the remaining analysis. Additional verification of this linear regression has been performed and can be found in Appendix D. The linear regression model for estimating European airports' access and egress travel speeds can, hence, be written as:

$$\hat{speed} = \beta_0 transit + \beta_1 egress + \beta_2 \ln(d) + \beta_3 night + \beta_4 urban + \beta_5 transit{*}night + \beta_6 transit{*}urban + \alpha \quad (1)$$

where:

- $transit = 1$ corresponds to transport mode choice *transit* and $transit = 0$ to *driving*
- $egress = 1$ corresponds to airport travel direction *egress* and $egress = 0$ to *access*
- d is the travel distance in kilometres
- $night = 1$ corresponds to travel time of day *night* and $night = 0$ to *day*
- $urban = 1$ corresponds to travel address' level of urbanisation *urban* and $urban = 0$ to *rural*
- α is the constant (or interception point)

See Fig. 11 for an illustration of the linear model for driving and transit.

This model distinguishes itself from the previous variations in that it incorporates interaction terms for transport mode and time of day and transport mode and level of urbanisation. This distinction has been made after it was discovered that the times of day and the levels of urbanisation have contrasting effects on estimated travel speed depending on the transport mode. For *driving*, the time of day *night* increases – ceteris paribus – the estimated travel speed by 4.31 km/h. For *transit*, however, the time of day *night* leads to a −2.52 km/h change in

Table 3
Linear travel speed models for European airports with increasing complexity from variation (1) to (4).

Coefficients	Notation	(1) Speed [km/h]	(2) Speed [km/h]	(3) Speed [km/h]	(4) Speed [km/h]
Mode: *transit*	β_0	−39.65*** (0.14)	−35.99*** (0.08)	−35.94*** (0.08)	−37.97*** (0.12)
Direction: *egress*	β_1		−1.66*** (0.08)	−1.65*** (0.08)	−1.65*** (0.08)
ln(*d*) [km]	β_2		12.33*** (0.03)	12.15*** (0.04)	12.05*** (0.04)
Time of Day: *night*	β_3			1.70*** (0.10)	4.31*** (0.13)
Urbanisation: *urban*	β_4			−0.95*** (0.09)	−4.01*** (0.11)
Mode: *transit* * Time of Day: *night*	β_5				−6.83*** (0.20)
Mode: *transit* * Urbanisation: *urban*	β_6				7.47*** (0.16)
Constant	α	68.02*** (0.08)	23.12*** (0.14)	23.82*** (0.17)	24.86*** (0.17)
Observations		85446	85446	85446	85446
R^2		0.4987	0.8142	0.8150	0.8217

*p < 0.10, **p < 0.05, ***p < 0.001 Standard errors in parentheses.

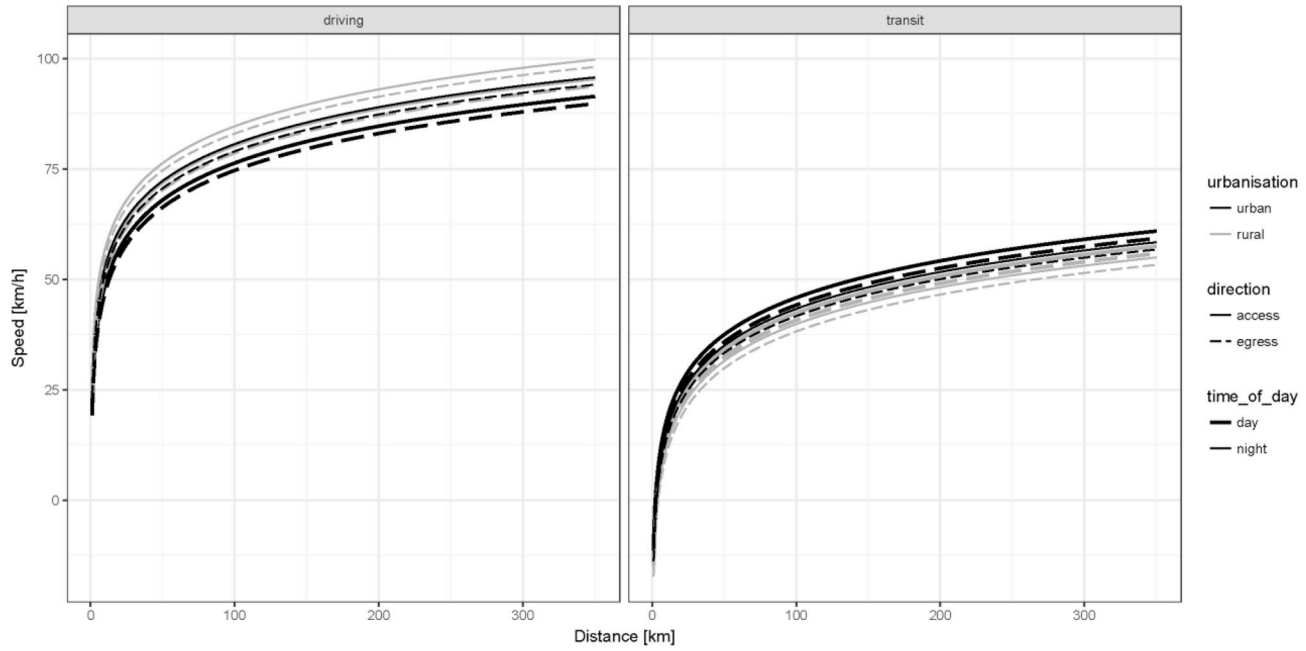

Fig. 11. Expected travel speeds [km/h] by travel distance [km] for *driving* and *transit*.

estimated travel speed. Similarly, the level of urbanisation proofed to have opposing effects on travel speed estimation. While estimated *transit* speeds benefit from the *urban* urbanisation level with a 3.46 km/h increase, estimated *driving* speeds decrease by 4.01 km/h. In contrast, when using variation (3), the time of day *night* and the level of urbanisation *urban* alter the estimated travel speed by 1.70 km/h and −0.95 km/h, respectively, regardless of transport mode.

The most influential factor on travel speed estimation is the transport mode: with the time of day *day* and the level of urbanisation *urban*, *transit* speeds are estimated to be 34.51 km/h slower than – ceteris paribus – *driving*. When changing the time of day and level of urbanisation to *night* and *rural*, respectively, the difference between estimated *driving* and *transit* speeds amounts to 40.49 km/h. The difference, between estimated *driving* and *transit* speeds, of the remaining combinations between times of day and levels of urbanisation lie between these two extrema, at 37.03 km/h (*night*, *urban*) and 37.97 km/h (*day*, *rural*).

For the transport mode *transit,* the linear model starts to estimate negative travel speeds below a distance of 4.20 km – using the slowest combination of variables (i.e. travel direction *egress*, time of day *night*, and level of urbanisation *rural*) as the reference point. Using the variable combination yielding the fastest transit speed estimations (i.e. travel direction *access*, time of day *day*, and level of urbanisation *urban*), negative travel speeds are still being estimated for distances below 2.23 km. The applicability of the presented model for short distances (i.e. distances of below 5 km) is, hence, limited and should be avoided. These negative travel speeds for distances below 5 km arise from the logarithmic inclusion of distance and Google Map's tendency to provide *walking* durations when no feasible *transit* connection can be found – which occurs with high frequency for short *transit* distance routing. Google Map's *driving* data, though, does not change its basis for estimation regardless of the trip length.

Based on the above-mentioned travel speed estimations, travel duration estimations [min] can be derived, written, and, subsequently, plotted as the ratio between travel distance and estimated travel speeds

$$\hat{duration} = \frac{d}{\hat{speed}} * 60 \quad (2)$$

where $\hat{speed}$ is the estimated airport access or egress travel speed from Eq. (1) in [km/h] and d is the travel distance in [km]. See Fig. 12 for an illustration of the estimated travel duration [min] as a function of travel distance [km].

Again, it is evident from Fig. 12 that, regardless of distance, airport access and egress travel times are significantly higher using *transit* as a transport mode instead of *driving*. The horizontal line marks the 25-min travel duration which, as it is required – both – for accessing and leaving an airport, would translate to a total requirement of 50 min for airport access and egress within an average intra-European air travel chain. While *driving* durations fall under the 25-min mark for distances below 24 km, *transit* durations continuously stay above the red line and, thus, do not cross it – estimating no *transit* travel durations of less than 25 min under any given circumstances. Asymptotic behaviour can be observed for estimated *transit* durations for travel distances within a few kilometres, due to the division by near-zero to negative travel speeds (see Fig. 11 and Eq. (2)).

5. Discussion

Through travel time mapping, travel time sampling, and, subsequently, the linear travel speed model it has become obvious that travel times, to and from airports, using public transport (*transit*) are significantly higher than when using private transport (*driving*). It is important, however, to remember the limitation of the presented analyses in that *driving* times do not include the time required for accessing one's car and, especially, parking at an airport. *Transit* times, on the other hand, do include walking and interchange times for the whole travel chain from door to airport and vice versa. Additionally, *transit* times might have been hampered by Google Maps' – possibly – incomplete public transport schedules. Further, relatively high *transit* speeds do not imply comprehensive public transport service coverage. Frankfurt Airport (FRA) showed the highest *transit* speeds in the sampling analysis while simultaneously having the lowest *transit* data coverage of all six major airports. Still, FRA's prominent position may be due to its direct motorway and high-speed rail access and could provide other European airports guidance in how to improve their accessibility.

The discrepancies between the various European airports and even between airports that serve the same city show that there is much potential for increasing public transport connectivity to/from European airports, as public transport does not yet provide an equivalent service quality, in terms of airport access/egress travel times, compared to *driving*. Yet, even when driving, the airport access/egress speeds do not suffice in view of the

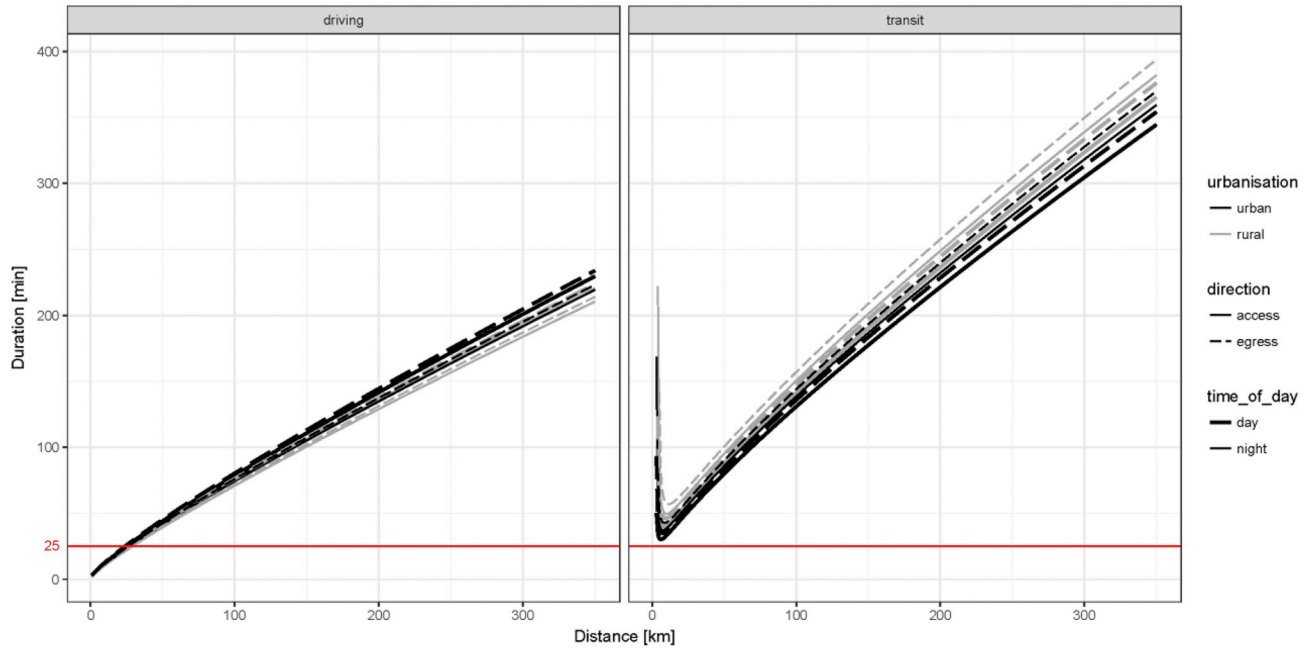

Fig. 12. Expected travel durations [min] by travel distance [km] for *driving* and *transit*; expected results based on negative *transit* speeds have been omitted; the horizontal line indicates the 25-min travel duration mark.

Flightpath 2050 goals of four hours door-to-door intra-European travel: subtracting the time requirements for other parts of the travel chain, merely 50 min remain for airport access and egress. After splitting the 50 min proportionally into available access (25.5 min) and available egress (24.5 min) times (based on the ratio of estimated airport *egress* versus *access* speeds), it is evident that the four hours door-to-door goal can only be achieved by driving from within 25 km of an airport (see Fig. 12). By using the GEOSTAT 2011 dataset, it is possible to derive the amount of people living within that distance to European airports. 33% of the EU population are living within 25 km of an airport with at least one million passengers in 2015 (see Appendix E). This percentage decreases to 11% when limiting the airport selection to large hub airports with more than ten million annual passengers – since smaller airports, oftentimes, do not offer the required amount of flights and connections (c.f. Lieshout et al., 2015).

While the presented analyses provide an initial assessment of airport access and egress times at European airports, further research would be viable in extending airport access/egress time analyses towards small and regional airports, identifying possible correlations between access/egress times and airport size, or contrasting European airport access/egress times with other regions. Additionally, more detailed, route-specific analyses could be performed in order to assess novel transport system concepts and provide possible recommendations for improving current transport systems.

6. Conclusion

In this study, airport access and egress times have been analysed for 22 European airports against the background of the European Commission's Flightpath 2050 goal of enabling four hours door-to-door intra-European travel, with the intention to provide further insight for policy makers when deciding on the implementation of measures to reduce overall door-to-door travel time and enhance the seamlessness of the transport system. For this purpose, travel times and speeds have been gathered via Google Maps for airport access and egress via private and public transport. Travel data was retrieved for different weekdays, times of day, and travel distances; so that a distinction between various influencing factors could be made. The resulting data was used to set up a linear regression model that estimates European airports' access/egress speeds and illustrates the dependence of access and egress speeds from the transport mode, the distance to the airport, the time of day, the level of urbanisation, and interactions between transport mode and time of day and transport mode and level of urbanisation.

The results show that the choice of transport mode has the highest impact on estimated travel speed, with public transport being significantly slower than access by car. Passengers with a higher value of time, including business travellers, for example, are therefore more likely to access the airport by car instead of public transport. The analyses have shown that current European airports' access and egress infrastructures are unable to provide satisfactory airport accessibility in view of the Flightpath 2050 goals. Especially, public transport services require connectivity improvements in order to provide a time-efficient alternative to private transport. Furthermore, in order to reduce road congestion and air pollution in urban areas, a shift towards a higher share of public transport as airport access mode is often considered by policy makers. Implementing measures to enhance both public transport travel times and reliability may incentivise more travellers to alter their choice of transport mode.

Severe differences in airport access/egress speeds between the analysed European airport show, however, that improvements in airport accessibility would be possible for most of Europe's airports. Associated herewith are other goals of the European Commission of, e.g., providing seamless travel and improving the integration of different transport modes. Reducing European airport access and egress times is, thus, an inevitable step in order to achieve the four hours door-to-door goal.

Acknowledgement

This research was supported by the European Union's DATASET2050 project. We thank our colleagues from Innaxis, Eurocontrol, and the University of Westminster who provided insight and expertise that greatly assisted the research.

Appendix F. Supplementary data

Supplementary data to this article can be found online at https://doi.org/10.1016/j.tranpol.2019.05.021.

Appendices

A. Google Maps results coverage and population maps of six major European airports

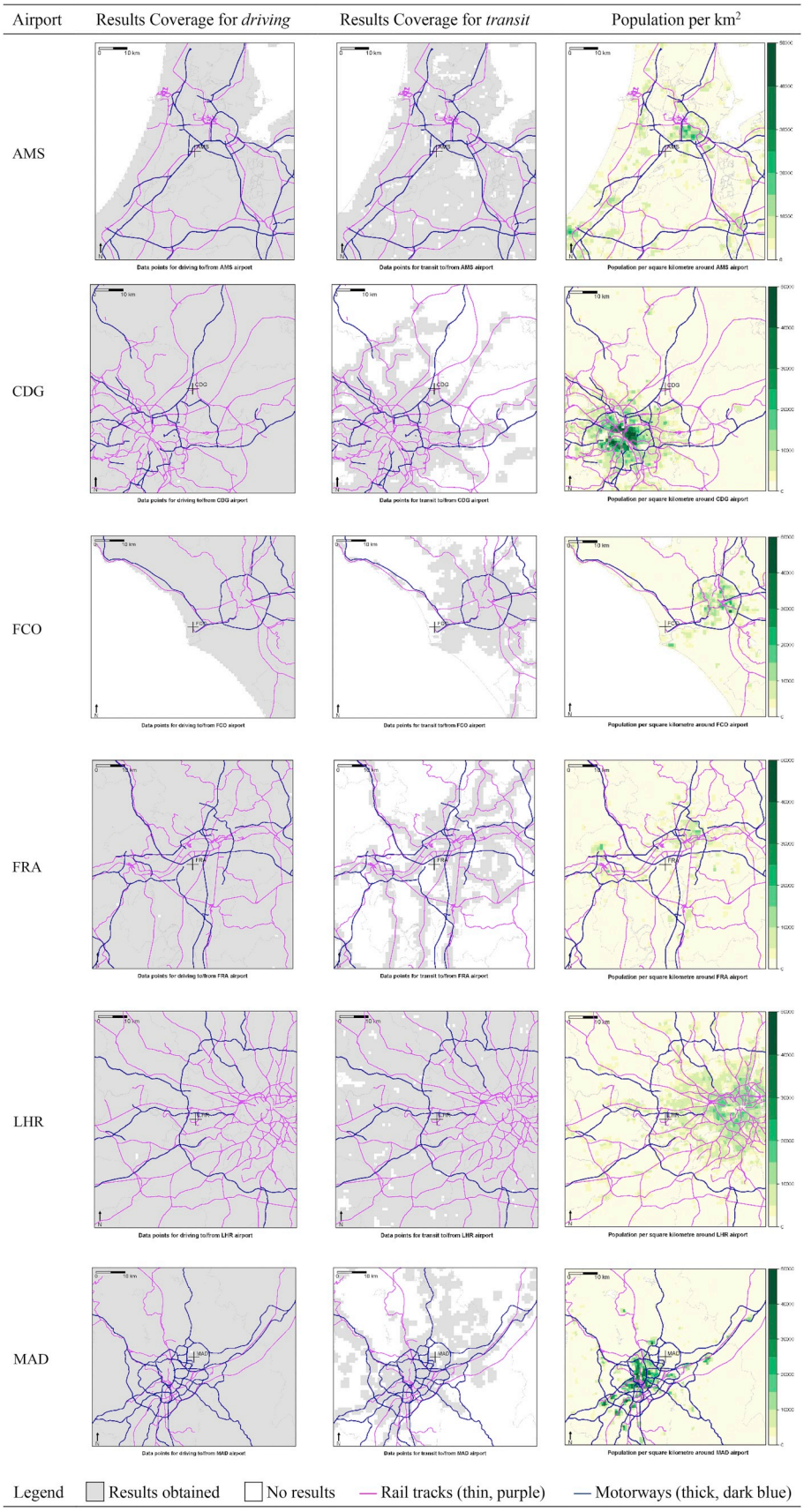

B. Maps of six major European airports for mean driving and transit times and the time difference of transit to driving

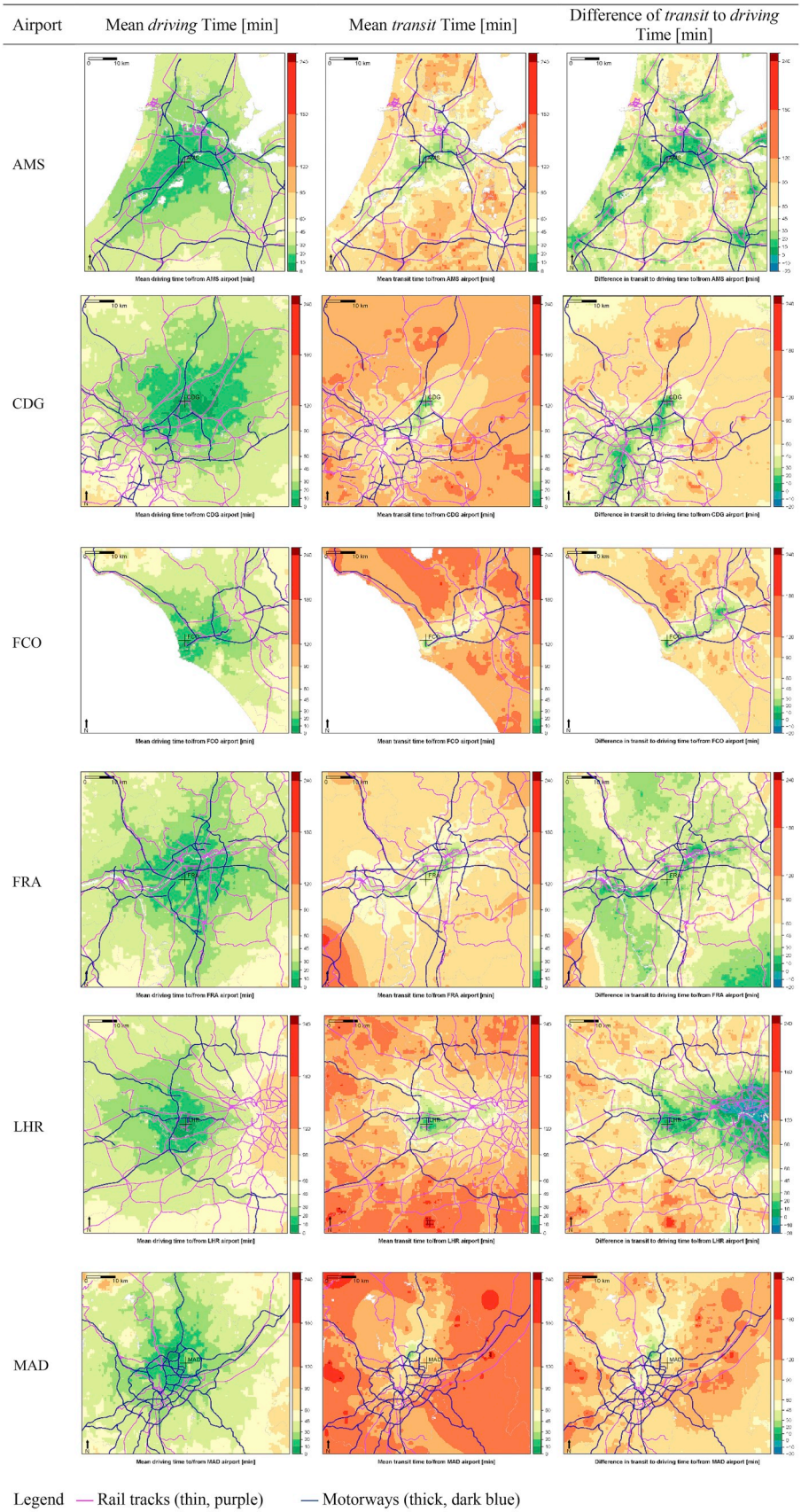

C. Mean driving and transit speeds for 22 European airports

Airport	Mean speed [km/h] for	
	driving	*transit*
AMS	72.64 (19.62)	32.62 (17.13)
BCN	65.36 (21.51)	22.55 (8.98)
BRU	68.61 (22.83)	30.81 (14.89)
CDG	71.39 (19.02)	27.54 (11.45)
CPH	68.67 (24.17)	31.30 (16.04)
DUB	59.11 (22.07)	21.84 (10.15)
DUS	75.00 (20.80)	31.32 (17.82)
FCO	66.65 (19.14)	31.68 (15.49)
FRA	73.08 (22.18)	38.06 (21.68)
LGW	66.30 (18.70)	31.33 (15.91)
LHR	62.10 (23.21)	28.29 (15.35)
LIS	70.82 (25.48)	16.33 (10.39)
MAD	73.98 (19.63)	19.04 (7.95)
MAN	60.85 (20.07)	26.67 (14.24)
MUC	74.25 (18.52)	30.55 (16.95)
ORY	65.57 (23.48)	19.13 (9.56)
OSL	62.84 (13.37)	26.92 (13.71)
PMI	54.94 (12.67)	15.99 (4.85)
STN	66.17 (19.45)	29.35 (16.68)
TXL	64.98 (25.43)	25.53 (14.22)
VIE	73.77 (19.32)	29.73 (14.17)
ZRH	66.00 (19.26)	32.91 (13.93)

Standard deviations in parentheses

D. Linear model variation (4) validation tests

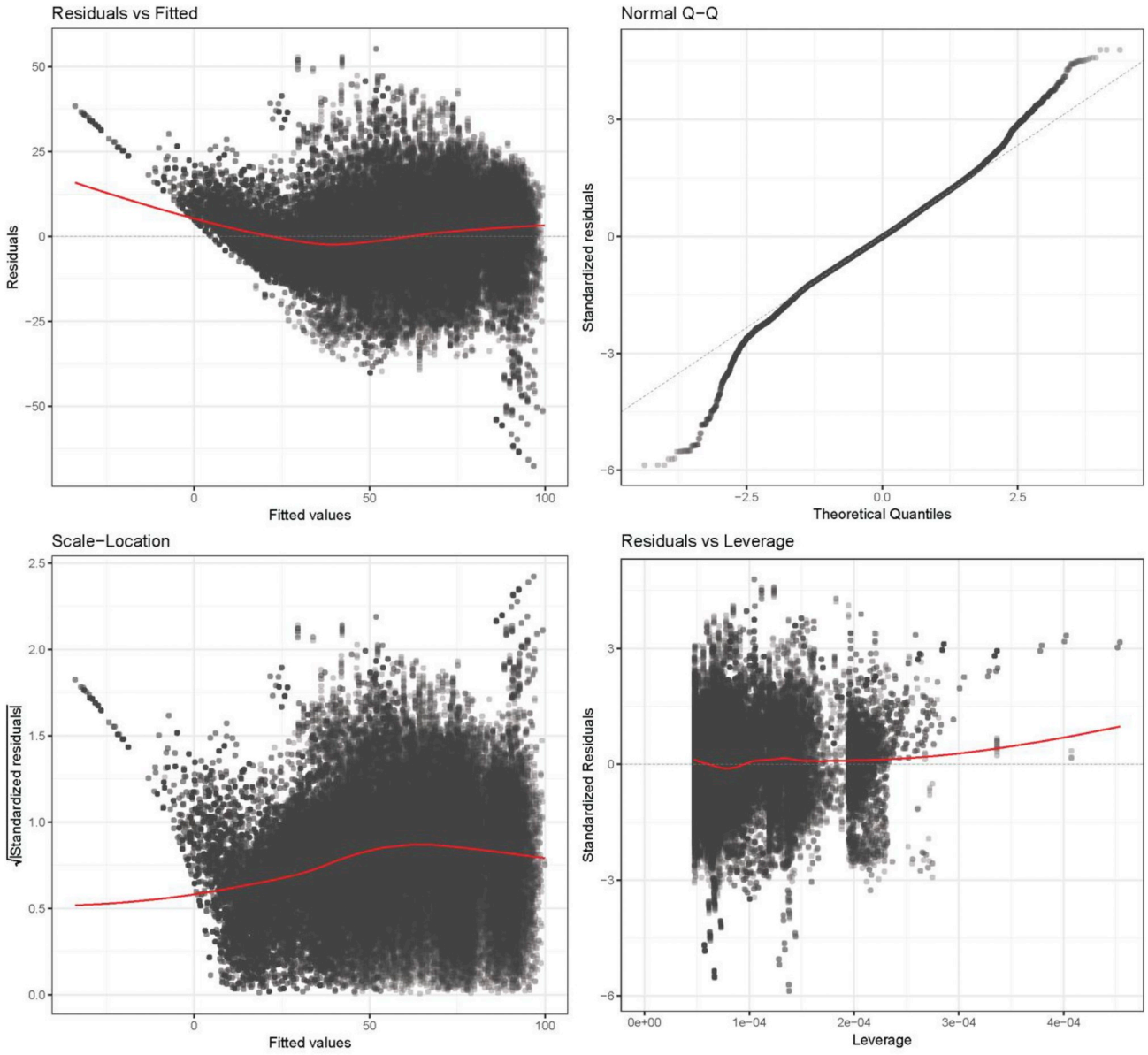

E. Share of EU population within 25 km of larger European airports

EU population within 25 km of airports with	Population count in m.	Population share*	Number of airports
more than 10 m annual passengers	58.34	11.29%	23
more than 5 m annual passengers	87.91	17.02%	41
more than 1 m annual passengers	169.53	32.82%	127

* with total EU population of 516.60 m.

References

ACARE, 2012. Strategic Research & Innovation Agenda, vol. 1 Retrieved from. http://www.acare4europe.org/sites/acare4europe.org/files/attachment/SRIA Volume 1.pdf.

European Commission, 2011. Flightpath 2050: Europe's Vision for Aviation, Report of the High Level Group on Aviation Research. Brussels. . https://doi.org/10.2777/50266.

European Commission, 2011. Roadmap to a Single European Transport Area–Towards a competitive and resource efficient transport system. Office for Official Publications of the European. https://doi.org/10.2832/30955.

Eurostat, 2016. Population Grids - Statistics Explained. https://www.doi.org/2443-8219.

Fujita, M., Thisse, J.F., 2013. Economics of Agglomeration : Cities, Industrial Location, and Globalization. Cambridge University Press.

Google Developers, 2017a. Developer's Guide | Google Maps Distance Matrix API | Google Developers. Retrieved April 21, 2017, from. https://developers.google.com/maps/documentation/distance-matrix/intro.

Google Developers, 2017b. Google Maps Distance Matrix API | Google Developers. Retrieved April 21, 2017, from. https://developers.google.com/maps/documentation/distance-matrix/.

Joustra, P.E., Van Dijk, N.M., 2001. Simulation of check-in at airports. In: Proceeding of the 2001 Winter Simulation Conference (Cat. No.01CH37304), vol. 2. IEEE, pp. 1023–1028. https://doi.org/10.1109/WSC.2001.977409.

Koster, P., Kroes, E., Verhoef, E., 2011. Travel time variability and airport accessibility. Transp. Res. Part B Methodol. 45 (10), 1545–1559. https://doi.org/10.1016/j.trb.2011.05.027.

Kouwenhoven, M., 2009. The role of accessibility in passengers' choice of airports. Compet. Interact. Between Airports, Airlines and High-Speed Rail 129–163. https://doi.org/10.1787/235278552305.

Lehner, S., Kölker, K., Lütjens, K., 2014. Evaluating temporal integration of European air transport. In: 29th Congress of the International Council of the Aeronautical Sciences, pp. 10. Retrieved from. http://www.icas.org/ICAS_ARCHIVE/ICAS2014/data/papers/2014_0617_paper.pdf.

Lieshout, R., 2012. Measuring the size of an airport's catchment area. J. Transp. Geogr. 25, 27–34. https://doi.org/10.1016/j.jtrangeo.2012.07.004.

Lieshout, R., Malighetti, P., Redondi, R., Burghouwt, G., 2015. The competitive landscape of air transport in Europe. J. Transp. Geogr. 50, 1–15. https://doi.org/10.1016/j.jtrangeo.2015.06.001.

Mączka, M., 2016a. Accessibility model for the evaluation of transport infrastructure policy. Trans. Instit. Aviation 245 (4), 116–133. https://doi.org/10.5604/05096669.1226430.

Mączka, M., 2016b. Evaluation of the transport policy in Poland using daily accessibility indicator - 2015 and 2030. Trans. Instit. Aviation 245 (4), 150–159. https://doi.org/10.5604/05096669.1226883.

Manataki, I.E., Zografos, K.G., 2010. Assessing airport terminal performance using a system dynamics model. J. Air Transp. Manag. 16 (2), 86–93. https://doi.org/10.1016/j.jairtraman.2009.10.007.

Marcucci, E., Gatta, V., 2011. Regional airport choice : consumer behaviour and policy implications. J. Transp. Geogr. 19 (1), 70–84. https://doi.org/10.1016/j.jtrangeo.2009.10.001.

Nießе, H., Grimme, W., 2014. Minimum travel times between European regions – an assessment of the ACARE 4h-goal. In: ATRS 2014, Retrieved from. http://elib.dlr.de/90548/1/ATRS2014-ACARE 4h goal_Final.pdf.

Nyquist, D.C., Mcfadden, K.L., 2008. A study of the airline boarding problem. J. Air Transp. Manag. 14 (4), 197–204. https://doi.org/10.1016/j.jairtraman.2008.04.004.

Piwek, K., Wiśniowski, W., 2016. Small air transport aircraft entry requirements evoked by FlightPath 2050. Aircraft Eng. Aero. Technol.: Int. J. 88 (2), 341–347. https://www.doi.org/10.1108/.

Poelman, H., 2013. Measuring Accessibility to Passenger Flights in Europe: towards Harmonised Indicators at the Regional Level. Retrieved from. http://ec.europa.eu/regional_policy/sources/docgener/focus/2013_09_passenger.pdf.

Schmitt, D., Gollnick, V., 2016. Air Transport System. Springer Vienna, Vienna. https://doi.org/10.1007/978-3-7091-1880-1.

Schultz, M., 2010. Entwicklung eines individuenbasierten Modells zur Abbildung des Bewegungsverhaltens von Passagieren im Flughafenterminal. Retrieved from. http://www.qucosa.de/fileadmin/data/qucosa/documents/8559/Dissertation_Michael_Schultz_IFL-TUDD.pdf.

Statistisches Bundesamt, 2000. Stadt-/Landgliederung nach der Zuordnung von Eurostat 2000. https://doi.org/10.1007/s001170170196.

Sun, X., Wandelt, S., Hansen, M., Li, A., 2017. Multiple airport regions based on inter-airport temporal distances. Transport. Res. E Logist. Transport. Rev. 101, 84–98. https://doi.org/10.1016/j.tre.2017.03.002.

Takakuwa, S., Oyama, T., 2008. Simulation analysis of international-departure passenger flows in an airport terminal. In: Proceedings of the 2003 International Conference on Machine Learning and Cybernetics (IEEE Cat. No.03EX693). IEEE, pp. 1627–1634. https://doi.org/10.1109/WSC.2003.1261612.

Tsamboulas, D.A., Nikoleris, A., 2008. Passengers ' willingness to pay for airport ground access time savings. Transport. Res. Part A 42 (10), 1274–1282. https://doi.org/10.1016/j.tra.2008.03.013.

Urban, M., Jessberger, C., Rothfeld, R., Schmidt, M., Batteiger, V., Plötner, K.O., Hornung, M., 2016. Multi-modal transport hub concept for inner-city airport operation. In: Deutscher Luft- und Raumfahrtkongress 2016 (DGLR), pp. 1–11. Retrieved from. http://www.dglr.de/publikationen/2016/420225.pdf.

Vickerman, R., 2007. Recent Evolution of Research into the Wider Economic Benefits of Transport Infrastructure Investments. Retrieved from. http://www.oecd-ilibrary.org/docserver/download/234770772187.pdf?expires=1493219582&id=id&accname=guest&checksum=92588F3A201E7CD68AE7D913E9FDF89C.

Vickerman, R., Spiekermann, K., Wegener, M., 1999. Accessibility and economic development in Europe. Reg. Stud. 33 (1), 1–15. https://doi.org/10.1080/00343409950118878.

Welch, T.F., Mishra, S., Wang, F., 2015. Interrelationship between airport enplanements and accessibility. Transport. Res. Rec.: J Trans Res Board 2501, 46–55. https://doi.org/10.3141/2501-07.

Wooldridge, J.M., 2009. Introductory Econometrics : a Modern Approach. Cengage Learning, South-Western.

B Rothfeld et al. (2020). Urban Air Mobility.

Reference: Rothfeld, R., Straubinger, A., Fu, M., Al Haddad, C., & Antoniou, C. (2020). Urban air mobility. In C. Antoniou, D. Efthymiou, & E. Chaniotakis (Eds.), *Demand for Emerging Transportation Systems - Modeling Adoption, Satisfaction, and Mobility Patterns* (1st ed., pp. 267–284). Elsevier.

Chapter 13

Urban air mobility

Raoul Rothfeld[1,2], Anna Straubinger[1], Mengying Fu[1], Christelle Al Haddad[2], Constantinos Antoniou[2]

[1]*Bauhaus Luftfahrt e.V., Taufkirchen, Germany;* [2]*Chair of Transportation Systems Engineering, Department of Civil, Geo and Environmental Engineering, Technical University of Munich, Munich, Germany*

Chapter outline

1. Introduction

Current technological advances in energy storage densities, as well as in electric and distributed propulsion, facilitate the development of passenger-carrying, short-haul air vehicles—so-called personal air vehicles (PAVs) or next-generation vertical takeoff and landing (VTOL) vehicles. These vehicle concepts, which promise to be quieter, safer, and cheaper to produce and operate than conventional helicopters, revitalize the idea of using urban airspace for intracity passenger transport, i.e., urban air mobility (UAM).

The concept of using urban aerial transportation is not novel, however, and had—at one time—been well established in, most notably, New York with New York Airways, which operated commercial helicopter-based passenger transport services from 1953 to 1979. After a series of fatal accidents and crashes, however, New York Airways ceased its operation and filed for bankruptcy shortly after. While this chapter of urban aerial mobility came to an abrupt end, today, various helicopter transport services have reemerged in traffic-stricken metropolises such as São Paulo, Mexico City, and, yet again, New York.

Companies like Fly Blade Inc. and Voom offer helicopter passenger transport services on an on-demand basis by making use of mobile applications for ad hoc ridehailing. For those helicopter services, flight schedules have, thus, been made obsolete by Internet-connected technologies. Now, with

Demand for Emerging Transportation Systems. https://doi.org/10.1016/B978-0-12-815018-4.00013-9

the advent of novel vehicle concepts for VTOL, an additional driver of UAM could be emerging.

Recently, a multitude of companies can be observed that race each other to advance VTOL technologies and to prototype and mass-produce the first next-generation VTOL vehicle, as illustrated by Shamiyeh et al., 2017). Besides the vehicles themselves, however, it is necessary to understand a vast array of research, as UAM requires the coordination and interaction of various fields, such as air traffic management, infrastructure development, integration with ground-based transport systems, public safety and acceptance, and regulations. The remainder of this chapter provides a literature overview of three key aspects for understanding potential demand, supply, and external effects of UAM by discussing its passenger adoption, transport modeling, and spatial as well as welfare effects.

2. Passenger adoption

By making use of aerial transport capacity, UAM is aimed at reducing problems facing the growing demand for mobility in an increasingly crowded environment, such as congestion, pollution, and scarcity of urban space. Advances in automation technology, notably for ground vehicles, could potentially also be applied for air mobility, leading to autonomous flying vehicles. The underlying assumption, feeding into the idea of widespread UAM usage, is that UAM vehicles will be fully autonomous in order to provide affordable on-demand aerial mobility for everyone.

The time frame for its potential implementation, however, remains unknown as it is subject to many challenges. These are mostly related to regulations, technology, safety, but also public and the potential passengers' acceptance; with social acceptance being one of the key components to UAM's implementation (c.f. Liu et al., 2017). As technological solutions are constantly evolving and regulations being negotiated, social acceptance remains one of the less predictable components and, therefore, a main challenge to UAM's introduction to the market.

Adoption and usage are the result of complex decision processes and depend on many unobserved variables. Therefore, many surveys focus on improving the understanding of people's perception toward new technologies, thereby identifying the most influential factors in their acceptance and adoption. Still, in the case of UAM, research lacks studies focusing on user perception and most existing surveys have been focusing on autonomous ground-based vehicles.

Only recently, research institutions have begun to take interest in UAM's social acceptance. A study by Garrow et al. (2018a) from the Georgia Institute of Technology, collected responses from about 2500 high-income workers in different areas of the United States, to more accurately predict demand for VTOL trips. NASA commissioned two comprehensive market studies (see

Cohen et al., 2018; Berger, 2018) looking at UAM from market, regulatory, societal barrier, and weather impact perspectives. In Germany, research on UAM has been facilitated by the city of Ingolstadt as part of the so-called Urban Air Mobility Initiative, supported by the European Commission. The Technical University of Munich has also taken interest in this topic, with first research into establishing mode choice models including autonomous ground- and air-based transport modes by Fu et al. (2019) and a factor study for passenger adoption among Munich residents by Al Haddad et al. (2019). Lately, several consulting groups including Berger (2018) and HorvathPartners (2019) focused on defining UAM success factors and assessing the UAM market potential, respectively.

Al Haddad et al. (2019) conducted an online survey and collected 221 responses, among which 97 were Munich residents, to extract the factors influencing the potential adoption and use of UAM. The initial findings confirmed that most of the respondents ranked safety as the most important factor affecting their adoption of UAM. By using exploratory factor analysis, the following factors were extracted and had a relatively high explanatory power: value of time savings, affinity to automation, safety concerns, data concerns, environmental awareness, and affinity to online services, social media, and sharing. Discrete choice models, i.e., ordered logit models, allowed to identify patterns for adoption, where uncertain adopters (uncertain about their time of UAM adoption) had similar attitudes to late adopters. Trust was found to be a key factor in the intention to adopt UAM and was positively influenced by the perceived reliability of automation, perceived vehicle's safety, perceived locus of control, previous automation experience, and the service provider's reputation.

Understanding passenger perception of UAM is a must to understand the technology as it allows the relevant stakeholders, such as governments or manufacturers, to take the corresponding measures to best address social acceptance. In this perspective, research should also focus on mode choice in an environment comprising both conventional modes of transport, which might be autonomous in the future, and UAM.

Current research concerning VTOL and UAM often focuses on technological and operational aspects (see e.g., Holden and Goel, 2016; Parker, 2017; Schuchardt et al., 2015). Only very little mode choice research can be found that analyzes the potential user preference among conventional transport modes and novel transport service, such as UAM. Though, based on a general review of factors affecting transport mode choice, as well as existing studies using choice theory to model various aspects of autonomous vehicles (AVs) and shared autonomous vehicles (SAVs), mode choice factors can be categorized into three groups when applied to UAM: (1) transportation service variables, (2) individual-specific variables, and (3) attitudinal/psychological variables.

With regard to transportation service variables, cost- and time-related attributes have been most commonly considered in transportation mode choice studies (c.f. Fu et al., 2019). Several other factors have been found relevant as well, particularly regarding the adoption of AVs and UAM. For instance, Winter et al. (2017) conducted a stated preference experiment and developed logit models to study mode choice among car-sharing, private car, public transportation (PT), and SAV in the Netherlands. Among the travel time-related attributes, waiting time for SAVs has been found to be insignificant. Nevertheless, other studies (e.g., Fagnant and Kockelman, 2018; Krueger et al., 2016) estimated the value of time (VOT) and willingness to pay of AVs and SAVs, showing an opposing view that waiting time is a critical service attribute of SAV operations. Similar to the findings of Krueger et al. (2016) on travel time and travel cost of SAVs, the recent mode choice study of Fu et al. (2019) concluded that travel time and travel cost might also be significant determinants of UAM adoption, although further research is expected to provide insights into the impact of waiting time and first- and last-mile services.

To understand individuals' willingness to pay for travel time savings, VOT measures have been commonly conducted for transportation mode choice studies in different countries or regions. For example, Atasoy et al. (2011) and Axhausen et al. (2006) have conducted studies in Switzerland regarding private car and public transportation usage. A Europe-wide meta-analysis (Wardman and Chintakayala, 2012) concerning VOT of conventional transportation modes has also been conducted with regard to different trip purposes, e.g., leisure or business purpose. Although rare, a few recent studies, which present VOT findings of autonomous transportation services, have been found as well. For instance, Correia et al. (2019) published VOT study results regarding SAVs in the Netherlands, while Fu et al. (2019) presented preliminary VOT estimations on SAVs and UAM. Nevertheless, it is worth noting that the measures of VOT differ greatly in-between studies and study areas, as the value of time can be affected by many, highly diverse factors, such as income level or quality and performance of existing transportation systems—all of which may vary greatly by study area and time.

The result of a general mode choice literature review indicates that socioeconomic variables, such as gender, age, and income have impact on mode choice behavior (see e.g., Fu et al., 2019; Atasoy et al., 2011; Vrtic et al., 2009). However, concerning the influence of personal and household characteristics on the choice to travel by AVs or SAVs, the before-mentioned research does not provide consistent findings (Fu et al., 2019). Assessing age as a factor, some studies state that younger individuals are more willing to adopt AVs (Bansal et al., 2016), while others found that SAVs could constitute an attractive mobility option especially for the elderly (Fagnant and Kockelman, 2018). Moreover, Bansal et al. (2016) and Kyriakidis et al. (2015) observed a positive relationship between willingness to pay for autonomous features and

income. In addition, a few studies also revealed a significant impact of education level and presence of children in the household (c.f Haboucha et al., 2017; Zmud et al., 2016). Similar aspects have been mentioned in recent research regarding flying vehicles and UAM: Castle et al. (2017) presented survey results which indicate that younger and more educated respondents are more willing to accept pilotless aircraft. Cohen et al. (2018) revealed greater excitement regarding UAM among middle- and upper-income households and younger and middle-aged respondents, as well as among respondents with higher level of educational attainment. Fu et al. (2019) mode choice study concerning UAM suggested that market penetration rate for UAM may be greater among younger respondents and older individuals with high income, who also have a relatively high propensity to use ground-based AVs.

Besides socioeconomic variables, other factors, such as current modality patterns, have also been found relevant to the adoption of AVs and UAM. For example, car users (drivers) are more likely to switch to SAVs than PT users (Krueger et al., 2016). Similar findings have been stated by Fu et al. (2019) that switching to either autonomous taxi or UAM is less likely if the individuals currently use PT or soft modes, i.e., walking and cycling, most often. Trip purpose may be another influencing factor. Similar to the results of the mode choice study including UAM (Fu et al., 2019) (as illustrated in Fig. 13.1), an Airbus study (Thompson, 2018), Garrow et al. (2018b), and Cohen et al. (2018) found that individuals may be particularly interested in using a flying taxi service for performing business and recreational trips.

Attitudinal factors, such as the preference for convenience, comfort, and flexibility have attracted increasing attention and found to be relevant to transportation mode choice behavior (Vredin Johansson et al., 2006). Existing literature highlights the impact of safety on AVs adoptions (e.g., Haboucha et al., 2017; Fu et al., 2019). Individuals who tend to use AVs or SAVs also express greater concern for the environment (Haboucha et al., 2017; Howard and Dai, 2014) and stronger technological awareness (Bansal et al., 2016;

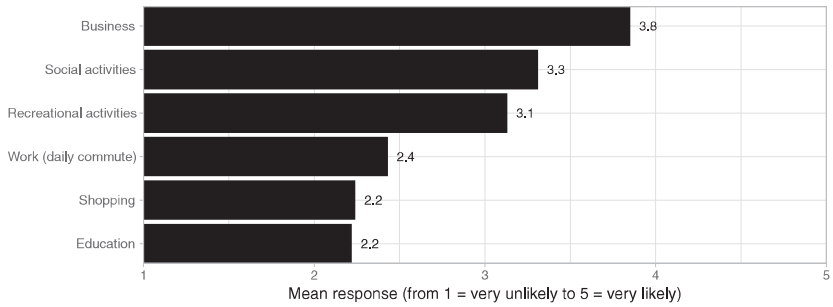

FIGURE 13.1 Survey results of likelihood to use UAM based on various trip purposes, own depiction based on Fu et al. (2019).

Schoettle and Sivak, 2014; KPMG, 2013). Amenities and vehicle automation have also been identified as being influential (Winter et al., 2017; Howard and Dai, 2014). Similarly, safety is regarded as one of the main psychological barriers to adopting flying vehicles (Cohen et al., 2018; Lineberger et al., 2018; Yedavalli and Mooberry, 2019). Interestingly with regard to automation, piloted aircraft are still generally preferred over fully autonomous flying vehicles (Cohen et al., 2018).

The impacts of other potential psychological factors, affecting UAM-related mode choice, have not been thoroughly studied yet. However, the survey results of Fu et al. (2019) regarding attitudes of different demographic groups indirectly reflect the potential technological and environmental concerns, which may affect choice behavior. Similar to the previously mentioned findings related to AV adoption (see Haboucha et al., 2017), Fu et al. (2019) survey results also indicate that younger individuals are more open toward new technologies (see top-left illustration in Fig. 13.2) and, thus, are more likely to adopt novel transport modes. Meanwhile, another group of potential adopters who are older and with high income may be more willing to pay for new technological and environmental-friendly transportation services. However, the low-income group with lower education level is likely to have less technological and environmental concerns and, therefore, may be less willing to accept novel transportation concepts, such as UAM.

Various findings have been presented by different UAM-related studies with focus on passenger adoption perspectives. Not all studies provide consistent conclusions regarding the factors affecting UAM adoption. However, several highly relevant demand drivers of UAM adoption, such as travel time, costs, value of time savings, safety concerns, income, environmental awareness, and affinity to sharing have been commonly highlighted in most of the mentioned studies.

3. Modeling urban air mobility

To provide a general picture of the operational UAM environment, current research focuses on investigating concept of operations by identifying various vehicle types, infrastructure requirements, environmental impact, and other potential constraints (c.f Holden and Goel, 2016; Antcliff et al., 2016; Kleinbekman et al., 2018; Vascik and Hansman, 2017a). In another study, Vascik and Hansman (2017b) provide specific operational suggestions regarding the identification of locations for VTOL infrastructure, so-called vertiports, and the capacity of air traffic control; while Balakrishnan et al. (2018) present an overview of routing strategies for UAM operation. General guidance in transportation network design and its various influencing factors is given by Rodrigue et al. (2017), with first studies confirming the importance of the number and distribution of UAM vertiport within a study area, as, e.g., shown by Rothfeld et al. (2018a) in the use case of Sioux Falls.

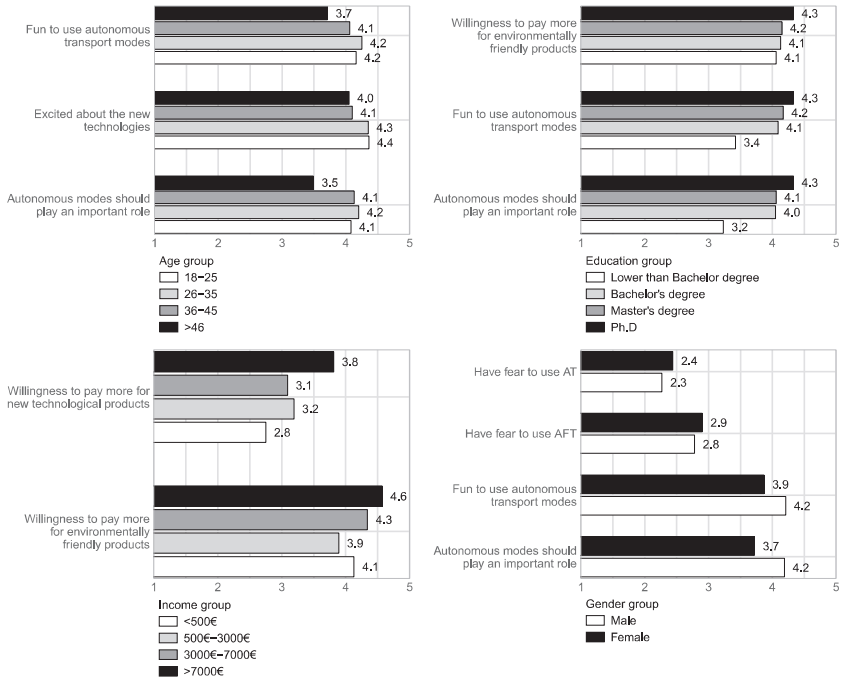

FIGURE 13.2 Survey result of technological and environmental concerns of different demographic groups, own depiction based on Fu et al. (2019).

Several studies analyze the UAM supply side based on modeling and simulation approaches. The object-oriented model developed by Kohlman and Patterson (2018) showed that a vehicle's recharging/refuelling rates can affect its ability to meet potential demand. Kohlman and Patterson (2018) also highlighted the importance of having a sufficient number of vertiports. Another simulation evaluation of Bosson and Lauderdale (2018) applied the so-called Autoresolver algorithm, which focused on the seamless integration of a new transport mode into an existing system by identifying valid vertiports locations. The Autoresolver algorithm has been proposed as a service with the potential to manage an entire UAM network with both strategic and tactical scheduling capabilities.

Meanwhile, estimating the demand and evaluating the demand drivers is a prerequisite for introducing UAM to the market (Straubinger and Rothfeld, 2018). A few studies address demand estimation of UAM-based on logit model for mode choice (e.g., Fu et al., 2019; Syed, 2017). The preliminary results of Syed (2017) show that the cost of on-demand VTOL must be kept rather low for UAM, for it to become a significant competitor to other modes.

Although not directly linked to UAM, Reddy and DeLaurentis (2016) explored demographic factors as well as stakeholder variables that affect public and stakeholder opinions about unmanned aircraft, using multinomial probit models. To identify a market niche, which can be filled by UAM, a few market studies (e.g., Berger, 2018; HorvathPartners, 2019) have been implemented based on analyzing market models. The UAM market potential has been projected, following a two-fold modeling approach, comparing the demand with and without considering current technological restrictions, economic constrains, and social barriers. One study (HorvathPartners, 2019) stated that UAM will play an important part in future multimodal mobility concepts.

Having been applied to modeling non-UAM types of on-demand aviation, the so-called strategic modeling method estimates future demand using socioeconomic and demographic information (see Moore and Goodrich, 2013; Smith et al., 2012). Strategic models are currently sensitive to many of the required behavioral impacts and can be adapted to represent changing behavior (Travel forecasting resource, 2018). The implementation of new mobility services, such as AVs or UAM, allows for and might require new strategies and policies. As the traditional trip-based models (such as four-step transport model) are not sufficiently sensitive to emerging policy and policy questions, many transport modelers now apply activity-based approaches which take, e.g., individual's budget, their time for activities, and travel patterns throughout a day into account (Travel forecasting resource, 2014).

Currently, the majority of studies modeling and simulating AV operations use MATSim (Horni et al., 2016), an open-source framework, to implement large-scale agent-based transport simulations. Bischoff and Maciejewski (2016a, 2016b) as well as Hörl (2016) estimated SAV demand using MATSim's agent-based model by utilizing the DVPR (Dynamic Vehicle Routing Problem) extension, in order to simulate a wide range of vehicle routing and scheduling processes. Moreno (2017) implemented another approach by modeling SAV services, while considering the feedback between land-use and changes in transportation systems, by coupling the land-use model SILO, the travel demand model MITO, and the transport model MATSim. Thus, providing a comprehensive modeling framework to account for the effects of AVs on transportation as well as land-use. Recently, this agent-based simulation approach using MATSim is also considered as a valid approach to analyze UAM performance.

First studies (e.g., Rothfeld et al., 2018a; Rothfeld et al., 2018b; Balac et al., 2018) regarding UAM infrastructure, vehicles' characteristics, network, and operational fleet capabilities; provide an initial basis for further UAM transport research. The modeling results indicate that the potential travel time reduction perceived by potential passengers, as well as UAM infrastructure and ground-based UAM processes, have an elemental influence on UAM adoption. For smaller study areas, such as Sioux Falls (Rothfeld et al., 2018b) and Zurich (Balac et al., 2018), the importance of short times for accessing

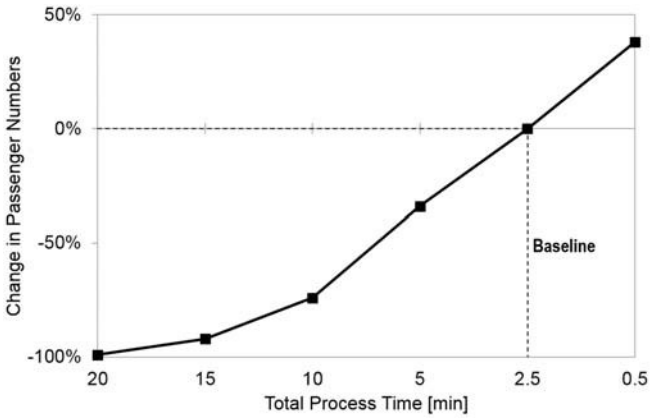

FIGURE 13.3 Impact of UAM process time variations on passenger numbers within a MATSim simulation of Sioux Falls, US (Rothfeld et al., 2018b).

vertiports and boarding UAM vehicles has been repeatedly highlighted. Compare, for example, Figs. 13.3 and 13.4, which show the greater effect of UAM process time increases versus faster UAM cruise speeds on passenger numbers. The travel time savings, gained by UAM's expected high travel speeds, when compared to, e.g., cars, could be negated by potentially long UAM processes before and/or after a UAM flight.

Initial research on UAM ground infrastructure has been presented by, e.g., Vascik and Hansmann (Vascik, 2019) or Fadhil (Fadhil, 2018), who take existing helicopter infrastructure as an approximation for future vertiports from a sizing and throughput perspective. Especially for the envisioned short-

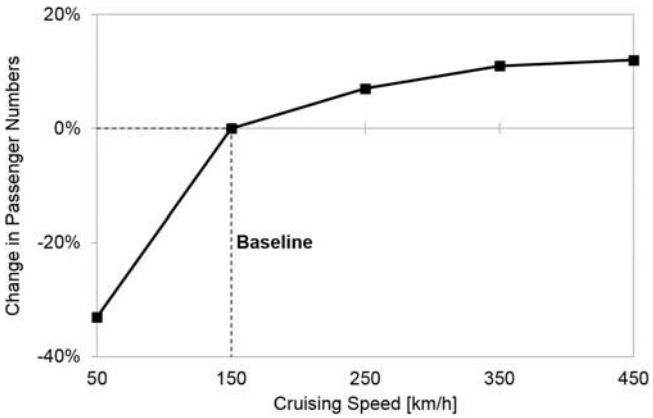

FIGURE 13.4 Impact of UAM cruise speed variations on passenger numbers within a MATSim simulation of Sioux Falls, US (Rothfeld et al., 2018b).

distance, i.e., intracity, usage of UAM, Wölfel (2019) identified the importance of infrastructure placement as a potential bottleneck for the implementation of UAM in Germany. Thus, space requirements and placement options for vertiports, in combination with the high impact of short access times, renders UAM infrastructure positioning as being a major factor in any potential UAM implementation and, thus, should receive even more attention in future UAM modeling research.

A well-functioning transportation system should allow the transport supply to meet transport demand. According to the results of a general literature review, current studies mainly focus on modeling UAM networks and operations. Further research is expected to consider both demand and supply sides of UAM as a whole, in order to enhance the understandings of the overall UAM environment and its impacts. Future studies on modeling UAM should, therefore, combine extended supply- and demand-side approaches to enable comprehensive analyses that fully encompass the various aspects of introducing UAM as a novel transport mode into existing transport systems.

With regard to existing UAM transport modeling approaches using MATSim, further improvements are required to reflect this merging of supply- and demand-side attributes, such as vehicle energy storage capacities, vertiport vehicle capacities, and ensuring vertical and horizontal separation of UAM vehicles during flight. Further, vehicle dispatching algorithms and fleet distribution optimization, as presented by, e.g., Hörl et al. (2019) for autonomous ridehailing services in Zurich, will be aspects relevant to UAM services and might be transferable in their approach to modeling of UAM.

4. Spatial and welfare effects

Besides the impact on the overall transport system, it is essential to understand the influence of UAM on the inhabitants' welfare and the implications for the city. Welfare changes should hereby not only consider shifts directly related to the transport market but also adjustments on other markets due to the introduction of UAM.

Transferring Milakis et al. (2017) methodology, who applied the ripple effect approach to the introduction of automated vehicles, one can differentiate between first-, second-, and third-order implications:

- First-order implications: travel costs, travel time, value of time, travel comfort, mode choice and modal shift, vehicle miles traveled, additional infrastructure
- Second-order implications: impact on other modes (road congestion, existing transport infrastructure, public transport usage), shifts in the location choice of companies and households, changes of the prices on

other markets (e.g., land market, commodity market, labor market), changes in the accessibility of different parts of the urban area
- Third-order implications: urban sprawl, negative environmental aspects: noise, visual annoyance, emissions, safety, social equity, economic impact, public health, energy consumption

While most of the first-order implications have been described in the previous chapters, the following discusses the resulting changes on related markets. Some discussions have already taken place in the literature (see, e.g., UBER, 2016; Holmes et al., 2017; Straubinger and Rothfeld, 2018) Yet, especially in contrast to the literature on the technology of VTOL vehicles, a lot of open questions remain in the field of wider economic impacts of UAM. Nevertheless, some of the findings from autonomous ground vehicle research (c.f Fagnant and Kockelman, 2013; Gruel and Stanford, 2016) can be transferred to UAM as both concepts are rather similar from an end-user perspective.

One decisive question is whether UAM will take car-based transport demand and shift it to the air, or whether additional transport demand will be induced by the introduction of UAM. Potentially, both effects might occur simultaneously. This is an effect that has already been identified in the field of autonomous ground-based vehicles. Duarte and Ratti (2018), for example, discuss the question of whether autonomous vehicles lead to more or less traffic on roads. Large parts of their reasoning can be transferred to UAM.

Additionally, potential modal shifts from public transport or soft modes to UAM are relevant, as this might result in increasing externalities. It is, therefore, essential to ensure a close linkage of any potential UAM introduction with existing transport systems, to reduce the probability of UAM drawing from the demand for PT or soft modes. According to Otte et al. (2018), an efficient integration of UAM and public transport is inevitable, not only from a physical perspective as in developing joint mobility hubs, but also from an organizational point of view with regard to ticketing and distribution platforms.

Besides mode choice, location choice of households and companies within cities can significantly influence the vehicle miles traveled. Thakur et al. (2016) and Duarte and Ratti (2018) already discussed these developments for autonomous ground-based vehicles and indicate that an influence on land rents and location choice is to be expected. Existing literature qualitatively proves that transport investments and, by that, positive changes in accessibility provoke rising land rents and increasing attractiveness of certain housing locations (see Cervero and Kang, 2011).

In the case of UAM, Straubinger and Verhoef (2018) expect two effects to occur: 1) the additional land demand for vertiport infrastructure will decrease the land supply for housing and company locations and 2) the land demand from households and companies will increase due to higher accessibility. These effects and their correlations are depicted in Fig. 13.5.

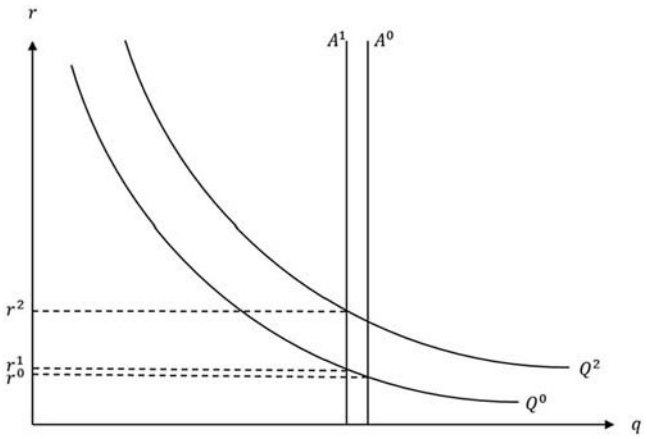

FIGURE 13.5 Changes in land rents in the suburbs due to additional demand and decreasing supply (Straubinger and Verhoef, 2018).

As described by Straubinger and Verhoef (2018), the x-axis denotes the quantity of land q, and the y-axis denotes the land rent per measurement unit r. The land supply for housing and company locations is fixed. A^0 hereby depicts the land supply in the suburb in a scenario without UAM. The introduction of UAM and the arising need for infrastructure result in a decreased land supply (A^1).

With the original demand for land from companies and households (Q^0), an initial price (r^0) is identified. The introduction of UAM is assumed to lead to increased connectivity of the suburb to the city and employment centers. High travel speeds, which UAM might offer, enable massive decreases in travel time. Together with the above-mentioned increasing attractiveness of suburban locations, due to transport service enhancements, the constancy of travel times (see Levinson and Kumar, 1997) allows to assume an increase in land demand by households and companies in the suburb (Q^2). In line with this increase of demand, the land rents in the suburb are expected to increase as well (r^2).

Straubinger and Verhoef (2018) reasoning shows that changes in land rents can arise based on the introduction of new mobility services. The decrease in travel time will also enable households to locate farther away from cities, where they can afford more land for housing. This effect could be reinforced with the advent of autonomous transport technology. Thakur et al. (2016) assume that, in the case of autonomous ground vehicles, people will relocate further away from the city. Additionally, the value of travel time savings decreases, since travel time could be used more productively with automated controls. Transferring this assumption to UAM strengthens the above-made

assumption on the relocation of households. Yet, this might not only have positive effects. Longer distances to the city center are likely to result in more vehicle miles traveled. Besides that, most cities do not favor their residents moving away from the city centers, as this leads to urban sprawl. Urban sprawl, i.e., the undesired relocation of people toward the suburbs, leads to lower population densities in city centers, which can result in massive inefficiencies in public services, such as with public infrastructure and public transport provisions (Squires, 2002).

Following Straubinger and Verhoef (2018) approach for UAM and transferring the findings of Thakur et al. (2016) and Duarte and Ratti (2018) for autonomous ground vehicles, relocation of households, due to a potential introduction of UAM, appears to be very likely. Thus, UAM involves the potential for causing undesired urban sprawl.

UAM's ecological impact strongly depends on all different aspects that have been mentioned so far. Only after estimating the vehicle miles traveled and modal splits of holistic transport system analyses, an assessment of UAM's ecological impact can be performed. Even when assuming UAM operators to exclusively use fully electric, shared, and on-demand vehicle services—by that trying to minimize the environmental effect of UAM with regard to, e.g., CO_2 and NOx emissions—noise and visual disturbance are externalities that cannot be avoided. Additionally, UAM also faces similar risks to those of autonomous cars (c.f Goodall et al., 2014; Hubaux et al., 2004; Maurer et al., 2015), in that loss of jobs due to automation, data privacy concerns, and ethical problems with regard to vehicle's automated decision making remain challenges yet to be tackled.

The externalities and other risks should be minimized and/or internalized by an adequate service design. The service design and interests of the service provider strongly relate to the market structure and business model. UAM has different submarkets and players: the vertiport infrastructure provider, the communication infrastructure provider, the air traffic management provider, the vehicle manufacturer, the vehicle owner, the service provider, and the platform provider. The various levels will face different intensities of competition within one level and vertical integration with players on other business levels (Cohen et al., 2018).

As multiple of the submarkets are likely to be dominated by a few market players, in combination with the above-discussed externalities, a potential UAM market is expected to be regulated like most of the other transport modes (see e.g., Baake and von Schlippenbach, 2014; Cairns and Liston-Heyes, 1996; Cantos and Maudos, 2001; de Palma and Lindsey, 2004; Haucap et al., 2015; Weiβ, 2003). Thus, regulation strategies, e.g., price regulation, quantity regulation, and quality regulation can be expected to be implemented for UAM services.

As indicated above, there is little to no research in the fields of urban economics and market regulation in the context of UAM. Thus, changes in location choice of households and companies, as well as changes in land rents

and urban form, often remain unconsidered. To improve the assessment of overall changes in vehicle miles traveled this is a necessary step. Besides that, households locating farther from the city center might lead to urban sprawl and, by that, to massive inefficiencies especially regarding infrastructure and traveling patterns. To minimize the negative effects of UAM, e.g., externalities (emissions, noise, congestion) and urban sprawl, it also is essential to address regulatory options in future research. The effects of different market regulating policies could be assessed together with UAM's impact on urban structures in an urban spatial computable general equilibrium (CGE) model as proposed by Straubinger and Verhoef (2018).

5. Conclusion

While research surrounding UAM steadily emerges with all its facets from vehicle performance, vehicle design, air traffic management, as well as its adoption, transport system modeling, and spatial and welfare effects; further understanding must be inspired. Only combining findings from the various disciplines of research into one coherent picture—while a formidable task—will facilitate in-depth analyses of the interdependencies of a potential UAM implementation within current transport systems and mobility patterns.

For UAM to become the reality that is currently being envisioned, a vast number of requirements must be fulfilled, from minimal noise levels, to trust building safety standards, and public accessibility that fosters public acceptance. It remains yet to be seen, however, whether manufacturers, transport planners, and researchers can live up to such promises.

The presented overview of research regarding UAM as a novel transport mode illustrates the uptake in UAM-related publications and research from other novel ground-based mobility concepts, such as autonomous ridehailing, that seems applicable to aerial mobility. Throughout the various discussed topics it became obvious that UAM research requires more in-depth analyses and, especially, conjoint studies that bridge multiple subject areas in order to gain a more widely applicable understanding of UAM, its acceptance, modeling, and further-reaching effects.

References

Al Haddad, C., Chaniotakis, E., Straubinger, A., Ploetner, K., Antoniou, C., 2019. User acceptance and adoption of urban air mobility. In: Transport Research: Part A (submitted).

Antcliff, K.R., Moore, M.D., Goodrich, K.H., 2016. Silicon Valley as an Early Adopter for On-Demand Civil VTOL Operations, pp. 1–17.

Atasoy, B., Glerum, A., Bierlaire, M., 2011. Mode choice with attitudinal latent class: a Swiss case-study. In: Second International Choice Modeling Conference, pp. 1–16.

Axhausen, K., Hess, S., König, A., Agay, G., Bates, J., Bierlaire, M., 2006. State of the Art Estimates of the Swiss Value of Travel Time Savings.

Baake, P., von Schlippenbach, V., 2014. Taximarkt: kein markt für eine vollständige liberalisierung. DIW-Wochenbericht 81 (31/32), 751–755.

Balac, M., Vetrella, A.R., Rothfeld, R., Schmid, B., 2018. Demand estimation for aerial vehicles in urban settings. IEEE Intelligent Transportation Systems Magazine.

Balakrishnan, K., Polastre, J., Mooberry, J., Golding, R., Sachs, P., 2018. BluePrint For The Sky - The Roadmap for the Safe Integration of Autonomous Aircraft.

Bansal, P., Kockelman, K.M., Singh, A., 2016. Assessing public opinions of and interest in new vehicle technologies: an Austin perspective. Transportation Research Part C: Emerging Technologies 67, 1–14.

Berger, R., 2018. Urban Air Mobility, the rise of a new mode of transportation. Technical Reports.

Bischoff, J., Maciejewski, M., 2016. Autonomous taxicabs in berlin—a spatiotemporal analysis of service performance. Transportation Research Procedia 19, 176–186.

Bischoff, J., Maciejewski, M., 2016. Simulation of city-wide Replacement of private cars with autonomous taxis in berlin. Procedia Computer Science 83 (Ant 2016), 237–244.

Bosson, C., Lauderdale, T.A., 2018. Simulation evaluations of an autonomous urban air mobility network management and separation service. In: 2018 Aviation Technology, Integration, and Operations Conference, p. 3365.

Cairns, R.D., Liston-Heyes, C., 1996. Competition and regulation in the taxi industry. Journal of Public Economics 59 (1), 1–15.

Cantos, P., Maudos, J., 2001. Regulation and efficiency: the case of European railways. Transportation Research Part A: Policy and Practice 35 (5), 459–472.

Castle, J., Fornaro, C., Genovesi, D., Lin, E., Strauss, D.E., Waldewitz, T., Edridge, D., 2017. Flying solo – How Far are We Down the Path Towards Pilotless Planes?, p. 53.

Cervero, R., Kang, C.D., 2011. Bus rapid transit impacts on land uses and land values in Seoul, Korea. Transport Policy 18 (1), 102–116.

Cohen, A., Susan, S., Emily, F., 2018. The potential societal barriers of urban air mobility, Executive Briefing urban air mobility (UAM) market study. Tech. Rep. Booz Allen Hamilton.

Correia, G.H.d.A., Looff, E., van Cranenburgh, S., Snelder, M., van Arem, B., 2019. On the impact of vehicle automation on the value of travel time while performing work and leisure activities in a car: theoretical insights and results from a stated preference survey. Transportation Research Part A: Policy and Practice 119 (November 2018), 359–382.

de Palma, A., Lindsey, R., June 2004. Congestion pricing with heterogeneous travelers: a general-equilibriumwelfare analysis. Networks and Spatial Economics 4, 135–160.

Duarte, F., Ratti, C., October 2018. The impact of autonomous vehicles on cities: a review. Journal of Urban Technology 25, 3–18.

Fadhil, D.N., 2018. A GIS-Based Analysis for Selecting Ground Infrastructure Locations for Urban Air Mobility. Master's Thesis. Technical University of Munich, Munich.

Fagnant, D., Kockelman, K., 2013. Preparing a nation for autonomous vehicles. Tech. Rep. Eno Center for Transportation.

Fagnant, D.J., Kockelman, K.M., 2018. Dynamic ride-sharing and fleet sizing for a system of shared autonomous vehicles in Austin, Texas. Transportation 45 (1).

Fu, M., Rothfeld, R., Antoniou, C., 2019. Exploring preferences for transportation modes in an urban air mobility environment: munich case study. In: Transportation Research Record. https://doi.org/10.1177/0361198119843858.

Garrow, L.A., German, B., Mokhtarian, P., Daskilewicz, M., Douthat, T.H., Binder, R., June 2018. If you fly it, will commuters come? A Survey to Model Demand for eVTOL Urban Air Trips (Atlanta).

Garrow, L.A., German, B.J., Ilbeigi, M., 2018. Conceptual models of demand for electric propulsion aircraft in intra-urban and Thin-haul markets. In: Transportation Research Board 97th Annual Meeting, Washington DC, United States.

Goodall, N.J., 2014. Machine ethics and automated vehicles. In: Meyer, G., Beiker, S. (Eds.), Road Vehicle Automation. Springer International Publishing, Cham, pp. 93–102.

Gruel, W., Stanford, J.M., January 2016. Assessing the long-term effects of autonomous vehicles: a speculative approach. Transportation Research Procedia 13, 18–29.

Haboucha, C.J., Ishaq, R., Shiftan, Y., 2017. User preferences regarding autonomous vehicles. Transportation Research Part C: Emerging Technologies 78, 37–49.

Haucap, J., Pavel, F., Aigner, R., Arnold, M., Hottenrott, M., Kehder, C., 2015. Chancen der Digitalisierung auf Märkten für urbane Mobilität: Das Beispiel Uber. In: DICE Ordnungspolitische Perspektiven 73. University of Düsseldorf, Düsseldorf Institute for Competition Economics (DICE).

Holden, J., Goel, N., 2016. Fast-forwarding to a Future of On-demand Urban Air Transportation. Tech. rep..

Holmes, B.J., Parker, R.A., Stanley, D., McHugh, P., Garrow, L., Masson, P.M., Olcott, J., Jan. 2017. NASA Strategic Framework for On-Demand Air Mobility - A Report for NASA Headquarters Aeronautics Research Mission Directorate.

Hörl, S., 2016. Implementation of an Autonomous Taxi Service in a Multi-Modal Traffic simulation Using MATSim. Department of Energy and Environment Chalmers University of Technology, p. 82. June.

Hörl, S., Ruch, C., Becker, F., Frazzoli, E., Axhausen, K., 2019. Fleet operational policies for automated mobility: a simulation assessment for zurich. Transportation Research Part C: Emerging Technologies 102, 20–31.

Horni, A., Nagel, K., Axhausen, K.W. (Eds.), 2016. The Multi-Agent Transport Simulation MATSim. Ubiquity Press.

Horvath, Partners, 2019. Business between Sky and Earth, Assessing the Market Potential of Mobility in the 3rd Dimension. Tech rep..

Howard, D., Dai, D., 2014. Public perceptions of self-driving cars: the case of Berkeley, California. MS Transportation Engineering 2014 (1), 21.

Hubaux, J.P., Capkun, S., Luo, J., May 2004. The security and privacy of smart vehicles. IEEE Security Privacy 2, 49–55.

Kleinbekman, I.C., Mitici, M.A., Wei, P., September, 2018. eVTOL arrival sequencing and scheduling for on-demand urban air mobility. In: AIAA/IEEE Digital Avionics Systems Conference - Proceedings, 2018.

Kohlman, L.W., Patterson, M.D., 2018. System-level urban air mobility transportation modeling and determination of energy-related constraints. In: 2018 Aviation Technology, Integration, and Operations Conference, p. 3677.

KPMG, 2013. Self-Driving Cars: Are We Ready? Retrieved from. https://home.kpmg/content/dam/kpmg/pdf/2013/10/self-driving-cars-are-we-ready.pdf/.

Krueger, R., Rashidi, T.H., Rose, J.M., 2016. Preferences for shared autonomous vehicles. Transportation Research Part C: Emerging Technologies 69, 343–355.

Kyriakidis, M., Happee, R., De Winter, J.C., 2015. Public opinion on automated driving: results of an international questionnaire among 5000 respondents. Transportation Research Part F: Traffic Psychology and Behaviour 32, 127–140.

Levinson, D.M., Kumar, A., 1997. Density and the journey to work. Growth and Change 28 (2), 147–172.

Lineberger, R., Hussain, A., Mehra, S., Pankratz, D., 2018. Passenger Drones and Flying Cars. Retrieved from. https://www2.deloitte.com/insights/us/en/focus/future-of-mobility/passenger-drones-flying-cars.html/.

Liu, Y., Kreimeier, M., Stumpf, E., Zhou, Y., Liu, H., May 2017. Overview of recent endeavors on personal aerial vehicles: a focus on the US and Europe led research activities. Progress in Aerospace Sciences 91, 53–66.

Maurer, M., Gerdes, J.C., Lenz, B., Winner, H., 2015. Autonomes Fahren: Technische, Rechtliche Und Gesellschaftliche Aspekte. Springer.

Milakis, D., van Arem, B., van Wee, B., 2017. Policy and society related implications of automated driving: a review of literature and directions for future research. Journal of Intelligent Transportation Systems 21 (4), 324–348.

Moore, M.D., Goodrich, K.H., 2013. High speed mobility through on-demand aviation. In: 2013 Aviation Technology, Integration, and Operations Conference, p. 4373.

Moreno, A.T., 2017. Autonomous Vehicles: Implications on an Integrated Landuse and Transport Modelling Suite, pp. 10–13.

Otte, T., Metzner, N., Lipp, J., Schwienhorst, M.S., Solvay, A.F., Meisen, T., September 2018. User-centered integration of automated air mobility into urban transportation networks. In: 2018 IEEE/AIAA 37th Digital Avionics Systems Conference (DASC). IEEE, pp. 1–10.

Parker, R.A., 2017. NASA Strategic Framework for On-Demand Air Mobility A Report for NASA Headquarters.

Reddy, L., DeLaurentis, D.A., 06 2016. Multivariate probit models and qualitative analysis of survey on public and stakeholder perception of unmanned aircraft. In: 16th AIAA Aviation Technology, Integration, and Operations Conference.

Rodrigue, J.-P., Comtois, C., Slack, B., 2017. The Geography of Transport Systems, fourth ed. Routledge.

Rothfeld, R., Balac, M., Ploetner, K.O., Antoniou, C., 2018. Initial analysis of urban air mobility's transport performance in sioux falls. In: 2018 Aviation Technology, Integration, and Operations Conference, p. 2886.

Rothfeld, R., Balac, M., Ploetner, K.O., Antoniou, C., 2018. Agent-based simulation of urban air mobility. In: 2018 Modeling and Simulation Technologies Conference, p. 3891.

Schoettle, B., Sivak, M., 2014. A survey of public opinion about connected vehicles in the U.S., the U.K., and Australia. In: 2014 International Conference on Connected Vehicles and Expo, ICCVE 2014 - Proceedings, No. July, pp. 687–692.

Schuchardt, B.I., Lehmann, P., Nieuwenhuizen, F., Perfect, P., 2015. Final List of Desirable Features/Options for the PAV and Supporting Systems.

Shamiyeh, M., Bijewitz, J., Hornung, M., 2017. A review of recent personal air vehicle concepts. In: Aerospace 6th CEAS Conference. Council of European Aerospace Societies, Bucharest, pp. 1–16 no. 913.

Smith, J.C., Viken, J.K., Guerreiro, N.M., Dollyhigh, S.M., Fenbert, J.W., Hartman, C.L., Kwa, T.-S., Moore, M.D., 2012. Projected demand and potential impacts to the national airspace system of autonomous, electric, on-demand small aircraft. In: 12th AIAA Aviation Technology, Integration, and Operations (ATIO) Conference and 14th AIAA/ISSM, vol. 5595. AIAA.

Squires, G.D., 2002. Urban Sprawl: Causes, Consequences, & Policy Responses. The Urban Institute.

Straubinger, A., Rothfeld, R., 2018. Identification of relevant aspects for personal air transport system integration in urban mobility modelling. In: Proceedings of 7th Transport Research Arena TRA 2018, (Vienna).

Straubinger, A., Verhoef, E.T., 2018. (Working Paper) Options for a Welfare Analysis of Urban Air Mobility (Hong Kong).

Syed, N., 2017. On Demand Mobility Commuter Aircraft Demand Estimation. Master Thesis. Faculty of the Virginia Polytechnic Institute and State University.

Thakur, P., Kinghorn, R., Grace, R., 2016. Urban form and function in the autonomous era. In: Australasian Transport Research Forum 2016 Proceedings.

Thompson, M., 2018. Panel: perspectives on prospective markets. In: Proceedings of the 5th Annual AHS Transformative VTOL Workshop, San Francisco, CA.

Travel forecasting resource, 2014. Benefits of Activity Based Models. http://tfresource.org/Benefits_of_Activity_Based_Models.

Travel forecasting resource, 2018. Autonomous Vehicles: Modeling Frameworks. http://tfresource.org/Autonomous_vehicles: _Modeling_frameworks.

UBER, Oct. 2016. Fast-Forwarding to a Future of On-Demand Urban Air Transportation.

Vascik, P., 2019. Development of vertiport capacity envelopes and analysis of their sensitivity to topological and operational factors. In: AIAA Scitech 2019 Forum, (San Diego, California, United States).

Vascik, P.D., Hansman, R.J., June 2017. Constraint Identification in On-Demand Mobility for Aviation through an Exploratory Case Study of Los Angeles. MIT International Center for Air Transportation (ICAT).

Vascik, P.D., Hansman, R.J., 2017. Evaluation of Key Operational Constraints Affecting On-Demand Mobility for Aviation in the Los Angeles Basin: Ground Infrastructure, Air Traffic Control and Noise, pp. 1–20.

Vredin Johansson, M., Heldt, T., Johansson, P., 2006. The effects of attitudes and personality traits on mode choice. Transportation Research Part A: Policy and Practice 40 (6), 507–525.

Vrtic, M., Schuessler, N., Erath, A., Axhausen, K.W., 2009. The impacts of road pricing on route and mode choice behaviour. Journal of Choice Modelling 3 (1), 109–126.

Wardman, M., Chintakayala, P., May 2012. European wide meta-analysis of values of travel time. Final Report.

Weiß, H.-J., 2003. Die Doppelrolle der Kommunen im ÖPNV. Tech. Rep. Diskussionsbeitr äge// Institut für Verkehrswissenschaft und Regionalpolitik.

Winter, K., Oded, C., Martens, K., van Arem, B., 2017. "Stated choice experiment on mode choice in an era of free-floating carsharing and shared autonomous vehicles: raw data. In: Transportation Research Board, 96th Annual Meeting, vol. 1, pp. 1–17.

Wölfel, P., 2019. An Analysis for an Imminent Implementation of Urban Air Mobility in Germany. Seminar paper. WHU - Otto Beisheim School of Management, Vallendar.

Yedavalli, P., Mooberry, J., 2019. An Assessment of Public Perception of Urban Air Mobility (UAM). Retrieved from. https://www.airbus.com/newsroom/news/en/2019/02/urban-air-mobility-on-the-path-to-public-acceptance.html.

Zmud, J., Sener, I.N., Wagner, J., 2016. Consumer Acceptance and Travel Behavior Impacts of Automated Vehicles Final Report PRC 15-49 F, p. 65.

C Rothfeld et al. (2021). Potential Urban Air Mobility Travel Time Savings.

Reference: Rothfeld, R., Fu, M., Balać, M., & Antoniou, C. (2021). Potential Urban Air Mobility Travel Time Savings: An Exploratory Analysis of Munich, Paris, and San Francisco. *Sustainability*, 13(4). https://doi.org/10.3390/su13042217

sustainability

MDPI

Article

Potential Urban Air Mobility Travel Time Savings: An Exploratory Analysis of Munich, Paris, and San Francisco

Raoul Rothfeld [1,*,†], Mengying Fu [2], Miloš Balać [3] and Constantinos Antoniou [1]

[1] Technical University of Munich, Chair of Transportation Systems Engineering, 80333 Munich, Germany; c.antoniou@tum.de
[2] Bauhaus Luftfahrt e.V., Economics and Transportation, 82024 Taufkirchen, Germany; mengying.fu@bauhaus-luftfahrt.net
[3] ETH Zürich, Institute for Transport Planning and Systems, 8093 Zurich, Switzerland; milos.balac@ivt.baug.ethz.ch
* Correspondence: raoul.rothfeld@tum.de; Tel.: +49-89-289-104-60
† Current address: Arcisstraße 21, 80333 München, Germany.

Abstract: The advent of electrified, distributed propulsion in vertical take-off and landing (eVTOL) aircraft promises aerial passenger transport within, into, or out of urban areas. Urban air mobility (UAM), i.e., the on-demand concept that utilizes eVTOL aircraft, might substantially reduce travel times when compared to ground-based transportation. Trips of three, pre-existent, and calibrated agent-based transport scenarios (Munich Metropolitan Region, Île-de-France, and San Francisco Bay Area) have been routed using the UAM-extension for the multi-agent transport simulation (MATSim) to calculate congested trip travel times for each trip's original mode—i.e., car or public transport (PT)—and UAM. The resulting travel times are compared and allow the deduction of potential UAM trip shares under varying UAM properties, such as the number of stations, total process time, and cruise flight speed. Under base-case conditions, the share of motorized trips for which UAM would reduce the travel times ranges between 3% and 13% across the three scenarios. Process times and number of stations heavily influence these potential shares, where the vast majority of UAM trips would be below 50 km in range. Compared to car usage, UAM's (base case) travel times are estimated to be competitive beyond the range of a 50-min car ride and are less than half as much influenced by congestion.

Keywords: urban aerial passenger transport; eVTOL; agent-based modeling; MATSim; motorized trip share

Citation: Rothfeld, R.; Fu, M.; Balac, M.; Antoniou, C. Potential Urban Air Mobility Travel Time Savings: An Exploratory Analysis of Munich, Paris, and San Francisco. *Sustainability* **2021**, *13*, 2217. https://doi.org/10.3390/su13042217

Academic Editor: Maria Nadia Postorino
Received: 23 January 2021
Accepted: 9 February 2021
Published: 19 February 2021

1. Introduction

The emergence of electrified and distributed propulsion for aerial vehicles might spur the proliferation of urban air passenger transport. Manufacturers of such novel vehicles that are capable of electric-powered vertical take-off and landing (eVTOL) promise reduced noise and emission footprints as well as cheaper and safer operation when compared to conventional helicopters. These developments might facilitate the spread and use of urban air mobility (UAM), which—in the context of this study—is understood as an on-demand aerial passenger transport via short-range eVTOL flights from, to, and/or within urban areas operating from dedicated eVTOL stations which passengers are required to access and egress from.

Occasionally, helicopter passenger transport services did exist with, for example, New York Airways operating between 1949 and 1979 in New York and Airbus' Voom offering on-demand helicopter transport in São Paulo, San Francisco Bay Area, and Mexico City from 2016 until recently ceasing operations in March 2020. Commercial helicopter services constitute a highly costly and situational—thus, a very niche—mode of transportation. Currently, the main benefit of helicopter transport services seems to be their relatively

short travel times that—generally—seem unaffected by conventional ground-based traffic congestion.

This study aims at exploring the potential travel time savings that various UAM implementations might allow. The main objectives of this study are to provide answers to the following three key research questions:

- What motorized trip shares could be achieved with what travel time savings?
- How much does ground-based congestion impact UAM travel times?
- On average, beyond which trip distances can UAM provide time savings?

2. Literature Review

2.1. Potential Demand

To understand demand drivers of UAM, Fu et al. [1] and Al Haddad et al. [2] conducted preliminary studies to gain insights into the potential user's choice behavior regarding currently available urban transportation modes and autonomous transportation services. Their results were integrated within the microscopic travel demand model, MITO [3], and applied to the Munich Metropolitan Region, resulting in UAM market share estimations ranging from 0.16% to 0.38% [4]. Similarly, Plötner et al. [5] concluded a potential modal split of 0.5% for UAM, trying to employ UAM in order to complement public transport. Both studies [4,5] conclude that UAM is expected to have a negligible impact on existing traffic patterns. A study by Wang and Ross [6], however, found that the majority of on-demand trips (taxi in their case) were transit-competing rather than transit-complementing or -extending. Since UAM is a similarly-functioning on-demand mode like taxi, the findings from Wang and Ross [6] might also be applicable to UAM. A study of Zurich, Switzerland, showed fewer than 2000 (0.34%) potential UAM trips [7], with a follow-up study—which introduced UAM process times and take-off and landing procedures—yielding a UAM trip share of 0.05% [8]. One of the main demand drivers for UAM service usage are potential travel time reductions.

Similar to this study, Postorino and Sarné [9] applied an agent-based simulation to analyze the impact of UAM usage on urban mobility. However, the authors focused on flying cars rather than UAM being a separate mode of transportation from a car that merits station access and egress. Within their simulation of grid-like transport networks, they conclude that "(i) [individual flying cars in urban contexts] are not necessarily more convenient and sustainable than current ground mobility when the demand level is increasing; (ii) the potential advantage is linked to the O/D pair distance [...]" ([9], p. 13). If one assumed UAM to be station-based, the placement of stations becomes highly relevant for the accessibility of the service, as early studies have shown [10].

2.2. Station Placement

The availability of ground infrastructure is one of the most important near-term limitations for UAM according to, e.g., Vascik and Hansman [11] and Liu et al. [12]. Similar to the minimum ground infrastructure requirements for helicopters, Vascik and Hansman [11] and Holden and Goel [13] defined several different UAM ground infrastructure concepts and designs. Focusing on UAM station placement, different methods and provided rationales for identifying UAM locations have been proposed (see, e.g., [5,14–16]). On the basis of two case studies for Los Angeles and Munich, Fadhil [15] conducted a geographic information system (GIS)-based analysis to identify areas of high suitability for UAM station locations. In another study based on the Upper Bavaria region of Germany, Plötner et al. [5] manually placed 130 UAM stations by conducting workshops with local experts, considering various trip purposes such as commuting, business, tourism, and leisure. Using the same study area, Arellano [16] developed a semi-automated procedure for allocating UAM station locations, following a GIS multi-criteria decision analysis framework similar to Fadhil [15], yet with the introduction of applying impedance minimization algorithms to derive specific station locations.

Other studies propose demand-driven implementations. Just like within the Uber Elevate white paper [13], Lim and Hwang [17] employed a *k*-means clustering algorithm which they applied on commute data from the Seoul Capital Area to identify centroids for trip origins and proposed those as suitable UAM station locations. The study set up 18 network schematics with the number of UAM stations ranging up to 36 stations. Notably, though, Lim and Hwang [17] suggest that location was more important than the number of UAM stations. Syed et al. [18] also used a *k*-means clustering algorithm to allocate stations in Northern California and the Baltimore–Washington metropolitan area. Aiming to minimize travel times to and from stations, their *k*-means implementation favored census tracts with high population and income. Based on four different scenarios with 200, 300, 400, and 1000 stations, the authors found that 20%, 25%, 30%, and 55% of potential demand was within 5 min of a UAM station for each scenario, respectively. Extending the study of German et al. [19] who attempt to place UAM stations for cargo delivery, Daskilewicz et al. [20] took the spatial distribution of jobs, in addition to population and income data, into account for the San Francisco Bay Area and Los Angeles region for allocating 10 to 40 UAM stations, with one of the studies' results being that the majority of UAM trips had lengths of less than 30 miles (48 km).

2.3. Environmental Impact

Another significant aspect to evaluate UAM is the environmental effect—that includes noise—of UAM vehicle operation (see, e.g., [21–23]). To understand the traffic-related emissions of eVTOL, Pukhova [21] conducted UAM simulations for the Munich Metropolitan Region and estimated the emissions of UAM operation with regard to CO_2 and NO_x levels. Based on comparing different scenarios with and without UAM, both with and without assumptions on various technological improvements, Pukhova [21] found that UAM can only be of environmental benefit if the electricity used by eVTOL vehicles originates from renewable sources. Still, electric ground-based vehicles may be more energy efficient than UAM, given the same electricity mix. Nevertheless, Kasliwal et al. [22] recently depicted an opposing view on the environmental impact of UAM. Their study found that, when comparing eVTOL vehicles at maximum occupancy (i.e., with three passengers) to cars with an average occupancy (i.e., 1.54 passengers), greenhouse gas emissions per passenger-kilometer of eVTOL flight are 50% lower than those from combustion engine cars and 6% lower than those of electric cars.

2.4. Modelling and Simulation

The multi-agent transportation simulation framework, MATSim [24], allows for the modeling and simulation of novel transportation concepts such as ride-sharing [25], car-sharing [26], and shared autonomous vehicles [27–29]. Likewise, UAM—another novel and autonomous mode—is also being modeled and studied using MATSim. The first such analysis of potential UAM demand was conducted for the city of Zurich, Switzerland by Balać et al. [8]. The study performed sensitivity analyses of various operational UAM parameters and proposed a mixed-integer linear program to optimize fleet size and minimize vehicle-kilometers traveled by UAM vehicles. However, the authors point out several limitations of the study, including a very specific modeling of the UAM service without dedicated UAM infrastructure. This was overcome with the development of the MATSim UAM-extension, first presented by Rothfeld et al. [30], which is developed based on the dynamic vehicle routing problem (DVRP) extension for MATSim by Maciejewski [31]. Rothfeld et al. [10] provided an initial analysis regarding the operational performance of a potential UAM implementation, considering eVTOL vehicle properties, dedicated eVTOL infrastructure placement, and the usage of urban airspace and aerial networks. For this, Rothfeld et al. [10] used the extended Sioux Falls MATSim scenario by Hörl [32] to do parameter–variation scenarios.

This initial sensitivity analysis for the MATSim UAM-extension prototype provides the first indications concerning the influence of UAM parameters, such as vehicle speed,

ground-based process time, and network structure, on UAM transport performance and potential adoption (see [5,10]). Further studies (cf. [7,33,34]) also made use of the UAM-extension for MATSim. Their key results suggest that UAM adoption is strongly influenced by the potential for travel time reduction perceived by passenger, UAM infrastructure placement, and duration of ground-based UAM processes. More than UAM vehicle speed and capacity, UAM accessibility and short process times seem to be highly significant for UAM to provide short travel times. However, most existent analyses either used prototyping study areas or focused on the impact of UAM service pricing while using assumptions on travel time savings that UAM can achieve. This study, however, intends to provide an insight into those—previously assumed—travel time savings.

3. Methodology

3.1. Simulation Framework and Base Scenarios

3.1.1. MATSim and Its Application

This study makes use of the aforementioned agent-based transport simulation, MATSim [24]. MATSim itself is an agent-based transportation simulation framework that models complex interactions of individuals and vehicles on transport networks. For that, each agent's daily activity plan—consisting of one or more trips—is iteratively modified, simulated, and scored, with agents generally seeking to minimize travel time and maximize time spent performing activities. This so-called MATSim loop is repeated until an equilibrium state is reached. MATSim has been designed to be easily extendable (see [24], Part II: Extending MATSim) and thus facilitates the development of numerous extensions and analysis interfaces. For modeling UAM transportation, an updated version of the open-source UAM-extension [35] as first presented by Rothfeld et al. [10], is utilized.

In order to obtain realistic trips and congestion levels, which are vital for this study, well-calibrated base scenarios are required. So-called MATSim scenarios contain all information about the respective study areas' synthetic population, each person's activities, and the region's transportation supply for an average day. For this study, the following three pre-existent scenarios are used: Munich Metropolitan Region (hereinafter abbreviated as MUC), Île-de-France (PAR), and San Francisco Bay Area (SFO), as listed in Table 1. While the MUC scenario has been authored by Moeckel et al. [36], PAR and SFO originate from Hörl and Balać [37], Balać and Hörl [38], with both sets of authors using different methods for generating and calibrating their respective scenarios.

Table 1. Overview of study areas.

Study Area	Abbreviation	Size [km^2]	Population [mil]
Munich Metropolitan Region	MUC	14,882	4.4
Île-de-France	PAR	12,070	11.8
San Francisco Bay Area	SFO	20,724	7.9

3.1.2. Munich Metropolitan Region Scenario

The MUC scenario was created by using the open-source microscopic transport orchestrator (MITO) [3] and OpenStreetMap data. MITO is an agent-based and trip-based travel demand model that follows the four-step transport modeling structure with (1) trip generation, (2) trip distribution, (3) modal split, and (4) traffic assignment. As an input, MITO requires a synthetic population that has been created using the land-use model SILO [39] and represents an anonymized replication of census data [40]. Trips, generated by the synthetic population's activities, are assigned a transportation mode using a nested logit mode choice model (see [3], Figure 1a for an illustration) which was estimated using the household travel survey Mobilität in Deutschland [41]. MITO itself also uses an iterative approach where MATSim's traffic volumes affect the next iteration's mode choice decisions until an equilibrium state is achieved. The calibrated MUC scenario includes trips towards five activity types home (42%), shop (9%), work (8%), education (3%), and

other (38%); using four modes of transportation car (57%), walk (23%), bicycle (15%), and public transport (PT) (5%). For comparability with the remaining scenarios, which use a different set of modes, the listed modes have been mapped to a reduced set of modes (i.e., car, PT, walk, and bike) that is coherent over all three scenarios. A down-sampled share of a synthetic population is used for analysis to reduce computation load. Thus, a 25% population sample was used for MUC which includes 3.8 million trips.

(**a**) Direct (i.e., Euclidean point-to-point) flight paths.

(**b**) Indirect (i.e., infrastructure-based) flight routes.

Figure 1. Direct (**a**) and indirect (**b**) UAM flight routing on the example of MUC with 24 UAM stations.

3.1.3. Île-de-France Scenario

Hörl and Balać [37] developed and calibrated an agent-based scenario for Île-de-France. Their scenario was built using only publicly-accessible data from sources such as population census, national and local household travel surveys, and tax registries to form a synthetic population with activity plans; and general transit feed specification (GTFS) schedules and OpenStreetMap to generate a multi-modal transport network. By using their self-developed framework eqasim [42,43], which builds on MATSim's functionality, but replaces plan scoring with discrete mode-choice models [44,45], Hörl and Balać [37] obtained each agent's mobility choices by applying a multinomial logit model. The calibrated PAR scenario includes trips towards six activity types' home (41%), leisure (13%), work (13%), errand (13%), shop (11%), and education (8%), using four distinct modes of transportation walk (43%), car (33%), PT (22%), and bike (1%). For PAR, a 10% population sample was used which includes 4.0 million trips with departure times, as using a 25% sample–as with MUC–exceeded available computational resources. Despite the lower sample size when compared to MUC, the sampled population of PAR provides more trips due to the scenario's high population density (cf. Table 1).

3.1.4. San Francisco Bay Area Scenario

Reapplying the methodology used for the Île-de-France scenario, Balać and Hörl [38] also created an agent-based scenario for the nine-county San Francisco Bay Area. As with the previous scenario, the SFO scenario was created using openly-available data sets like the USA census estimates for 2017, the California household travel survey (CHTS) from 2012, GTFS schedules of public transport operators, and OpenStreetMap data. A multinomial logit mode-choice model was estimated based on the CHTS and paired with the mobility simulation of MATSim, in the same way as for Île-de-France. The calibrated SFO scenario includes trips towards six activity types home (35%), leisure (18%), work (13%), shop (10%), education (4%), and other (20%), using three distinct modes of transportation car (74%), walk (19%), and PT (7%). As with PAR and for the same reasons, a 10% population sample was used for SFO which includes 2.5 million trips. To be used with the UAM-extension though, each scenario requires some preparation, such as providing UAM station locations, UAM vehicle properties, and UAM flight routes.

3.2. Scenario Preparation

3.2.1. Zoning

MATSim itself uses each trip's precise origin and departure coordinates for calculating travel times without the need for subdividing the study area into smaller zones. However, such a reduction in spatial complexity greatly facilitates visualising and analysing study areas and aides in placing UAM stations. Thus, rasterized layers have been created for each of the three study areas, using a population-based incremental segmentation approach inspired by Moeckel and Donnelly [46].

3.2.2. Station Placement

Arellano [16] presented the application of an impedance minimization location–allocation algorithm for the automated placement of UAM stations for a given study area, which has been adapted and applied for this study. Similar to that approach, the location-allocation algorithm was used in iterations with an increasing number of desired UAM stations, defined to be 4, 8, 24, 76, and 130. These UAM station numbers were chosen to ensure comparability of this study with existing literature that assumed a relatively low number of UAM stations (e.g., [17,19]) as well as studies with more numerous UAM stations (e.g., [5,16]). In contrast to Arellano [16], who gathered expert judgement within a Delphi process to create an artificial location suitability weight, this study uses each zone's aggregated, normalised, and densified number of motorized trip origins and destinations as the single demand weight for station allocation.

As potential UAM station locations, out of which the algorithm derives the pre-defined number of stations that—in total—minimizes travel time impedance, evenly-spaced grid points (see [16]) and manually-placed potential locations by local experts (see, e.g., [5,10]) have been combined, as illustrated by Figure 2a. These combined points serve as the input for the station placement algorithm. For each study area, a local expert has been asked to manually place between 50 and 150 potential UAM station locations based on their knowledge of the area with regard to major transportation hubs (e.g., airports and train stations), major points of interest (e.g., tourist attractions), and major commuter destinations (e.g., company headquarters). The grid point spacings have then been set so that the total number of potential station locations per study area does not exceed a given software limit of 1000 points, resulting in a grid point spacing of 4 km for MUC and PAR, and 5 km for SFO.

Figure 2b shows one result of the impedance minimizing location–allocation algorithm for MUC with 24 stations. The translucent black lines connect all zones' centroids (i.e., weighted demand points) to the algorithmically-selected, impedance-minimizing UAM station locations (white). See Appendix A for illustrations of each scenario's potential input and selected output locations for 4, 24, and 130 UAM stations.

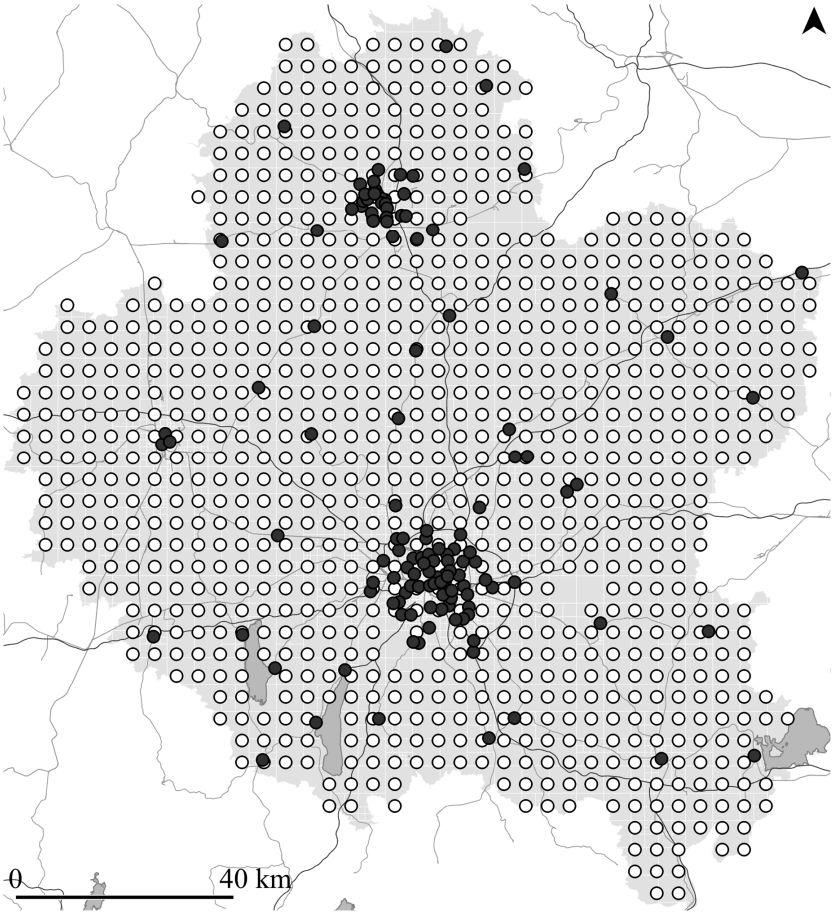

(**a**) Potential locations via manual placement (black) and via a regular grid (white).

Figure 2. *Cont*.

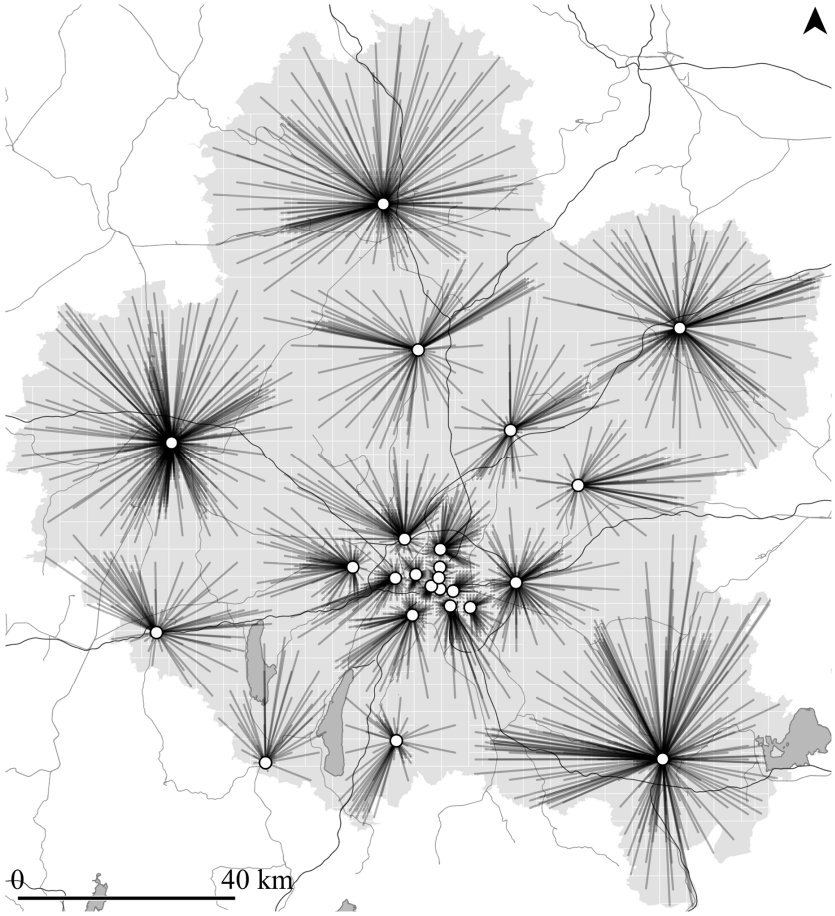

(**b**) Resulting 24 UAM station locations (white) for impedance minimization to each zone's centroid.

Figure 2. Location–allocation input (**a**) and impedance minimization output (**b**) on the example of MUC.

3.2.3. Flight Path Routing

Numerous UAM studies (e.g., [8,10,16]) assume Euclidean, i.e., straight-line, flight distances in their analyses. To compensate for in-flight route deviation and for real-life navigation of helicopters along existing ground infrastructure (cf. [11,47]), a few studies have started to include static detour factors to all Euclidean flight distances (see, e.g., [5]). However, using Euclidean connections (as exemplarily illustrated in Figure 1a) led to "straight station-to-station routes that often traversed over population" ([16], p. 92). Vascik and Hansman [11,48] examined possible UAM flight constraints for Los Angeles, CA, USA, and identified overflight rules that UAM operation will probably have to adhere to.

In order to identify the impact of flight path routing and mimic urban, real-life, low-altitude overflight—comparable to today's helicopter operation—an exploratory ground-infrastructure-based approach for flight route definition is proposed. Instead of connecting all UAM stations via Euclidean flight paths, ground-based transport infrastructure is used as a proxy for overflight, where larger infrastructure with high noise emissions and traffic capacity is preferred for UAM overflight. For that, road and rail infrastructure data from OpenStreetMap have been combined and categorized into three groups from high to low capacity: (1) regional and high-speed rail, motorways, and primary roads, (2) secondary and tertiary roads, and (3) all remaining road and rail infrastructure.

The combined ground-transport infrastructure layer was then used as the network for automated path finding between all UAM station locations for each scenario and all numbers of stations. The categorisation was the basis for defining an artificial path finding cost parameter which replaces path length. Thus, instead of the shortest paths, the results

are paths that predominately follow high-capacity road and rail infrastructure, as illustrated in Figure 1b for MUC with 24 station locations. After initial tests with various category weights (see [49]), a weight (i.e., cost) factor of three has been applied for this study.

3.3. Travel Time Calculation

3.3.1. Eligibility Criteria

Two subsequent conditions have been used to define whether or not a base scenario trip is eligible for UAM usage. First, only motorized trips are considered as potentially UAM-eligible. For non-motorized trips, i.e., walk or bike, UAM as a mode of transportation is not assumed to be a viable substitution. This leaves 67% of trips in MUC, 59% in PAR, and 86% in SFO potentially eligible for UAM usage given this first condition of motorization. However, the vast majority of those motorized trips are rather short. The median and 3rd quartile of each scenario's Euclidean motorized trip distances are 6 km and 10 km for MUC, 5 km and 10 km for PAR, and 6 km and 14 km for SFO—showing that only a few motorized trips are long-range.

The second subsequent condition is based on the availability of UAM stations within a dynamic search radius around a trip's origin and destination. This dynamic search radius for UAM stations has been derived from a study by (Pukhova [21], pp. 34–35) where "the sum of the [Euclidean] distances to and from UAM stations should not be longer than one third of the total trip length", with the total trip length denoting the trip's Euclidean distance. This condition limits UAM use to trips where a significant part of the trip would be served by UAM vehicles, i.e., flying. However, an initial analysis showed that the constraint as presented by Pukhova [21] seems too restrictive. Thus, an alternative implementation has been used in which the maximum-allowed access and egress distances—each individually—may constitute up to one third of the total trip length. Combined, the summed distance of a UAM trips' access and egress legs can make up two-thirds of the overall trip length within this study.

Figure 3 illustrates the shares of UAM-eligibility for motorized trips per scenario based on the station accessibility conditions for various UAM station numbers. It is evident that the share of UAM-eligible motorized trips heavily relies on the number and distribution of UAM stations within the study area, with higher station numbers providing larger UAM-eligibility shares. An additional analysis of the share of motorized trips that are UAM-eligible over Euclidean distance showed another trend: longer trips (i.e., trips with Euclidean distance of more than 50 km) experience higher shares of UAM-eligibility. Thus, even though the overall shares of motorized trips that are UAM-eligible remain below 50% for all scenarios, longer trips are generally included, which is important, since those trips are expected to benefit most from the introduction of UAM.

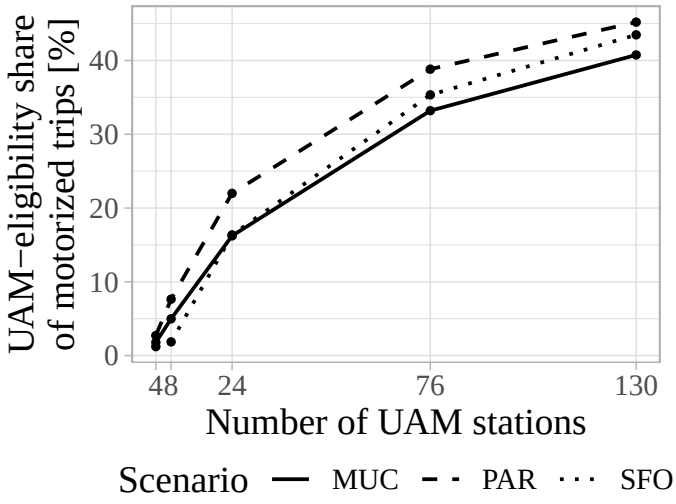

Figure 3. Share of UAM-eligible motorized trips per number of UAM stations.

3.3.2. Traffic Congestion

For this study, traffic congestion affects each mode (i.e., car, PT, and UAM) in different ways. For car travel times, previously-run MATSim simulations of each scenario provided the base traffic- and congestion-levels, which were then taken into account for calculating car travel times. Furthermore, MATSim's car travel times do not include access/egress or parking search times. Travel times using PT do include public transport station access and egress walks, potential waiting times for transfers (e.g., when changing from bus to train), and are primarily schedule-based. Travel times for UAM combine the workings of car and PT, as both modes—as well as walking—are available for UAM station access/egress. Total UAM trip times include access, flight, and egress legs, as well as static waiting, check-in, boarding, and deboarding times. These passenger process times are summarized under the terms pre- and post-flight processes. For each trip, the combination of two UAM stations and access and egress modes that result in the shortest overall UAM trip time was calculated as each trip's potential UAM option.

Figure 4 illustrates the mean door-to-door car speed developments during the simulated day per scenario. Those speeds are derived by dividing the door-to-door trip Euclidean distance by the trip's total travel time and averaging them based on a 30 min time window with regard to the trip's departure time. The illustrated mean speeds for car show distinct traffic peak times. For latter categorization of peak and off-peak trips, the 75th percentile of car mean speeds was used as a threshold per scenario, resulting in peak times of 10:00 a.m.–11:30 a.m. and 3:00 p.m.–6:30 p.m. for MUC, 7:30 a.m.–9:30 a.m. and 4:30 p.m.–7:30 p.m. for PAR, and 7:30 a.m.–10:00 a.m. and 4:30 p.m.–7:00 p.m. for SFO.

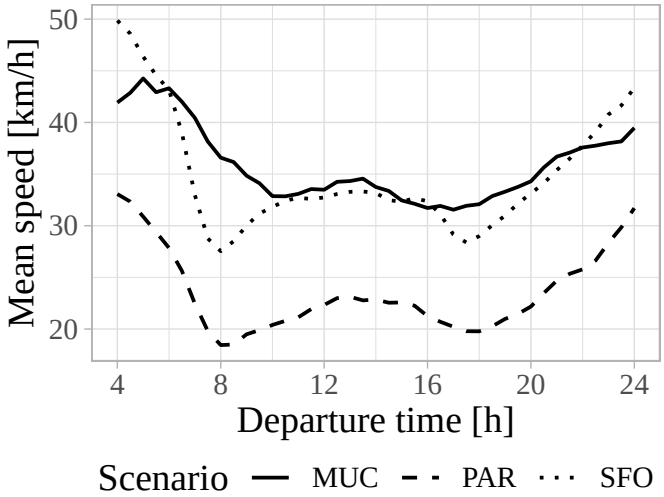

Figure 4. Car mean speeds per departure time of day in 30-min bins.

3.3.3. UAM Parameters and Base Case

Variations of four different UAM system parameters have been applied: (1) number of UAM stations, (2) UAM vehicle cruise speed, (3) total processing time, and (4) type of flight routes. As previously mentioned, the numbers of UAM stations were 4, 8, 24, 76, and 130 stations, distributed within each study area. Flight speeds have been varied between 60 and 300 km/h in steps of 20 km/h based on a VTOL vehicle overview by (Shamiyeh et al. [50], Table 1, p. 3). Per trip, a total of 120 s has been added to account for take-off and landing of the UAM vehicle. In addition to the duration for VTOL operations, total passenger process time variations were included with 0, 15, and 30 min. In order to facilitate understanding, a distinct UAM base case has been defined. The base case aims at representing a realistic—albeit optimistic—case for potential future on-demand UAM operations with the following parameters:

- UAM station count: 24 stations
- UAM vehicle cruise speed: 180 km/h
- UAM total process time: 15 min
- UAM VTOL duration: 120 s in total
- UAM flight routes: direct (i.e., Euclidean) flight paths

4. Results

4.1. Travel Time Savings Ratio

For comparing travel times between UAM and the trip's respective original, ground-based, motorized mode (i.e., car or PT), the following ratio of change in trip travel time is being utilized (Equation (1)):

$$r_{tts} = 1 - \frac{t_{uam}}{t_{gb}} \quad (1)$$

where the ratio of travel time savings (r_{tts}) is the relative difference between a trip's respective ground-based travel time (t_{gb}) and that trip's potential UAM travel time (t_{uam})—which comprises access, egress, flight, and process times. Positive travel time savings ratios (r_{tts}) do, thus, denote that the calculated UAM trip time is shorter than the original trip's travel time, whereas a negative ratio indicates that UAM would offer no travel time savings.

4.1.1. Motorized Trip Shares

Assuming UAM-usage given at least a minimal travel time savings (i.e., for $r_{tts} > 0$), UAM motorized trip shares for MUC, PAR, and SFO are 3%, 13%, and 7% under base-case parameters. There is indication that these UAM's motorized trip shares are largely drawn from trips that originally were using public transport. For MUC, 49% of UAM trips were originally PT trips (while PT makes up only 9% of motorized trips), 74% for PAR (PT has a motorized trip share of 40%), and 40% for SFO (PT has a motorized trip share of 8%). UAM's motorized trip share, given $r_{tts} > 0$, however, varies greatly with changes in UAM parameters. Figure 5a illustrates the motorized trip share development depending on UAM's assumed cruise flight speed and process time for 24 UAM stations. At the base-case cruise flight speed of 180 km/h, a motorized trip share increase of 3 percentage points (pp) for a decrease in process time from 30 to 15 min and, from there, an additional 11 pp increase for no process times can be observed for MUC. The same reductions in process time lead to share increases of 6 pp and 11 pp for PAR and 2 pp and 6 pp for SFO at base-case cruise speed.

Figure 5b, on the other hand, illustrates the motorized trip share development depending on UAM's assumed cruise flight speed and number of UAM stations. Again, at base-case cruise flight speed, the respective motorized trip shares of UAM are 0.4%, 1%, 3%, 7%, and 9% for 4, 8, 24, 76, and 130 stations for MUC; 1%, 4%, 13%, 22%, and 26% for PAR; and 0.6%, 1%, 7%, 12%, and 13% for SFO. Evidently, the share increase is largest when increasing the number of stations from 8 to 24 and again from 24 to 76—an increase from 76 to 130 stations only leads to a marginal increase in motorized trip share. Figure 5a,b also illustrate the impact of UAM cruise flight speed on trip shares. With 24 stations and 15 min process time (base case), UAM's motorized trip share increases from 1% at 60 km/h to 5% at 300 km/h for MUC, 8% and 14% for PAR, and 4% and 8% for SFO. The marginal motorized trip shares for flight speed increases between 60 to 180 km/h are 1.8, 4.8, and 2.5 times higher than those from flight speed increases from 180 to 300 km/h for MUC, PAR, and SFO, respectively.

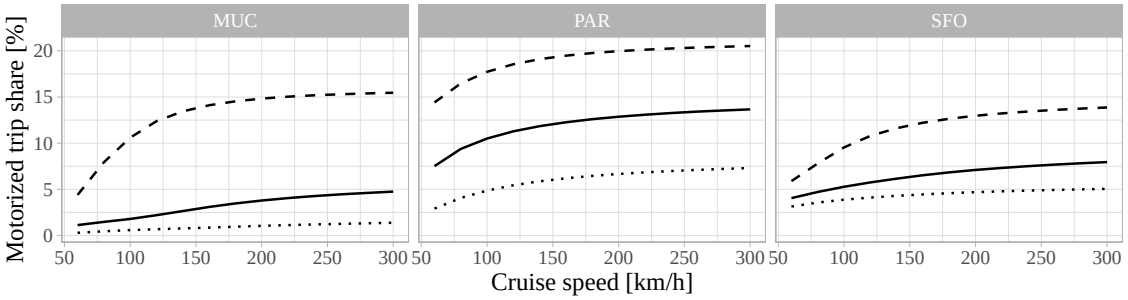

(**a**) Process time variations.

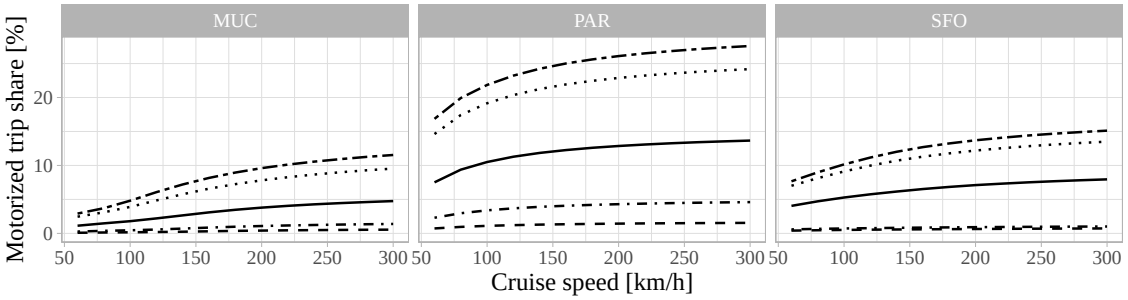

(**b**) UAM station number variations.

Figure 5. UAM motorized trip share for $r_{tts} > 0$ over cruise flight speed.

A slight impact on flight distances can also be observed from the number of stations. Figure 6 illustrates the median (50th), upper quartile (75th), and maximum (100th percentile) Euclidean trip distances over station number for UAM (base case) usage given $r_{tts} > 0$. In general, for all three scenarios, the distributions of Euclidean trip distances per mode are heavily skewed towards very short trips. The median trip distances for car and PT are 5–6 km, except for PT in SFO, which has a median trip distance of 10 km. Similarly, the upper quartiles are between 9 and 13 km, which SFO's upper PT quartile being 23 km. The vast majority of motorized trips are, thus, relatively short. UAM's median trip distances are consistently higher, i.e., longer, than cars with 10, 11, and 27 km with 24 stations for MUC, PAR, and SFO, respectively.

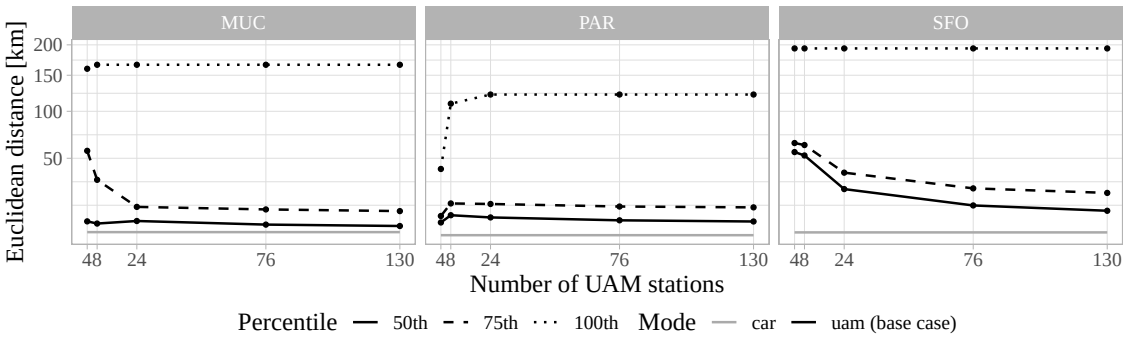

Figure 6. Euclidean trip distance percentiles for car and UAM over number of UAM stations.

An increase in number of stations leads to a slight decrease of median trip distance for MUC and PAR with a 19% and 14% drop when increasing the number of stations from 24 to 130. For SFO, a more substantial decrease of 46% can be observed. Most importantly, however, is that even the upper quartile is comparatively short with 16, 18, and 38 km for MUC, PAR, and SFO for 24 stations—indicating that the vast majority of potential UAM trips would be far below 50 km.

4.1.2. Sensitivity Analysis

As was already indicated by the change in motorized trip shares, the travel time savings ratios themselves are highly dependent on and vary greatly with the underlying UAM assumptions, such as the number of UAM stations or process time. Figure 7 illustrates the distribution of UAM travel time savings ratios for UAM parameters (a) number of UAM stations, (b) cruise speed, (c) process time, and (d) flight path routing and for non-UAM parameters (e) trips' original modes and (f) scenario. For each figure, base-case assumptions were used except for the specified UAM parameter that is being varied for Figure 7a–d. For readability, the graph's ratio-axis has been set to only show values for $r_{tts} > -2$.

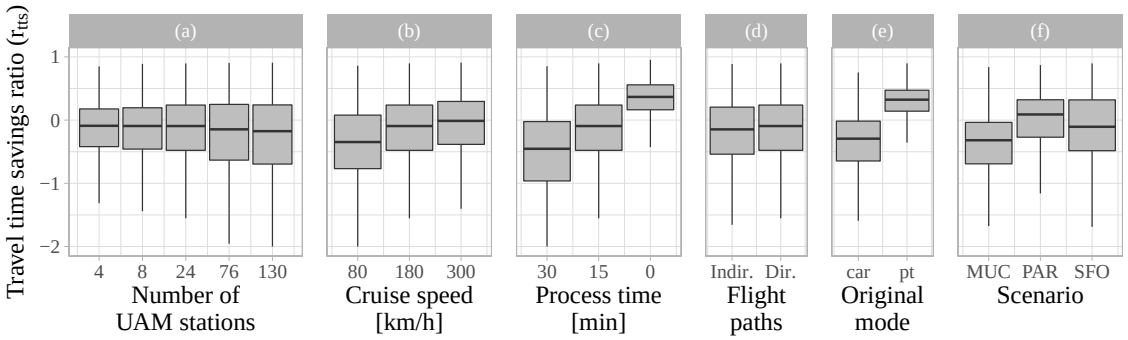

Figure 7. Sensitivity of travel time savings ratio (r_{tts}) to UAM parameters and scenario.

While more numerous UAM stations do significantly increase service coverage, as can be seen from Figure 5b, the potential for travel time savings does not improve—as is evident from Figure 7a. On the contrary, the median travel time saving slightly decreases. For cruise speed, the median ratios increase by 0.35 between 80 km/h ($MED = -0.37$) and 300 km/h ($MED = -0.02$). More drastic is the impact of UAM process time with a 0.91-increase in median travel time savings ratio from -0.54 with 30 min to 0.37 without process time—even further, the spread of ratios is also significantly reduced. Whether UAM flight paths are direct (station-to-station) or indirect (routed), paths makes a ratio difference of 0.06 when comparing their respective medians ($MED_{direct} = -0.10$, $MED_{indirect} = -0.16$). The median travel time savings ratio for UAM over PT trips is significantly higher than for car trips, with median ratios of 0.32 and -0.30 for trips that originally were PT and car trips, respectively. Finally, there is quite a difference in the distribution of travel time savings ratios between the scenarios themselves (see Figure 7e). MUC has the lowest median ratio with $MED = -0.33$. In-between MUC and PAR lies SFO with $MED = -0.11$; PAR has highest median ratio with $MED = 0.09$.

4.2. Travel Speed Comparisons

4.2.1. Impact of UAM Operation Parameters

As seen from the time savings ratio's sensitivity analysis (see Figure 7), the UAM operation parameters, cruise flight speed and process time, have a significant impact on travel time and, hence, travel speeds. Figure 8a illustrates the mean trip travel speeds over Euclidean distance in 5 km-bins and shows the speed impact of different UAM cruise flight speeds. Except for the described variations in cruise flight speed, base-case parameters are set for UAM. At the base-case cruise speed of 180 km/h, UAM's mean trip travel speed surpasses that of car at 60, 35, and 40 km/h for MUC, PAR, and SFO. While each scenario's distance is slightly different, with their respective speeds, they all equate to a 50–55 min car ride. Beyond these Euclidean trip distances, UAM is—on average—expected to provide at least some travel time savings. When UAM's cruise flight speed is reduced to 80 km/h, however, UAM' mean speeds do not clearly surpass those of cars but merely approach them for PAR and SFO for distances larger than 100 km. Compared to PT speeds, however, even an 80 km/h-cruise speed results in consistently higher mean speeds. A cruise flight

speed increase from 180 to 300 km/h leads to a reduction in intersection points between car and UAM, with them being 35 (MUC), 25 (PAR), and 30 km (SFO).

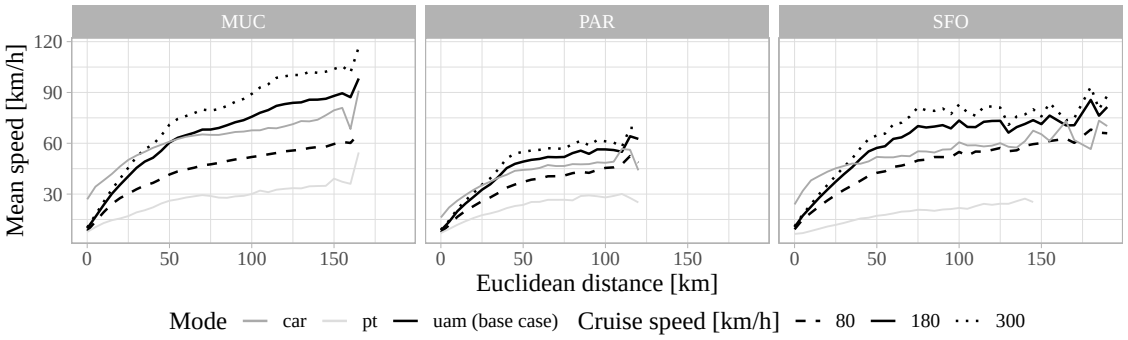

(**a**) Cruise flight speed variations.

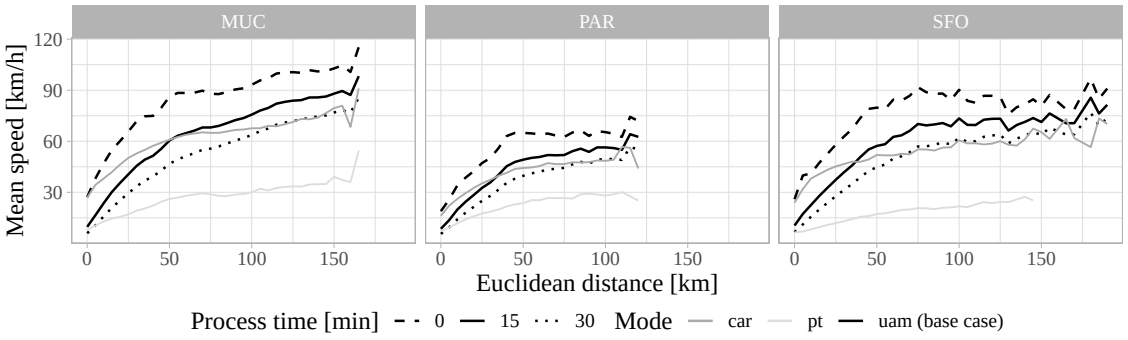

(**b**) Process time variations.

Figure 8. Mean trip speeds for car and UAM over Euclidean trip distance in 5 km-bins.

In contrast to the above, Figure 8b illustrates the change of mean speeds for variations in assumed UAM process time. Most significant is the impact of reduced process times for short-range trips. When decreasing the process times from 15 min (base case) to zero, the mean UAM trip speeds start off and remain above those cars for all three scenarios. For an increase of process times to a total of 30 min at a cruise flight speed of 180 km/h, mean UAM trip speeds do not sufficiently surpass car speeds but begin being competitive beyond 120, 80, and 70 km for MUC, PAR, and SFO.

4.2.2. Impact of Flight Path Routing and Congestion

As non-UAM operation parameters, flight path routing and congestion also affect mean UAM trip speeds. For routed, i.e., indirect flight paths that follow ground-based infrastructure as discussed in Section 3.2.3, a decrease in mean trip speeds is expected due to prolonged flight distances while the trips' Euclidean distances remain unchanged. Overall, a mean speed reduction by 5% (MUC), 4% (PAR), and 7% (SFO) can be observed. However, the mean speed reduction varies with different trip distances, as shown in Figure 9. The impact of indirect flight paths increases proportionally with longer Euclidean trip distances up to ca. 35 km, before starting to decrease with distances beyond ca. 100 km. Notably, the impact of indirect paths over distance is more volatile for SFO than for MUC or PAR. An auxiliary analysis showed that a very low number of long-range trips and the scenario's topography, i.e., the presence of a vast and central body of water, are two primary factors for said volatility. Beyond 130 km, SFO only has one third the number of trips when compared to MUC and, additionally, those trips are spread over a wider range of distance bands.

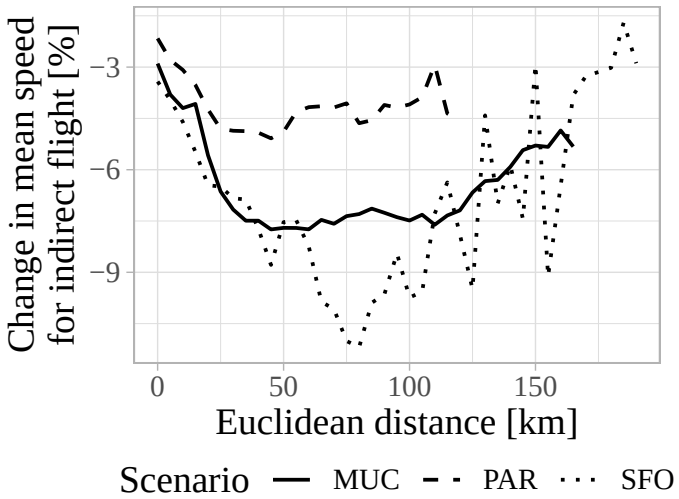

Figure 9. UAM (base case) trip speed impact of indirect, i.e., infrastructure-based, flight paths.

The overall impact of peak times, i.e., congestion, on mean UAM (base case) trip speeds is a reduction by 4% (MUC), 5% (PAR), and 2% (SFO). For car, the equivalent mean speed reductions are 9% for MUC and 14% for PAR and SFO. Thus, UAM is 51% (MUC), 63% (PAR), and 82% (SFO) less affected by ground-based traffic congestion compared to cars. Figure 10 shows how the impact of ground-based congestion changes with variations in stations' numbers.

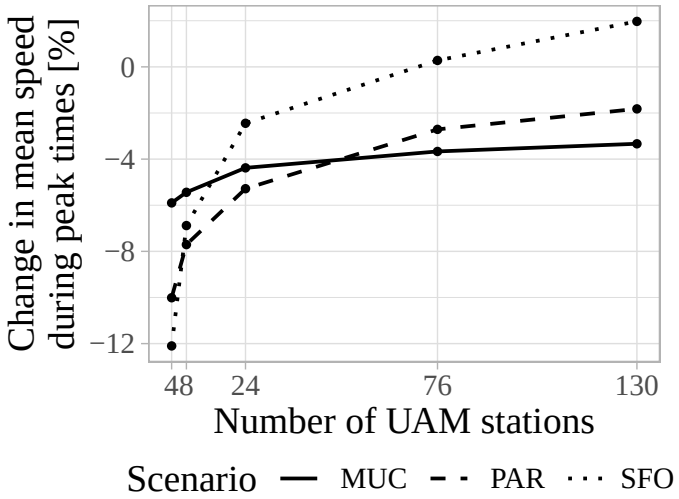

Figure 10. UAM (base case) trip speed impact of congestion, i.e., peak time departure.

5. Discussion

The importance of the number and distribution of UAM stations, for UAM to be a feasible alternative to ground-based transportation modes, can not be overstated. The restriction, of trips being UAM-eligible only if the flight distance is at least one third of the overall trip's Euclidean distance, shows how few motorized trips actually have origins and destinations within reasonable UAM station distances. Even with 130 stations being distributed over the respective study areas, the share of UAM-eligible motorized trips remains a slight minority, thus limiting UAM's trip share regardless of UAM's potential travel times savings. Since UAM is assumed to be a station-based transportation system, like public transport, UAM's potential for travel time reduction hinges on the accessibility of the system's entry and exit points, i.e., UAM stations. This study's observed UAM-eligibility rates, which are leveling off at 40–45% for 130 UAM stations, seem comparable

to the findings of Syed et al. [18] (see Section 2.2), who applied a stricter radius limitation, but also placed more stations.

Higher station numbers substantially increased service coverage, yet did not significantly reduce median travel times. Rather than shortening overall access and egress distances, the number of very short-range trips grows. Even with base-case assumptions of 24 stations, most potential UAM trips have Euclidean distances of less than 50 km—confirming the results of Daskilewicz et al. [20]. Especially for those short-range trips, the impact of process time duration heavily outweighs UAM's cruise flight speeds. The results from early simulations (c.f. [10]), in that potential future UAM operators should focus on station placement and processes instead of vehicle speed, must be reaffirmed. This can be linked with the finding that indirect flight paths (i.e., overlying ground-based infrastructure) do not overly reduce UAM travel times. It seems fair to assume that, for potential real-life UAM implementations, a regulatory requirement to circumvent certain non-fly zones or to follow ground-based infrastructure for noise-avoidance and safety reasons might be worth the trade-off with slightly-prolonged travel times.

On average, travel time savings are expected to be achieved beyond a 35–60 km range, which stands in contrast to most UAM trips being very short-range. One could reasonably argue, however, that UAM should not be encouraged as a transportation mode for such short-range trips. With UAM vehicles' take-off and landing operations being the most energy-intensive flight phases, UAM's questionable sustainability (c.f. [21]) would be improved with longer trip distances. Disallowing UAM trips, with less than, say, 50 km Euclidean distance, would reduce the motorized trip shares of UAM by more than 75% (see Figure 6). It is important to note that the sustainability of a potential future UAM realization very much depends on a multitude of factors, such as vehicle capacity, average load factors, or the share of renewable energy production. Still, high base usage fees for UAM might be an economic measure to reduce unsustainable short-range flights.

Since potential UAM service prices and costs are still very much speculation, pricing has purposefully not been included within this study. Thus, the reported motorized trip shares present the maximum possible shares, with the inclusion of pricing substantially reducing UAM's trip shares—given that UAM is expected to be a more costly service than private car or PT usage. Especially when discussing UAM as a potential alternative for trips that originally were done using PT, it is fair to question whether such substitution can be assumed or—more importantly—desired. In light of making transport more sustainable and decreasing social inequality, reducing the trip share of PT for a more individualistic mode of transportation is wholly unwanted—despite UAM potentially offering shared services at some point in the future. Assuming that PT substitution would not occur, either due to economic or regulatory measures, the reported motorized trip shares for UAM would decrease by 40–79%.

6. Limitations and Future Research

This study primarily analyzes travel times savings without the inclusion of pricing. Combining various stated-preference surveys—especially the emerging study for San Francisco Bay Area by Garrow et al. [51]—with the presented information could enable more detailed insight into potential UAM demand. Furthermore, more localized analyses of the study areas' ground infrastructure and topography might lead to particular flight connections that prove to be useful despite being, e.g., short-range.

With UAM station selection being such a central influence on its coverage and trip shares, it is a topic worth its own analysis in the lines of Chakour and Eluru [52], whose approach specifically addresses the issue of different sequences in passengers' decisions for departure stations in whether the access mode or station precedes. Additionally, required UAM infrastructure throughput, potential for passenger pooling, public acceptance, and sustainability of UAM operations also warrant further investigation.

7. Conclusions

Urban air mobility, understood as short-range on-demand aerial passenger transport, is expected to provide a novel, time-saving mode of transportation. Except for potential future UAM realizations with vast numbers of UAM station, however, the majority of motorized trips are UAM-ineligible due to prolonged access and egress trips. Thus, the number and distribution of stations are key to achieving wide-spread UAM service coverage. Under base-case assumptions, UAM could provide travel time savings for 3–13% of motorized trips. Due to the necessity of accessing/egressing UAM stations, ground-based congestion does affect UAM travel times–compared to cars, however, UAM travel times are 51–82% less affected. UAM (base case) is estimated to provide time savings beyond respective distances of a 50–55 min car ride.

While UAM is not believed to be suitable for mass transport, based on the derived trip shares, the underlying technologies could provide valuable alternatives to conventional helicopters that are in use for emergency, touristic, or occasional passenger transport services. However, UAM might be a suitable addition to existing transportation systems in areas with, for example, ground terrain that causes large detours for ground-based transportation. For UAM manufacturers or intended UAM service providers, it is recommended to focus on UAM stations' accessibility and distribution, rather than maximizing UAM vehicle cruise flight speed.

Author Contributions: Conceptualization, R.R.; methodology, R.R.; software, R.R. and M.B.; validation, R.R. and M.F.; formal analysis, R.R.; investigation, R.R.; resources, R.R.; data curation, R.R.; writing—original draft preparation, R.R.; writing—review and editing, R.R., M.F., M.B., and C.A.; visualization, R.R.; supervision, C.A.; All authors have read and agreed to the published version of the manuscript.

Funding: This work was supported by the Technical University of Munich within the Open Access Publishing Funding Program.

Institutional Review Board Statement: Not applicable.

Informed Consent Statement: Not applicable.

Data Availability Statement: The data presented in this study are available on request from the corresponding author. The data are not publicly available due to privacy concerns.

Conflicts of Interest: The authors declare that they have no conflict of interest.

Appendix A

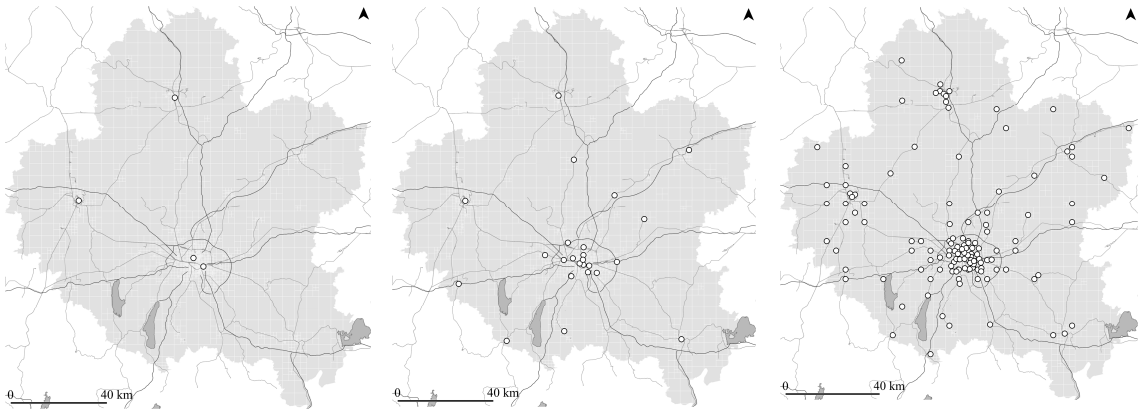

(**a**) MUC with 4 stations. (**b**) MUC with 24 stations. (**c**) MUC with 130 stations.

Figure A1. *Cont*.

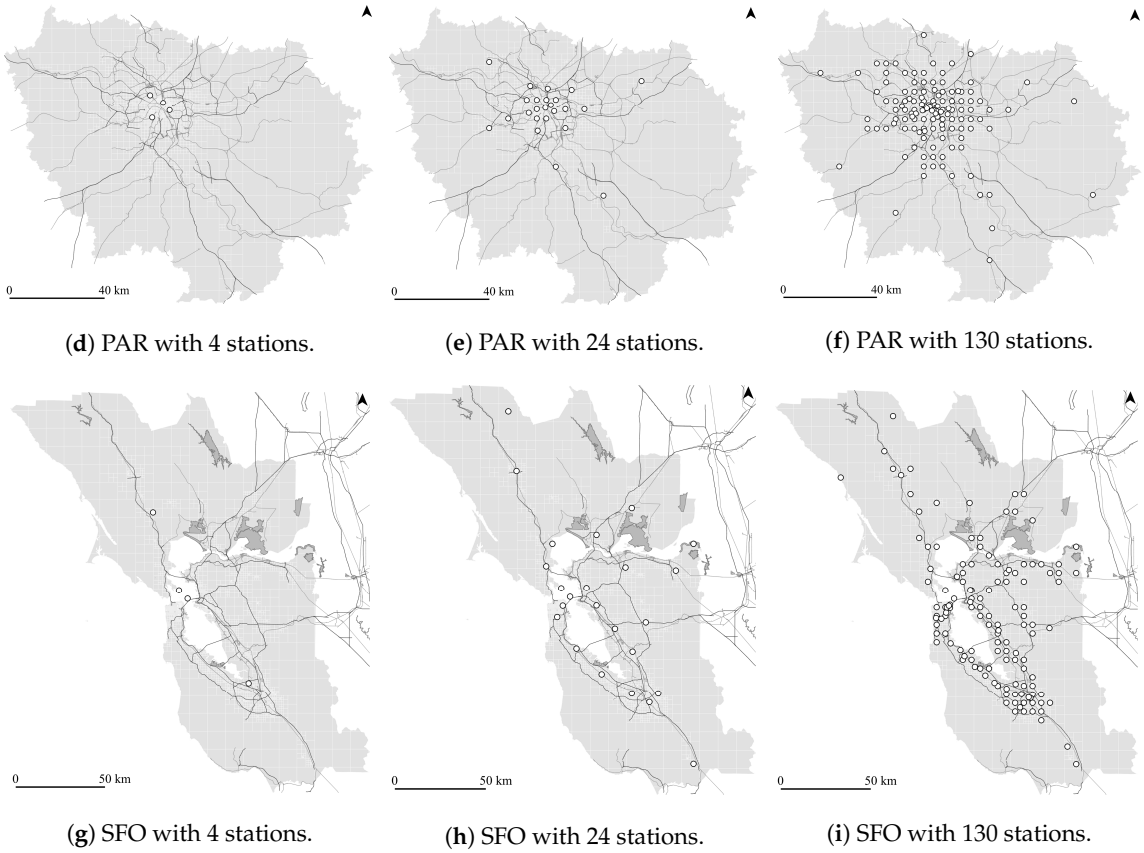

(**d**) PAR with 4 stations. (**e**) PAR with 24 stations. (**f**) PAR with 130 stations.

(**g**) SFO with 4 stations. (**h**) SFO with 24 stations. (**i**) SFO with 130 stations.

Figure A1. Location–allocation impedance minimization outputs for 4, 24, and 130 UAM stations for MUC, PAR, and SFO.

References

1. Fu, M.; Rothfeld, R.; Antoniou, C. Exploring Preferences for Transportation Modes in an Urban Air Mobility Environment: Munich Case Study. *Transp. Res. Rec.* **2019**. [CrossRef]
2. Al Haddad, C.; Chaniotakis, E.; Straubinger, A.; Plötner, K.; Antoniou, C. Factors affecting the adoption and use of urban air mobility. *Transp. Res. Part A Policy Pract.* **2020**, *132*, 696–712. [CrossRef]
3. Moeckel, R.; Kuehnel, N.; Llorca, C.; Moreno, A.; Rayaprolu, H. Agent-Based Simulation to Improve Policy Sensitivity of Trip-Based Models. *J. Adv. Transp.* **2020**, *2020*. [CrossRef]
4. Pukhova, A.; Llorca, C.; Moreno, A.; Zhang, Q.; Moeckel, R. Urban air mobility: Another disruptive technology or just an insignificant addition. In Proceedings of the European Transport Conference, Dublin, Ireland, 9–11 October 2019.
5. Plötner, K.; Rothfeld, R.; Shamiyeh, M.; Kabel, S.; Frank, F.; Straubinger, A.; Llorca, C.; Fu, M.; Moreno, A.; Pukhova, A.; et al. Long-term Application Potential of Urban Air Mobility Complementing Public Transport: An Upper Bavaria Example. *CEAS Aeronaut. J. Off. J. Counc. Eur. Aerosp. Soc.* **2020**. [CrossRef]
6. Wang, F.; Ross, C.L. New potential for multimodal connection: Exploring the relationship between taxi and transit in New York City (NYC). *Transportation* **2019**, *46*, 1051–1072. [CrossRef]
7. Balać, M.; Vetrella, A.R.; Rothfeld, R.; Schmid, B. Demand Estimation for Aerial Vehicles in Urban Settings. *IEEE Intell. Transp. Syst. Mag.* **2019**, *11*, 105–116. [CrossRef]
8. Balać, M.; Rothfeld, R.; Hörl, S. The Prospects of on-demand Urban Air Mobility in Zurich, Switzerland. In Proceedings of the 2019 IEEE Intelligent Transportation Systems Conference, ITSC 2019, Auckland, New Zealand, 27–30 October 2019; pp. 906–913. [CrossRef]
9. Postorino, M.N.; Sarné, G.M. Reinventing mobility paradigms: Flying car scenarios and challenges for urban mobility. *Sustainability* **2020**, *12*, 3581. [CrossRef]
10. Rothfeld, R.; Balać, M.; Plötner, K.; Antoniou, C. Initial Analysis of Urban Air Mobility's Transport Performance in Sioux Falls. In Proceedings of the 2018 Aviation Technology, Integration, and Operations Conference, Atlanta, GA, USA, 25–29 June 2018; pp. 1–13. [CrossRef]
11. Vascik, P.D.; Hansman, R.J. Scaling Constraints for Urban Air Mobility Operations: Air Traffic Control, Ground Infrastructure, and Noise. In *2018 Aviation Technology, Integration, and Operations Conference*; MIT International Center for Air Transportation (ICAT), Department of Aeronautics & Astronautics, Massachusetts Institute of Technology, American Institute of Aeronautics and Astronautics: Reston, VA, USA, 2018. [CrossRef]

12. Liu, Y.; Kreimeier, M.; Stumpf, E.; Zhou, Y.; Liu, H. Overview of recent endeavors on personal aerial vehicles: A focus on the US and Europe led research activities. *Prog. Aerosp. Sci.* **2017**, *91*, 53–66. [CrossRef]
13. Holden, J.; Goel, N. *Fast-Forwarding to a Future of On-Demand Urban Air Transportation*; Uber Technologies, Inc.; San Francisco, CA, USA, 2016; pp. 1–98.
14. Antcliff, K.R.; Moore, M.D.; Goodrich, K.H. Silicon valley as an early adopter for on-demand civil VTOL operations. In Proceedings of the 16th AIAA Aviation Technology, Integration, and Operations Conference, Washington, DC, USA, 13–17 June 2016; American Institute of Aeronautics and Astronautics, Ed.; American Institute of Aeronautics and Astronautics: Washington, DC, USA, 2016. [CrossRef]
15. Fadhil, D.N. A GIS-based Analysis for Selecting Ground Infrastructure Locations for Urban Air Mobility. Master's Thesis, Technical University of Munich, Munich, Germany, 2018.
16. Arellano, S. A Data- and Demand-Based Approach at Identifying Accessible Locations for Urban Air Mobility Stations. Master's Thesis, Technical University of Munich, Munich, Germany, 2020.
17. Lim, E.; Hwang, H. The Selection of Vertiport Location for On-Demand Mobility and Its Application to Seoul Metro Area. *Int. J. Aeronaut. Space Sci.* **2019**, *20*, 260–272. [CrossRef]
18. Syed, N.; Rye, M.; Ade, M.; Trani, A.; Hinze, N.; Swingle, H.; Smith, J.C.; Marien, T.; Dollyhigh, S. ODM commuter aircraft demand estimation. In Proceedings of the 17th AIAA Aviation Technology, Integration, and Operations Conference, Denver, CO, USA, 5–9 June 2017.
19. German, B.; Daskilewicz, M.; Hamilton, T.K.; Warren, M.M. Cargo Delivery in by Passenger eVTOL Aircraft: A Case Study in the San Francisco Bay Area. In *2018 AIAA Aerospace Sciences Meeting*; American Institute of Aeronautics and Astronautics: Reston, VA, USA, 2018; Number 210059, pp. 1–13. [CrossRef]
20. Daskilewicz, M.; German, B.; Warren, M.M.; Garrow, L.A.; Boddupalli, S.S.; Douthat, T.H. Progress in Vertiport Placement and Estimating Aircraft Range Requirements for eVTOL Daily Commuting. In *2018 Aviation Technology, Integration, and Operations Conference*; American Institute of Aeronautics and Astronautics: Reston, VA, USA, 2018; pp. 1–11. [CrossRef]
21. Pukhova, A. Environmental Evaluation of Urban Air Mobility Operation. Master's Thesis, Technical University of Munich, Munich, Germany, 2018.
22. Kasliwal, A.; Furbush, N.J.; Gawron, J.H.; McBride, J.R.; Wallington, T.J.; De Kleine, R.D.; Kim, H.C.; Keoleian, G.A. Role of flying cars in sustainable mobility. *Nat. Commun.* **2019**, *10*, 1–9. [CrossRef] [PubMed]
23. Eißfeldt, H. Sustainable urban air mobility supported with participatory noise sensing. *Sustainability* **2020**, *12*, 3320. [CrossRef]
24. Horni, A.; Nagel, K.; Axhausen, K.W., Eds. *The Multi-Agent Transport Simulation MATSim*; Ubiquity Press: London, UK, 2016. [CrossRef]
25. Segui-Gasco, P.; Ballis, H.; Parisi, V.; Kelsall, D.G.; North, R.J.; Busquets, D. Simulating a rich ride-share mobility service using agent-based models. *Transportation* **2019**, *46*, 2041–2062. [CrossRef]
26. Balać, M.; Becker, H.; Ciari, F.; Axhausen, K.W. Modeling competing free-floating carsharing operators—A case study for Zurich, Switzerland. *Transp. Res. Part C Emerg. Technol.* **2019**, *98*, 101–117. [CrossRef]
27. Liu, J.; Kockelman, K.M.; Boesch, P.M.; Ciari, F. Tracking a system of shared autonomous vehicles across the Austin, Texas network using agent-based simulation. *Transportation* **2017**, *44*, 1261–1278. [CrossRef]
28. Winter, K.; Cats, O.; Martens, K.; van Arem, B. *Relocating Shared Automated Vehicles Under Parking Constraints: Assessing the Impact of Different Strategies for On-Street Parking*; Number 0123456789; Springer: New York, NY, USA, 2020. [CrossRef]
29. Kim, J. Assessment of the DRT system based on an optimal routing strategy. *Sustainability* **2020**, *12*, 714. [CrossRef]
30. Rothfeld, R.; Balać, M.; Plötner, K.; Antoniou, C. Agent-based Simulation of Urban Air Mobility. In Proceedings of the 2018 Modeling and Simulation Technologies Conference, Kissimmee, FL, USA, 8–12 January 2018; pp. 1–10. [CrossRef]
31. Maciejewski, M. Dynamic Transport Services. In *The Multi-Agent Transport Simulation MATSim*; Horni, A., Nagel, K., Axhausen, K.W., Eds.; Ubiquity Press: London, UK, 2016; Chapter 23, pp. 145–152. [CrossRef]
32. Hörl, S. Implementation of an Autonomous Taxi Service in a Multi-Modal Traffic Simulation Using MATSim. Master's Thesis, ETH Zurich, Zurich, Switzerland, 2016. [CrossRef]
33. Shamiyeh, M.; Rothfeld, R.; Hornung, M. A Performance Benchmark of Recent Personal Air Vehicle Concepts for Urban Air Mobility. In Proceedings of the 31st Congress of the International Council of the Aeronautical Sciences, ICAS, Belo Horizonte, Brazil, 9–14 September 2018.
34. Fu, M.; Straubinger, A.; Schaumeier, J. Scenario-based Demand Assessment of Urban Air Mobility in the Greater Munich Area. In *AIAA AVIATION 2020 FORUM*; American Institute of Aeronautics and Astronautics: Reston, VA, USA, 2020; pp. 1–16. [CrossRef]
35. Rothfeld, R.; Balać, M.; Militão, A. MATSim-UAM. Available online: https://github.com/BauhausLuftfahrt/MATSim-UAM (accessed on 19 February 2021).
36. Moeckel, R.; Kuehnel, N.; Llorca, C.; Moreno, A.; Rayaprolu, H. Microscopic Travel Demand Modeling: Using the Agility of Agent-Based Modeling Without the Complexity of Activity-Based Models. In Proceedings of the Annual Meeting of the Transportation Research Board, Washington, DC, USA, 8–12 January 2019.
37. Hörl, S.; Balać, M. Reproducible scenarios for agent-based transport simulation. *Arbeitsberichte Verkehrs Raumplan.* **2020**, *1499*. [CrossRef]

38. Balać, M.; Hörl, S. Synthetic Population for The State of California Based on Open-data: Examples of San Francisco Bay Area and San Diego County. In Proceedings of the 100th Annual Meeting of the Transportation Research Board,Washington, DC, USA, 5–29 January 2021.
39. Moeckel, R. Constraints in household relocation: Modeling land-use/transport interactions that respect time and monetary budgets. *J. Transp. Land Use* **2017**, *10*, 211–228. [CrossRef]
40. Moreno, A.; Moeckel, R. Population Synthesis Handling Three Geographical Resolutions. *ISPRS Int. J. Geo-Inf.* **2018**, *7*, 174. [CrossRef]
41. Mobilität in Deutschland. Available online: https://www.mobilitaet-in-deutschland.de (accessed on 19 February 2021).
42. Hörl, S.; Balać, M. Eqasim-org. Available online: https://github.com/eqasim-org (accessed on 19 February 2021).
43. Hörl, S.; Balać, M. Introducing the eqasim pipeline: From raw data to agent-based transport simulation. Presented at the ABMTRANS, Warsaw, Poland, 23–26 March 2021.
44. Hörl, S.; Balać, M.; Axhausen, K.W. A first look at bridging discrete choice modeling and agent-based microsimulation in MATSim. *Procedia Comput. Sci.* **2018**, *130*, 900–907. [CrossRef]
45. Hörl, S.; Balać, M.; Axhausen, K.W. Pairing discrete mode choice models and agent-based transport simulation with MATSim. In Proceedings of the Transportation Research Board 98th Annual Meeting, Washington, DC, USA, 13–17 January 2019.
46. Moeckel, R.; Donnelly, R. Gradual Rasterization: Redefining Spatial Resolution in Transport Modelling. *Environ. Plan. B Plan. Des.* **2015**, *42*, 888–903. [CrossRef]
47. Hansman, R.J.; Vascik, P.D. Operational Aspects of Aircraft-Based On-Demand Mobility Aircraft-Based On-Demand Mobility. 21 April 2016. Available online: https://www.faa.gov/about/office_org/headquarters_offices/ang/library/events/jup/april2016/MIT/MIT_ICAT_Parker_Vascik.pdf (accessed on 12 February 2021).
48. Vascik, P.D.; Hansman, R.J. Evaluation of Key Operational Constraints Affecting On-Demand Mobility for Aviation in the Los Angeles Basin: Ground Infrastructure, Air Traffic Control and Noise. In Proceedings of the 17th AIAA Aviation Technology, Integration, and Operations Conference, Denver, CO, USA, 5–9 June 2017; American Institute of Aeronautics and Astronautics: Reston, VA, USA, 2017. [CrossRef]
49. Rothfeld, R.; Fu, M.; Antoniou, C. Analysis of Urban Air Mobility's Transport Performance in Munich Metropolitan Region. In Proceedings of the mobil.TUM 2019, Munich, Germany, 11–12 September 2019. [CrossRef]
50. Shamiyeh, M.; Bijewitz, J.; Hornung, M. A Review of Recent Personal Air Vehicle Concepts. In Proceedings of the Aerospace Europe 6th CEAS Conference, Bucharest, Romania, 16–20 October 2017; Number 913, pp. 1–16.
51. Garrow, L.A.; Mokhtarian, P.; German, B.; Boddupalli, S.S. Commuting in the Age of the Jetsons: A Market Segmentation Analysis of Autonomous Ground Vehicles and Air Taxis in Five Large U.S. Cities. In *AIAA AVIATION 2020 FORUM*; American Institute of Aeronautics and Astronautics: Reston, VA, USA, 2020. [CrossRef]
52. Chakour, V.; Eluru, N. Analyzing commuter train user behavior: A decision framework for access mode and station choice. *Transportation* **2014**, *41*, 211–228. [CrossRef]